A developed 3(4) step synthesis strategy for radiolabeling Flumazenil with carbon-11 in the carbonyl position and establishment of a process for [^{11}C]-methylation of Flumazenil

Master's Thesis in Medical Technology

by

Synnøve Hodnekvam

Department of Chemistry
University of Bergen

June 1, 2023

Scientific environment

This study is carried out at the department of chemistry at University of Bergen and at the PET centre at Haukeland University Hospital. The work is supported by the Tracer Development Center in Bergen through the 180°N consortium and by the Bjørsvik Research Group. The work is funded by the 180°N consortium which again is funded by Trond Mohn Foundation and Tromsø Research Foundation.

UNIVERSITY OF BERGEN

Bjørsvik Research Group

180°N
NORWEGIAN NUCLEAR MEDICINE CONSORTIUM

Haukeland University Hospital

Acknowledgements

First of all, I would like to thank my supervisor, Tom Christian Holm Adamsen for guidance and for giving me so much freedom when planning the work on my thesis. Also for facilitating my hot experiments through assisting me with the cyclotron, helping me order liquid nitrogen in advance and generally assisting me in the laboratory.

I am also very grateful for 180°N for giving me the opportunity to network in the nuclear medicine environment, and to have gotten the chance to present my work in front of pioneers in the field, getting valuable feedback upon topics that were hard to come by through literature search.

I would also like to thank my co-supervisor, Hans-René Bjørsvik for giving me advice and guidance every time i got stuck on my synthesis, for allowing me to use the Bjørsvik Group laboratories and making me a part of his research group.

I am very grateful for the other master's students in the Bjørsvik Research Group, Eline, Marie, Kjetil, Julianne, Jenny-Mari and last but not least our PhD candidate, Sara. Thank you for helping me with all kinds of problems, teaching me new techniques in the lab and also for making a fun and safe environment and a year I will not forget.

Also, a huge thank you to Bjarte Holmelid and Jarl Underhaug. Bjarte for helping me whenever I had questions or issues with the LC-MS instrument, and Jarl for helping me with improving my NMR spectra and structural elucidation whenever I had questions or problems in regard to this.

Thank you, Unni and Chubina for helping me in the hot-lab. Unni for helping me with questions regarding the instruments and Chubina for helping me with mathematical problems and design of experiments.

Lastly, I would like to thank my family and friends for the support throughout this year and especially to my partner, Andreas. Thank you.

Synnøve Hodnekvam
Bergen, 31.05.2023

Abstract

Even though carbon-11 has some very interesting features for PET imaging, its potential has still not been fully exploited. Reasons for this could be that its short half-life requires an efficient and fast synthesis route, or that its primary synthons are quite unreactive, limiting its chemistry. However, great engineering work has been done, and carbon-11 chemistry is on the rise, moving towards novel methods aside from the main strategy, [^{11}C]-methylation. Previously, Flumazenil, a selective $GABA_A$ receptor antagonist, has been radiolabeled in different positions with the aim to perform nuclear imaging of $GABA_A$ receptors in the brain. Due to metabolites, the best candidate is [^{11}C]-methylated Flumazenil. However, for research purposes, it could be interesting to radiolabel Flumazenil in the carbonyl position, giving a possibility to learn more about Flumazenil and its metabolite in the brain, while also performing novel carbon-11 chemistry and developing precursor synthesis routes that also can be adaptable towards other targets. The aim of this study is therefore to synthesize a precursor for Flumazenil that can be radiolabeled in the carbonyl position of the ester group and then to radiolabel it through [^{11}CO]-carbonylation. Another goal of this study is to establish an efficient process for [^{11}C]-methylation of Flumazenil using design of experiments as a tool. In this work, a synthesis strategy for generating precursors that can be radiolabeled in the carbonyl position of an ester group next to heteroatoms on heteroaromatic rings has been developed. Establishment and partly optimization of a process for [^{11}C]-methylation of Flumazenil using design of experiments has been done.

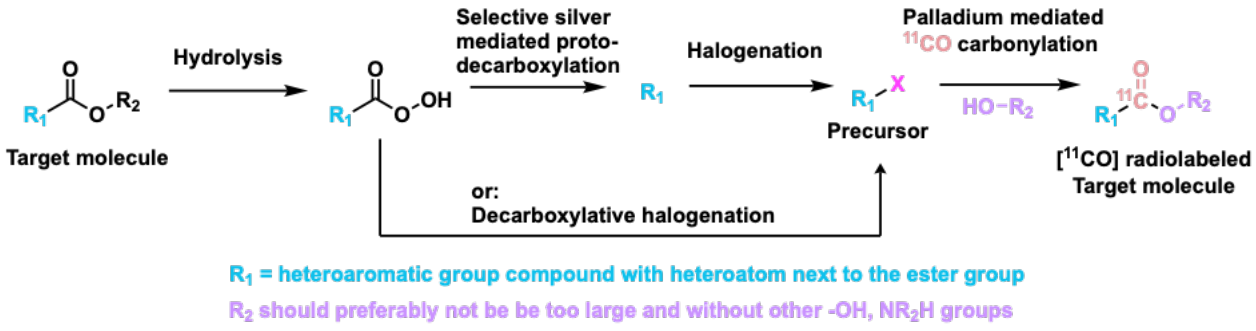

Figure 1: The developed [^{11}CO]-precursor synthesis strategy.

Contents

Abbreviations

^{13}C-NMR	Carbon-13 Nuclear Magnetic Resonance
^{1}H-NMR	Proton Nuclear Magnetic Resonance
AcOH	Acetic acid
Ag_2CO_3	Silver Carbonate
$AgNO_3$	Silver Nitrate
Ag_2O	Silver Oxide
α	alpha
BBB	Blood Brain Barrier
Bq	Becquerel
CH_2O	Aldehyde
CH_3NO_2	Nitromethane
CH_4	Methane
Ci	Curie
CO	Carbon Monoxide
CO_2	Carbon Dioxide
$COCl_2$	Phosgene
COSY	Correlation spectroscopy
CS_2	Carbon Disulfide
CT	Computer Tomography
CuI	Copper Iodide
DBrH	N,N'-Dibromo-5,5-dimethylhydantoin
DCH	N,N'-Dichloro-5,5-dimethylhydantoin

DCM	Dichlormethane
DHH	N,N'-Dihalo-5,5-dimethylhydantoin
DIH	N,N'-Diiodo-5,5-dimethylhydantoin
DIPEA	N,N-Diisopropylethylamine
DMF	Dimethylformamid
DMSO	Dimethyl Sulfoxide
DoE	Design of Experiments
ESI	Electron Ionization
ESI	Electron Spray Ionization
EtOAc	Ethyl Acetate
EtOH	Ethanol
GABA	γ-Aminobutyric Acid
$GABA_A$	γ-Aminobutyric Acid - A
GC-MS	Gass Chromatography Mass Spectrometry
H_2	Hydrogen gas
HCl	Hydrochloric Acid
HCl	Hydrochloric Acid
HCN	Cyanide
He	Helium
HF	Hydrofluoric Acid
HI	Hydroiodic Acid
HMBC	Heteronuclear multiple-bond correlation spectroscopy
HPLC	High Pressure Liquid Chromatography
HSQC	Heteronuclear single-wuantum correlation spectroscopy
I_2	Iodine
LC	Liquid Chromatography
LC-MS	Liquid Chromatography Mass Spectrometry
MeI	Methyl Iodide

$MeNH_2$	Methylamine
MeOH	Methanol
MeOTf	Methyl Triflate
MR	Magnetic Resonance
N_2	Nitrogen gas
$Na_2S_2O_3$	Sodium Thiosulfate
$NaNO_2$	Sodium Nitrate
NaOH	Sodium Hydroxide
NBS	N-Bromosuccinimide
NH_4OH	Ammonium Hydroxide
Ni	Nickel
NIS	N-Iodosuccinimide
NMR	Nuclear Magnetic Resonance
NOESY	nuclear Overhauser effect spectroscopy
O_2	Oxygen gas
p	proton
Pd	Palladium
$Pd(OAc)_2$	Palladium Acetate
PET	Postitron Emission Tomography
QC	Quality Control
RCP	Radiochemical Purity
RCY	Radiochemical Yield
RSM	Response Surface Methodology
SA	Specific Activity
Semi-Prep HPLC	Semi-Preparative High Pressure Liquid Chromatography
S_N2	Nucleophilic Substitution Reaction with both substrate and nucleophile involved in rate limiting step

SPECT	Single Photon Emission Computed Tomography
THF	Tetrahydrofuran
TIC	Total Ion Chromatogram
$TiCl_3$	Titanium(III)chloride
TLC	Thn Layer Chromatography
UV-VIS	Ultra Violet-Visual
Xe	Xenon
Zn	Zinc

List of Figures

List of Tables

Chapter 1

Introduction

1.1 Aim of Study

The aim of this study is to synthesize a precursor that can participate in a palladium mediated [^{11}CO]-carbonylation of Flumazenil and to perform [^{11}CO]-carbonylation of this precursor. The aim is also to establish and optimize an efficient method for producing [^{11}C]-Flumazenil through [^{11}C]-methylation using a Synthra MeI Plus Research synthesizer.

1.2 Objectives

Can Flumazenil be radiolabeled with carbon-11 in the carbonyl position of the ester group? Can the process for [^{11}C]-methylation og Flumazenil be optimized using different design of experiments tools?

1.3 Contribution

This work should give Haukeland University Hospital two different methods for producing Flumazenil that can be used to learn more about metabolite activity of Flumazenil in the brain. The work will increase the competence in carbon-11 chemistry at Haukeland University Hospital and in the 180°N consortium environment. The work should give more knowledge in which factors that are important for an increased radiochemical yield in [^{11}C]-methylations. Gained knowledge about how to optimize separation and isolation of Flumazenil from its precursors is also to be obtained. The work will also contribute towards gained knowledge of precursor synthesis, especially on chemistry done on imidazole rings and esters or carboxylic acids located next to a heteroatom on an aromatic ring.

Chapter 2

Background

2.1 Nuclear Medicine

Nuclear medicine is the application of radionuclides in medicine. The advantage of nuclear medicine is that although radioactive nuclides have different physical properties compared to corresponding stable nuclides, they still exhibit the same chemical properties (13). This means that a stable nuclide can be replaced with a radioactive nuclide of the same atom in a drug. After introducing the radioactive drug into a body, one can achieve non-invasive, in vivo images of the behavior of the drug by using detectors suitable for the type of radiation and combine this with other imaging techniques such as a Computed Tomography, CT, or Magnetic Resonance, MR, scan. By imaging the behavior of a drug, one can access pharmacodynamic and pharmacokinetic behavior of the drug, use it as a biomarker for diseases, monitor disease or treatment progress and learn more about different processes in the body.

There are two types of nuclear imaging techniques: Single Photon Emission Computed Tomography, SPECT and Positron Emission Tomography, PET. SPECT arises from nuclides emitting gamma rays, while PET arises from nuclides emitting positron particles. A positron is the positively charged counter particle of an electron. As soon as a positron meets an electron, they will annihilate and turn into two 511 KeV photons that travel in the opposite direction of each other. This thesis will focus on the radioactive nuclide carbon-11, which is a positron emitter. It is also possible to use radioactive nuclides for therapy. If an alpha emitting nuclide is put on a drug with well-known pharmacokinetics, this can be used to destroy tumor tissue, as the alpha particle radiation is destructive to the surrounding tissue. This paper will however focus on radiotracers for PET.

For a radioactive nuclide to be a useful candidate for nuclear imaging purposes, it

should exhibit certain features:

- The unstable nuclide should emit sufficient amounts of the desired radiation (gamma radiation or positron emission).
- For safety reasons, the nuclide should preferably be a low energy emitter. The perfect combination is when for example a positron emitting nuclide emits low energy positrons and has a high fraction of positron emission (14).
- The nuclide should have a relatively short half-life that is comparable to the time required for the administered radiotracer to localize the tissue of interest (15).
- The ideal nuclide can be prepared in sufficient amounts, using nuclear reactions that do not generate larger amounts of additional undesirable radioisotopes that causes a waste concern after production.
- The chemistry of the nuclide must allow for it to be integrated into a target molecule in an applicable way.

In Table 2.1 an overview of commonly used radionuclides in nuclear imaging along with their half-lives, method of production and what type of scan they are used for can be viewed. As one can see, carbon-11 has one of the shortest half-lives, something that is a good match for drugs that has a rapid uptake in the body. It is also useful for research purposes as the short half-life allows for multiple scans in the same subject in one day. Carbon-11 will be more in-depth described later in this chapter.

Radionuclide	**Half-life**	**Production method**	**Type of scan**
^{82}Rb	1.27 min	Generator	PET
^{15}O	2 min	Cyclotron	PET
^{15}N	10 min	Cyclotron	PET
^{11}C	20 min	Cyclotron	PET
^{68}Ga	68.3 min	Generator	PET
^{18}F	110 min	Cyclotron	PET
^{99m}Tc	6.03 h	Generator	SPECT
^{123}I	13.2 h	Cyclotron	SPECT
^{111}In	2.8 d	Cyclotron	SPECT
^{201}Tl	3.05 d	Cyclotron	SPECT
^{67}Ga	3.26 d	Cyclotron	SPECT
^{133}Xe	5.25 d	Reactor	SPECT

Table 2.1: The most commonly used radionuclides used for nuclear imaging.

2.2 Brain Receptor Imaging

Receptors are typically protein structures located on cellular membranes that, when interacting with specific ligands, trigger a signal resulting in defined responses mediated by either secondary messengers or ion channels. Receptors play a critical role in brain function by serving as the sites where neurotransmission occurs at the postsynaptic membrane. They also regulate presynaptic sites for neurotransmitter reuptake and feedback and can modulate various functions of the cell membrane. The distribution, density and activity of receptors can be visualized by radioactive tracers that are labeled for SPECT and PET scans, giving a great, non-invasive insight in brain function. Through tracer kinetic modelling one can also quantify receptor binding (16).

2.3 $GABA_A$ Receptors

GABA, γ-Aminobutyric Acid, is the most important inhibitory neurotransmitter. The transmission of this neurotransmitter is altered in epilepsy, as well as in anxiety and other psychiatric disorders. GABA is abundant in the cortex and very sensitive to damage. The fact that it is sensitive to damage makes it a biomarker for neural integrity, and can be used to investigate damage after for example an ischemic stroke in the brain and in other various neurodegenerative diseases. Benzodiazepines are a class of psychoactive drugs that act as central nervous system depressants and have a range of therapeutic uses. They work by enhancing the activity of GABA at $GABA_A$ receptors, which results in increased inhibition of neuronal activity in the brain (16). The central benzodiazepine receptor, a part of the $GABA_A$ receptor complex, gates the Cl^- ion channel and specifically mediates all pharmacological properties of the benzodiazepines. Knowledge about receptor binding of pharmaceuticals to the $GABA_A$ receptor can give great insight to the pharmacodynamics of benzodiazepines.

2.4 Carbon-11

Carbon-11 is a radioactive nuclide with a short half-life of 20.4 minutes. It decays to boron-11 mainly through positron emission (99.77%), see Figure 2.1 and to a very short extent through electron capture (0.23%) (1; 17). Carbon-11 has some very attractive features for radiolabeling, as carbon is the main building block of most organic compounds and therefore also in most pharmaceuticals. Its short half-life also allows for multiple PET-scans in one day on the same subject, something that potentially can boost the speed of acquired data and the throughput of subjects (17). However, its

short half-life also offers some productional challenges. The rule of thumb is that the production time of a radiotracer should not exceed around 3 half-lives of the radionuclide, which limits the production of carbon-11 radiotracers to a production time of approximately 60 minutes, including quality control. The radiotracer should be ready for injection no later than 6 half-lives, which for carbon-11 means no later than 120 minutes after the end of bombardment in the cyclotron. This requires efficient synthesis routes and fast work-up. When working with carbon-11, Design of Experiments is a very useful tool which can be used to get the most yield out of as little production time as possible. Design of Experiments is explained more thoroughly in subsection 3.5.1 in Methods.

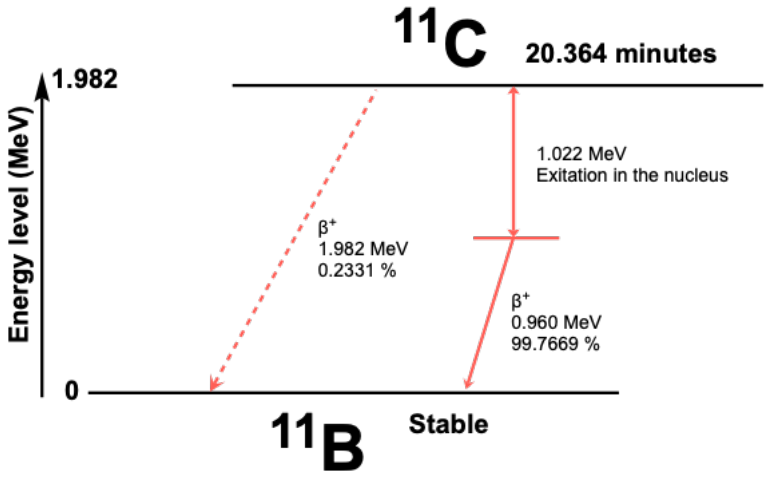

Figure 2.1: The radioactive decay route of carbon-11. Figure taken from page 39 in Karlsruhe Nuclide Chart (1).

2.4.1 Production and Common Synthons

Carbon-11 is produced in a cyclotron through proton bombardment of nitrogen gas, giving the radiochemical equation $^{14}N(p,\alpha)^{11}C$. The carbon-11 nuclide will exist as a part of different chemical species, depending on the environment the bombardment occurs in, see Figure 2.2. The presence of oxygen (0.5-1%) will yield [^{11}C]CO_2, while the presence of hydrogen (5-10%) will yield [^{11}C]CH_4 (17). [^{11}C]CO_2 and [^{11}C]CH_4 freshly produced from the cyclotron are called primary synthons. In this paper, [^{11}C]CO_2 is the primary synthon of use, and the paper will therefore focus on this method.

The mostly used reaction pathway in carbon-11 chemistry is ^{11}C-methylation using the secondary synthons, [^{11}C]methyl iodide or [^{11}C]methyl triflate. However, the use of other carbon-11 synthons have also been explored, expanding the possibilities for

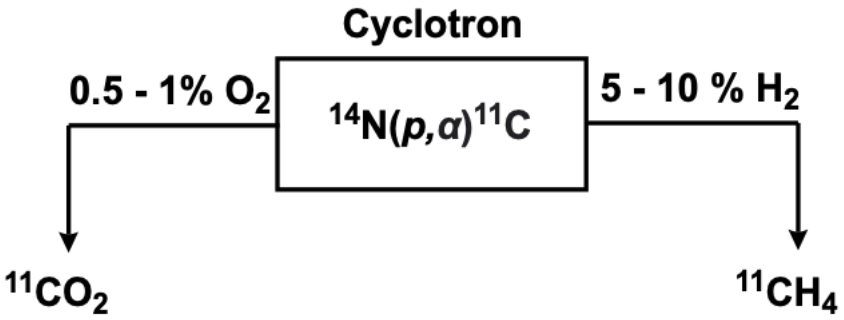

Figure 2.2: The production of carbon-11 and its primary synthons.

radiolabeling with carbon-11. Such synthons are [^{11}C]CO_2, [^{11}C]CS_2, [^{11}C]CH_2O, [^{11}C]CO, [^{11}C]CH_3NO_2, [^{11}C]$COCl_2$ and [^{11}C]HCN (18). This thesis will focus on [^{11}C]methyl iodide or [^{11}C]methyl triflate and [^{11}C]CO.

2.4.2 Methylation

[^{11}C]-methylations are by far the most commonly used method for introducing carbon-11 into a molecule (19). The most common methylation substrate is [^{11}C]methyl iodide. When methyl iodide is not sufficiently reactive, [^{11}C] methyl triflate is often used. The methylation happens through a S_N2 reaction where the molecule to be labeled acts as a nucleophile attacking the methyl group, kicking out the iodide or the triflate ion that acts as a leaving group, see Figure 2.3

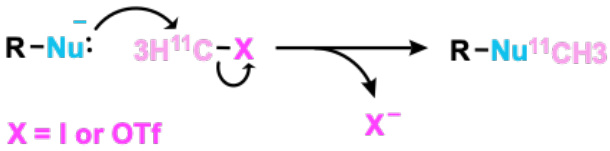

Figure 2.3: Methylation reaction used for labeling with [^{11}C]MeI or [^{11}C]MeOTf.

To produce [^{11}C]MeI when using [^{11}C]CO_2 as a primary synthon, the following steps are needed and also illustrated in Figure 2.4. Firstly, a CO_2 trap is needed to contain the [^{11}C]CO_2 produced from the cyclotron. From the cyclotron, [^{11}C]CO_2 is transported with the target nitrogen gas. For the next step hydrogen gas is used, and therefore the CO_2 trap is needed so that one can concentrate it and switch gas for the next step. Secondly, the [^{11}C]CO_2 is passed through a nickel oven using hydrogen as a carrier gas. The nickel oven functions as a catalyst when hydrogen is present during heating, turning [^{11}C]CO_2 into [^{11}C]CH_4. Hydrogen gas is no longer needed, therefore a methane trap is required in order to switch to an inert carrier gas, for example

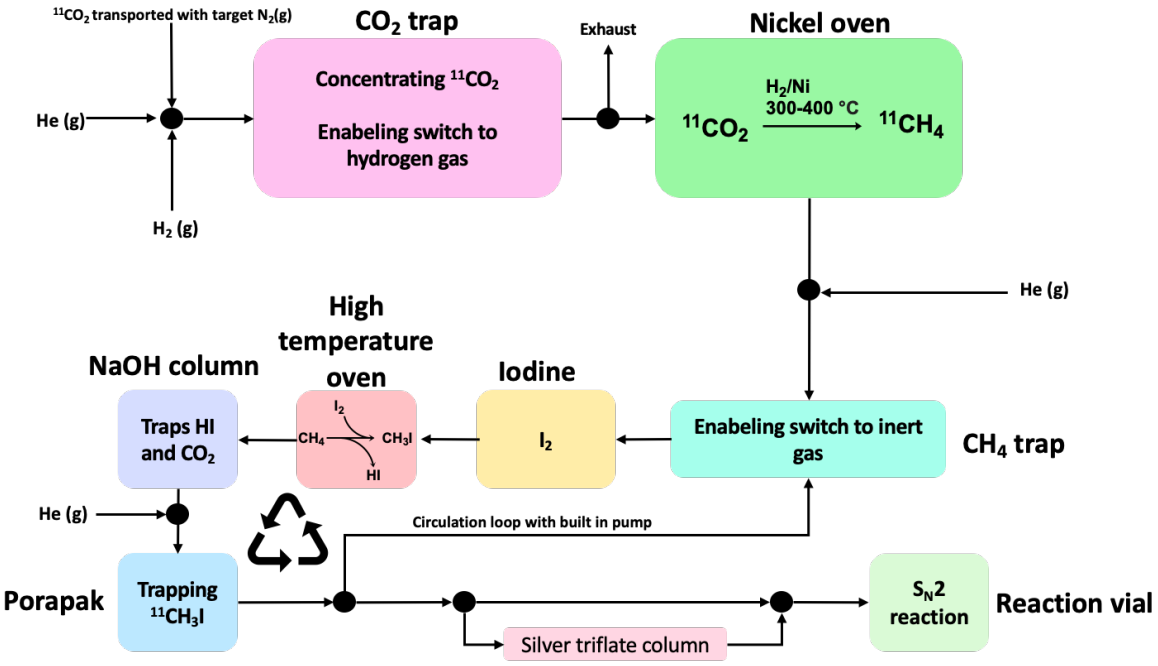

Figure 2.4: The production of $[^{11}C]CH_3I$ or $[^{11}C]CH_3OTf$ from $[^{11}C]CO_2$.

helium. Thirdly, the trap is heated and $[^{11}C]CH_4$ is passed through an iodine column, a high temperature oven, a NaOH column and a Porapak column. The iodine column and the high temperature oven turns $[^{11}C]CH_4$ into $[^{11}C]CH_3I$, the NaOH traps residue $[^{11}C]CO_2$ and hydroiodic acid, while the Porapak column is cooled to trap and concentrate $[^{11}C]CH_3I$. As not all of the $[^{11}C]CH_4$ will react to yield $[^{11}C]CH_3I$, the carrier gas needs to circulate $[^{11}C]CH_4$ through the system several times to increase the yield. Lastly, the Porapak column is heated to release the methyl iodide and the $[^{11}C]CH_3I$ is bubbled into a solution containing the precursor to be labeled in the solvent of choice, often DMSO or DMF. It is to prefer a polar aprotic solvent as this supports S_N2 reactions. If $[^{11}C]CH_3OTf$ is desired, $[^{11}C]CH_3I$ can be passed through a heated silver triflate column before being bubbled into the reaction mixture.

2.4.3 Carbonylation

Carbonylation is the introduction of carbon monoxide into organic or inorganic molecules. $[^{11}C]CO$ can be achieved through reduction of $[^{11}C]CO_2$ over a zinc or molybdenum column (20). $[^{11}C]CO$ can participate in palladium mediated ^{11}C-carbonylation reactions to produce a great variety of functional groups (17; 21). This thesis will focus on $[^{11}C]$-alkoxy carbonylation where a halo-aryl substrate Pd(0) mediated reacts with an alcohol and $[^{11}C]CO$ in a basic environment to yield an ester, see Figure 2.5.

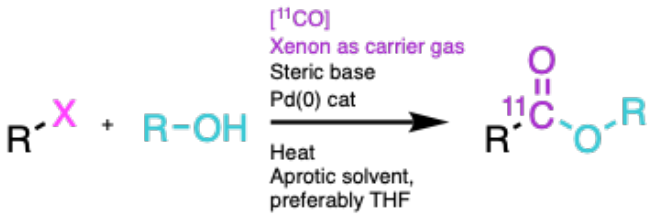

Figure 2.5: Palladium mediated alkoxy carbonylation with [^{11}C]CO.

The mechanism for Pd(0)-catalyzed carbonylation of organohalides using [^{11}C]CO can be viewed in Figure 2.6 (21).

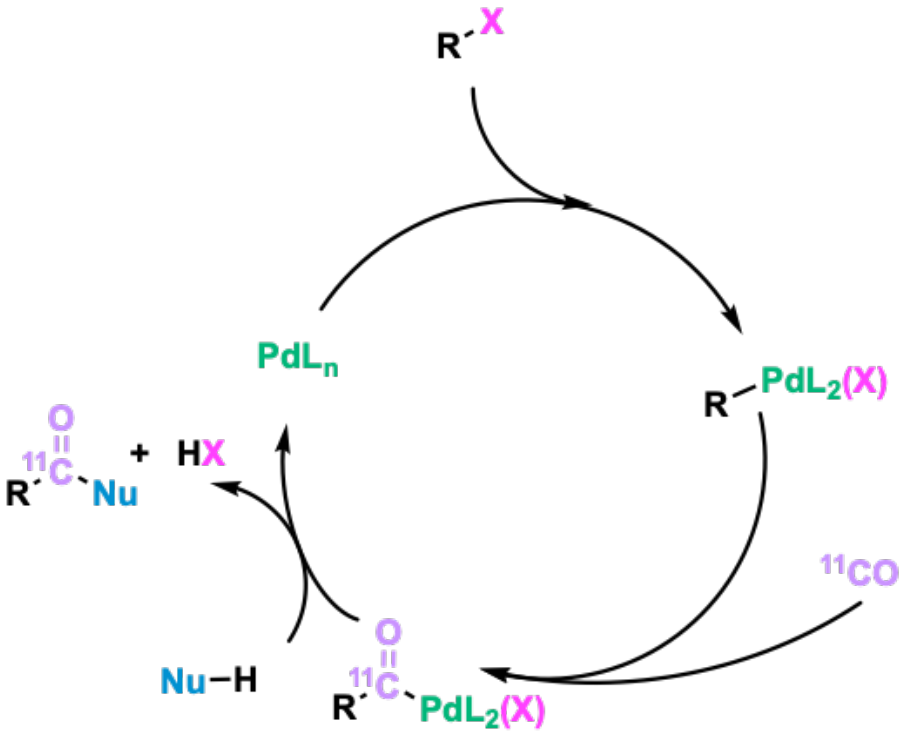

Figure 2.6: Mechanism for Pd(0)-catalyzed carbonylation of organohalides using [^{11}C]CO.

One of the problems with using [^{11}C]CO has been its low solubility and retention different organic solvents (17). There have also been problems when using Zinc as a reducing agent, as nitrogen oxides from the target gas in the cyclotron destroys the column, leading to drastically worse conversion to [^{11}C]CO for each production. Different approaches have been investigated to solve these problems. In order to solve the problem with the Zinc column, Kihlberg and Langström developed a method in 2004 that entails trapping [^{11}C]CO_2 at low temperature using a trap cooled down to -196°C (22). The trap is then heated to room temperature and released using a stream of helium as a carrier gas. The stream then flows through a silica gas purification column, removing all undesired residues from the target gas, and allowing purified [^{11}C]CO_2 to enter

the Zinc column. Other solutions to this problem, have been to decrease the amount of oxygen in the nitrogen target gas in the cyclotron to 0.1 % instead of 0.5-1 %. For the problem with the solubility of CO in different organic solvents, different approaches have been developed. The most applicable one, which do not involve high pressure micro-autoclaves and takes place at ambient pressure, was developed by Eriksson et al in 2012 (23). The method is based on using Xenon as a carrier gas for [^{11}C]CO. Xenon has a high solubility in THF, and by using THF as a solvent for palladium mediated [^{11}CO] carbonylation, [^{11}C]CO can be successfully trapped in the reaction mixture, allowing for higher yields.

In Figure 2.7, a method for the production of [^{11}C]CO can be viewed. Here, only 0.1 % oxygen is used in the target gas to avoid the problem with nitrogen oxides destroying the zinc column. [^{11}C]CO_2 is firstly trapped, concentrating [^{11}C]CO_2 and allowing for switch to inert carrier gas. [^{11}C]CO_2 is then transported to a Zinc column at 400 °C for the reduction of [^{11}C]CO_2 to [^{11}C]CO. It is important that it is exactly 400 °C, as higher temperatures will destroy the column. Residue [^{11}C]CO_2 is then trapped in an Ascarite column, while [^{11}C]CO is trapped in a [^{11}C]CO trap, allowing for a switch from the previous carrier gas to Xenon gas. The trap is heated, and Xenon is bubbled into the reaction vial, using THF as solvent.

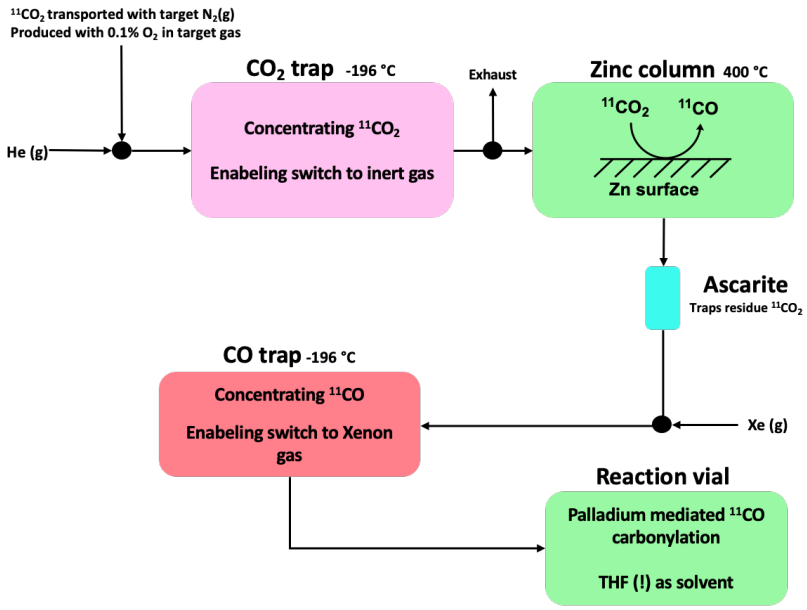

Figure 2.7: The production of [^{11}C]CO from [^{11}C]CO_2.

2.5 Previous Work - Raclopride

Previously, Raclopride, that routinely is radiolabeled using a methylation strategy, has been redesigned to be radiolabeled in the carbonyl position using palladium mediated carbonylation (24). This was done with the aim to radiolabel using a new method and compare the effect of the different ways of radiolabeling the drug in non-human primate using PET. The comparison was done with regards to quantitative outcome measurements, metabolism of the labeled tracer and protein binding. In this work they performed novel carbon-11 chemistry while also learning more about the pharmacokinetics and pharmacodynamics of Raclopride. This work has been of inspiration to the following section about Flumazenil.

2.6 Flumazenil

Flumazenil is a selective $GABA_A$ receptor antagonist. Therapeutically it is used as an antidote against overdoses of benzodiazepines through competitive inhibition. Its selectivity towards $GABA_A$ receptors also makes it a great radiotracer for mapping the distribution of $GABA_A$ receptors in the brain. Previously, Flumazenil has been radiolabeled in the positions that can be seen in Figure 2.8, using ^{123}I, ^{18}F and ^{11}C in the methyl and ethyl postition of the molecule, with the [^{11}C]-methylated version being the most frequently used (25–27).

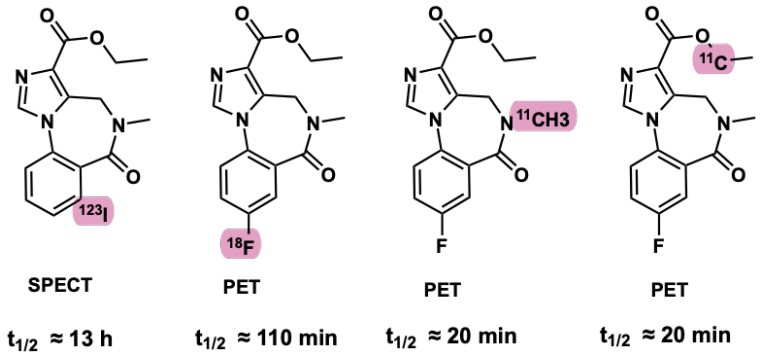

Figure 2.8: Previous radiolabeling of Flumazenil.

In Figure 2.9 the main metabolic pathways of Flumazenil can be viewed. If this illustration is compared to the [^{11}C]-radiolabelings in Figure 2.8, one can see that both the ethylated and methylated [^{11}C]-radiolabelings are metabolized through Hydrolysis and N-dealkylation, respectively. The N-dealkylated metabolite of Flumazenil also passes the blood brain barrier (BBB) - being the reason why the [^{11}C]-methylated ver-

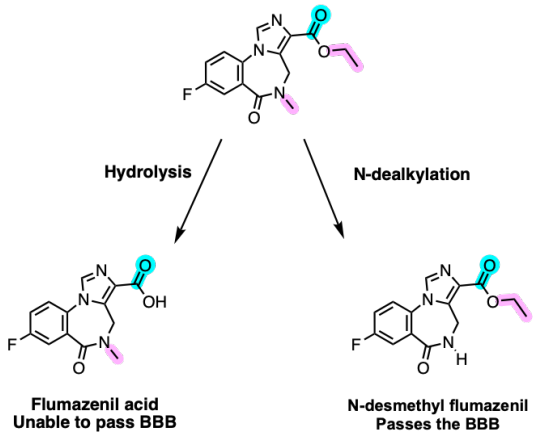

Figure 2.9: Main metabolic pathways of Flumazenil.

sion is the most frequently used, as this is the only radiolabeling that does not also have radiolabeled metabolites passing the BBB. However, it would also be interesting to radiolabel Flumazenil with carbon-11 in the carbonyl position, marked in blue in Figure 2.9. By having the radiolabel in this position, one can use this radiolabeled version of Flumazenil to study the behavior or the effects of the N-dealkylated metabolite in the brain. This is something that already have been possible with the fluor-18 version of Flumazenil, however when using carbon-11, which is the same radioactive signal source as for the [^{11}C]-methylated version, this hopefully can lead to more precise measurements of metabolite activity in the brain. It would also be a great way to broaden the library of carbon-11 chemistry by performing [^{11}CO]-carbonylation and develop new strategies for precursor synthesis.

Theoretically, compound **7x** should be able to participate in a palladium mediated [^{11}CO]-carbonylation reaction, yielding [^{11}CO]-Flumazenil, as in Figure 2.10. To generate the precursor **7x**, where X indicates a halogen Cl, Br or I, is the overall goal of this thesis as well as establishing a production process for [^{11}C]-methylation of Flumazenil.

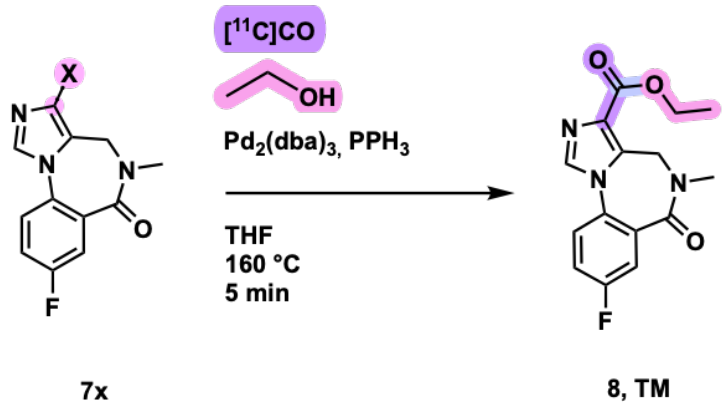

Figure 2.10: Palladium mediated [^{11}C]CO-carbonylation of Flumazenil.

Chapter 3

Methods and theory of methods

3.1 Literature Search

It was desirable to find an already established radiotracer that previously had been [^{11}C]-methylated, but also had the potential to be, and had not yet been [^{11}CO]-carbonylated. A literature search using Google Scholar and conversations with experts in the field was therefore done to localize the radiotracer of interest, landing on Flumazenil. SciFinder^{n} and Google Scholar were used to find synthesis routes for the synthesis of the precursor for radiolabeling Flumazenil in the carbonyl position.

3.2 Radiochemistry

The Cyclotron at Haukeland University Hospital was used to produce [^{11}C]CO_2. Synthra MeI Plus Research inside a lead workstation was used for radiolabeling. For measurement of specific activity, SA, radio chemical yield, RCY, and radio chemical purity, RCP, an analytical radio HPLC system from Agilent Technologies was used.

3.2.1 Synthra MeI Plus Research

Synthra MeI Plus Research is a flexible and completely automated synthesis system for routine production of a wide variety of [^{11}C]-labeled compounds, based on the generation of gas-phase [^{11}C]methyl iodide or optional [^{11}C]methyl triflate synthesis. The module can be used for solid support heterogeneous as well as homogeneous reactions. The synthesizer has two reaction vessels and the capability to produce [^{11}C]HCN as well as [^{11}C]CO for further labeling procedures. The Synthra MeI Plus Research module can be viewed in Figure 3.1.

In Figure 3.2 the graphical user interface for the Synthra module can be viewed.

h

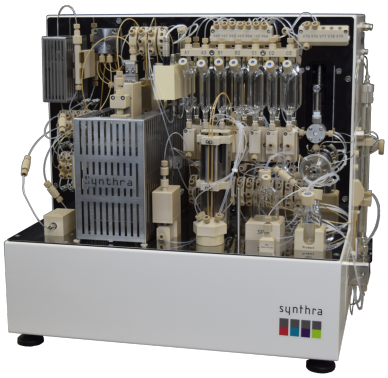

Figure 3.1: The Synthra MeI Plus Research module

Before the synthesis starts, the run is programmed into a script that controls and monitors all the valves, temperatures and flow rates. One can also override the script during a run. This gives great control over the process, and the system should be applicable for performing design of experiments.

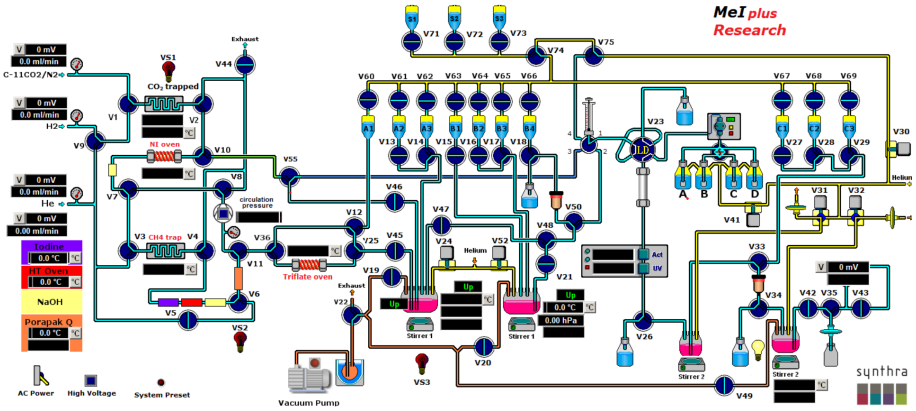

Figure 3.2: Synthra Graphical User Interface for [^{11}C]-methylation chemistry.

3.2.2 Analytical Radio HPLC

Analytical HPLC is a low scale analytical method used to perform quantitative or qualitative analysis. It separates compounds in a sample using a HPLC column. The amounts of sample loaded on to the HPLC column is of very low amounts and only to perform quantitative or qualitative analysis. On normal HPLC there is a detector, normally UV/VIS detector that can measure the intensity of substance leaving the column, which then can be used to detect and quantify the substance. With radio HPLC, there is also a detector for measuring radioactivity of the substance leaving the column. In this way, one can also measure the SA, RCY and RCP parameters from the

production of a radiopharmaceutical. SA is calculated using Equation 3.1, where A_R is the activity of the radiopharmaceutical and m_R is the mass of the radiopharmaceutical. RCY is calculated using Equation 3.2, where A_R is the activity of the radiopharmaceutical and A_S is the activity of the starting material. RCP is calculated using Equation 3.3, where A_R is the activity of the radiopharmaceutical and A_{total} is the total activity.

$$SA = \frac{A_R}{m_R} \quad (3.1) \qquad RCY = \frac{A_R}{A_S} \quad (3.2) \qquad RCP(\%) = \frac{A_R}{A_{total}} \quad (3.3)$$

HPLC is described more thoroughly in Section 3.4.

3.2.3 Semi-Preparative Radio HPLC

Preparative HPLC is a method for isolating and purifying a product of interest. Semi preparative HPLC functions in the same way as for preparative HPLC, only for smaller quantities, and is done on analytical or slightly larger sized columns. This scale is suitable for radiochemistry as the tracers often are made in very small quantities. As for the analytical radio HPLC, there is a normal detector such as UV/VIS along side with a detector for radioactivity at the end of the column where the species elute, allowing for collection of the product when the detectors indicate the presence of the desired product.

3.3 Precursor Synthesis - Reaction types, Mechanisms and Techniques

3.3.1 Imidazole Tautomerism

An imidazole ring where there are no groups attached to the nitrogen on the ring will undergo tautomerism and can lead to isomers when participating in reactions, see figure 3.3. This must be considered when performing synthesis involving imidazole rings where there are no groups attached to the nitrogen.

Figure 3.3: Imidazole tautomerism

3.3.2 Microwave Assisted Synthesis

Microwave-assisted synthesis is a technique in which microwaves are used to heat reaction mixtures. In a microwave-assisted synthesis, the reaction mixture is placed in

a microwave reactor that permits microwaves into the reaction mixture. The mixture is then exposed to microwave radiation, which causes the molecules in the mixture to rapidly rotate and generate heat. This has many benefits, allowing for a lower energy consumption through heating more rapidly and homogeneously compared to conventional heating methods such as the use of an oil bath. It can allow for a faster reaction time, higher yields, use of greener solvents (e.g. water, ethanol, methanol and acetone, which are responsive to microwave irradiation) and sometimes even the use of less or no solvents (28).

3.3.3 Nucleophilic Aromatic Substitution through a Meisenheimer Complex

A Meisenheimer Complex is an intermediate that can be formed during certain types of chemical reactions, such as nucleophilic aromatic substitution reactions. When a nucleophile attacks an aromatic compound, such as a benzene ring, it can displace a leaving group and form a highly unstable intermediate known as an arenium ion. The arenium ion can then rearrange to form a more stable Meisenheimer complex. The Meisenheimer complex is typically formed by the addition of a nucleophile to a highly electron-deficient aromatic ring, such as a substituted nitro benzene, see Figure 3.4 (2).

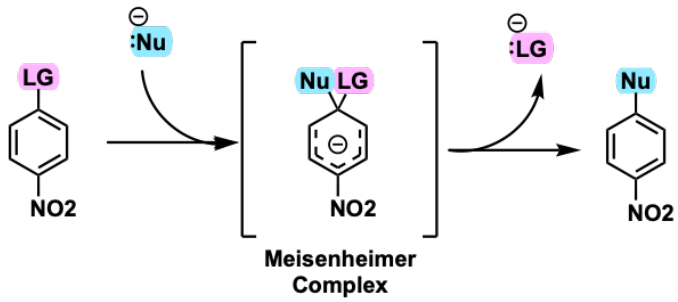

Figure 3.4: A nucleophilic aromatic substitution reaction proceeding through a Meisenheimer Complex (2).

3.3.4 Conversion of Esters into Carboxylic Acids: Hydrolysis

In the presence of an aqueous base or an aqueous acid, esters can be hydrolyzed, yielding a carboxylic acid and an alcohol, see Figure 3.5. When the reaction is catalyzed by an aqueous base, the reaction proceeds through a typical nucleophilic acyl substitution where the hydroxide ion acts as the nucleophile (29).

3.3.5 NBS Bromination: Wohl-Ziegler Reaction

N-Bromo succinimide, also known as NBS, is a versatile chemical reagent commonly utilized in organic chemistry for radical substitution, electrophilic addition, and elec-

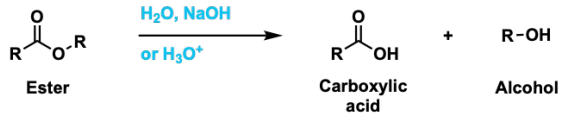

Figure 3.5: Acid or base catalyzed hydrolysis of an ester.

trophilic substitution reactions. NBS is a convenient source of the bromine radical. A Wohl-Ziegler reaction is a chemical reaction where a bromination of a hydrocarbon in an allylic or benzylic position occurs, using NBS and a radical initiator (RI), see Figure 3.6 (30; 31).

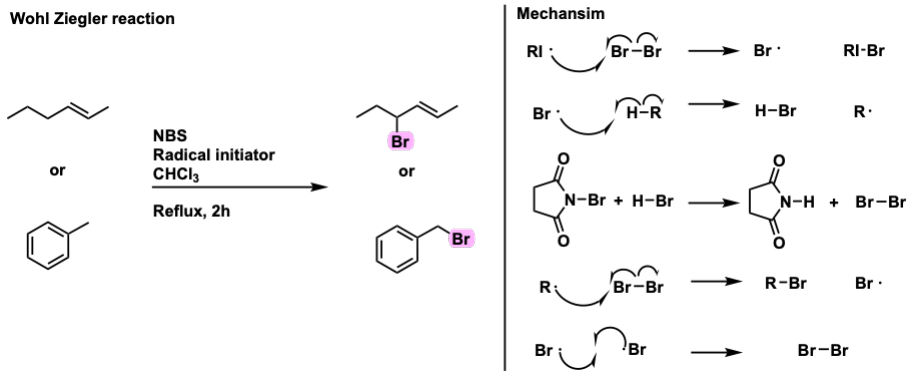

Figure 3.6: Wohl-Ziegler reaction along with the Goldfield proposed mechanism (3).

3.3.6 Silver Mediated Protodecarboxylation of Heteroaromatic Carboxylic Acids

A carboxylic acid can be removed (protodecarboxylated), mediated by a silver salt, when the carboxylic acid sits next to a heteroatom on an aromatic ring. The proposed mechanism for this reaction can be seen in Figure 3.7 (4).

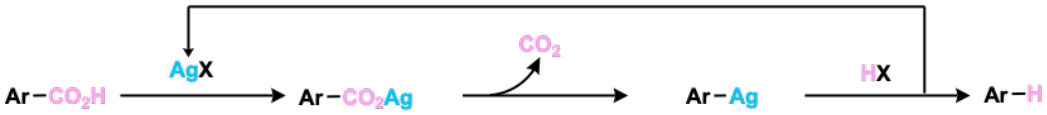

Figure 3.7: Proposed mechanism for silver catalyzed protodecarboxylation of ortho-substituted benzoic acid and carboxylic acids in position next to a heteroatom on an aromatic ring (4).

3.3.7 Halogenation of Imidazole using DIH

The *N,N'*-dihalogenated analogues of 5,5-dimethyl hydantoin, carry two electrophilic equivalents of halogen that can be used as a halogenation source in the presence of a Brønsted Acid. A proposed mechanism for the activation of the *N,N'*-diiodo-5,5-dimethyl hydantoin (DIH) can be viewed in Figure 3.8 (5).

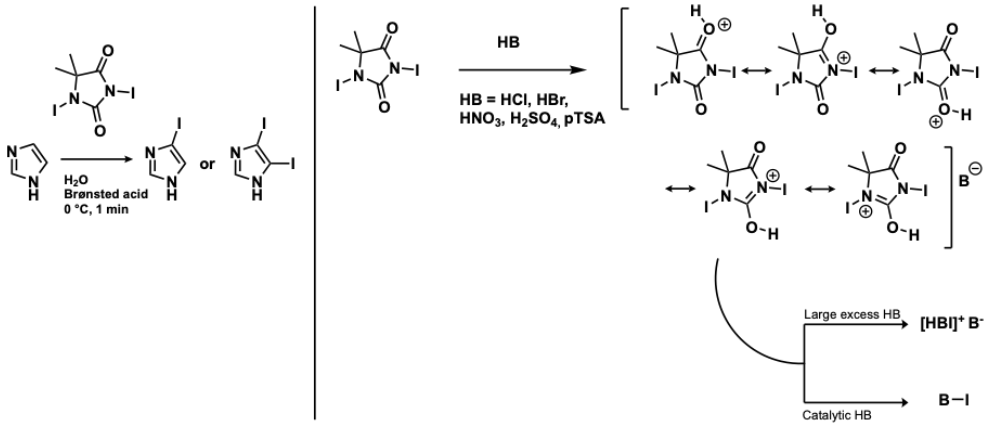

Figure 3.8: Di-and mono-iodation of imidazole using DIH and the proposed mechanism for the activation of DIH (5).

Previous work done by Sandtorv in 2013 has shown that DIH can selectively an quickly lead iodide in the 4 and 5 positions on an imidazole ring in excellent yields when done in the presence of a Brønsted base, see Figure 3.8. (5)

3.3.8 Decarboxylative Halogenation of Heteroaromatic Compounds

Different approaches can be used to perform decarboxylative halogenation of Heteroaromatic compounds. Four examples of this can be seen in Figure 3.9 (6–8). The examples involve using CuI or NIS as a source of halogen with or without palladium acetate as a catalyst under inert conditions or an excess of oxygen. The last example uses a biphasic system with pH control at room temperature and iodine dissolved in the organic phase as a source of halogen (6–8).

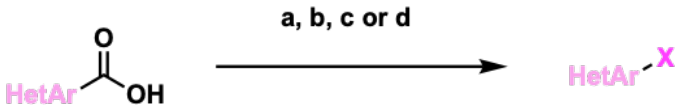

Figure 3.9: Different approaches for decarboxylative Halogenation of Heteroaromatic Compounds.a: 0.02 eqv $Pd(OAc)_2$, 1.05 eqv NIS, DMF, 80°C 3 h, Ar (6), b: 0.1 eqv $Pd(OAc)_2$, 1.2 eqv CuI, DMSO, 160°C 20 h, O_2 (7) c: 1.2 eqv CuI, DMSO, 160°C 30 h, O_2 (7) d: I_2, DCM/Brine, pH = 12, rt, 18h quench $Na_2S_2O_3$ pH = 7(8).

3.4 Analytical Methods and Tools

3.4.1 High Pressure Liquid Chromatography, HPLC

Chromatography is a separation technique where components of a mixture are separated based on their physical properties. Liquid chromatography is when a mobile phase flows through a stationary phase, and the components in the mobile phase are separated based on their affinities to the mobile and stationary phase. High pressure liquid chromatography is when the mobile phase can flow through the stationary phase at high flow rates, generating high pressure, yielding an efficient separation. To quantify and detect when the components elute from the column, a detector is needed. The detector is often a UV/VIS detector, which is the type of detector used in this paper.

3.4.2 Mass Spectrometry, MS

Mass Spectrometry is an analytical method that can measure the mass-to-charge ratio m/z of a compound. This is done by ionizing the analyte with the charge z. Then the analyte is accelerated in an electric field V to gain a speed v. When the analyte with the mass m, charge z and speed v that was gained from the electric field V is sent into a magnetic field B, it will curve in a circle with the radius r. When B, V and r is known, the mass m can be calculated and measured based on equation 3.4, 3.5 and 3.6

$$\frac{1}{2}mv^2 = zV \qquad (3.4) \qquad r = \frac{mv}{zB} \qquad (3.5) \qquad \frac{m}{z} = \frac{B^2r^2}{2V} \qquad (3.6)$$

By filtering based on the radius the detector is measuring at, the m/z ratio can be measured, as the electrical field V and magnetic field B are being kept constant. In Figure 3.10 an illustration of how a mass spectrometer generally looks like can be viewed, with a sample inlet, ion source, mass analyzer, detector, and data system. The illustration is taken directly from (9).

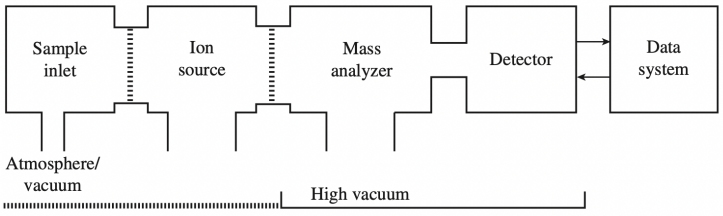

Figure 3.10: Illustration of the compartments of a MS-instrument. Illustration taken directly from (9).

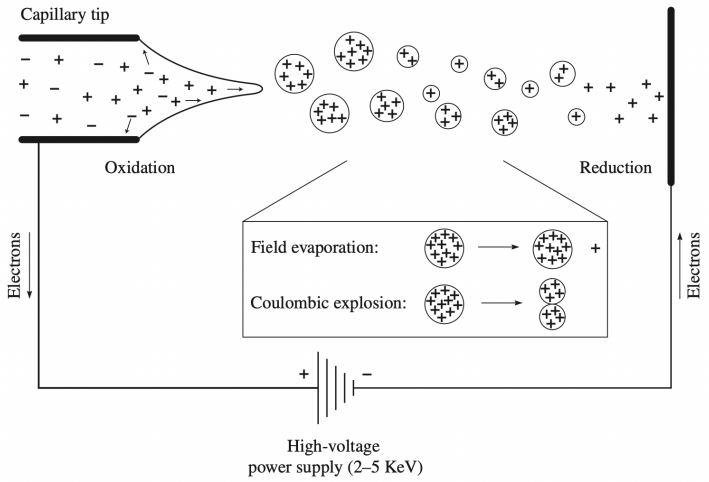

Figure 3.11: Illustration of the ESI process showing evaporation and the colombic explosion after reaching the Raygleigh limit. Illustration is borrowed directly from (10) which reprinted this from (11).

There are different ways to ionize the analyte. In this thesis, Electrospray Ionization, ESI, and Electron Ionization, EI, have been used. ESI is a soft ionization method where fragmentation of the molecular ion can be avoided. A solution containing the analyte is sprayed out of the end of a fine capillary and into a heated chamber at atmospheric pressure. The capillary that the solution now has passed through has a high voltage potential across its surface, resulting in small, charged droplets of the solution being thrown into an ionization chamber. A drying gas in the ionization chamber quickly evaporates the solvent and the charge density of each droplet increases until they reach the Rayleigh limit and break into smaller droplets. This process continues until there only are solvent-free sample ions left in the gas phase that are accelerated into the mass analyzer (10). An illustration of the ESI process can be viewed in Figure 3.11. The illustration has been taken directly from (10). ESI is very useful as it presents the molecular ion without fragmentation, giving a definite result. In positive ESI, the molecular ion can appear as $M+1, M+23, M+1+M$ and $M+23+M$. 1 is hte mass of a proton, while 23 is the mass of sodium.

EI is a "hard" ionization method where a beam of high-energy electrons is emitted from a filament that is heated to several thousand degrees Celcius. The beam strikes the stream of molecules that has been introduced from the sample inlet system. This result in electrons being stripped from the molecule, creating a cation. Newly created ions are then directed towards a series of accelerating plates through a repeller plate. A large potential difference applied across the accelerating plates produces a beam of rapidly traveling positive ions. Lastly, before the ions are sent into the mass analyzer, they are directed into a uniform beam by a focusing slit (12). An illustration of the electron

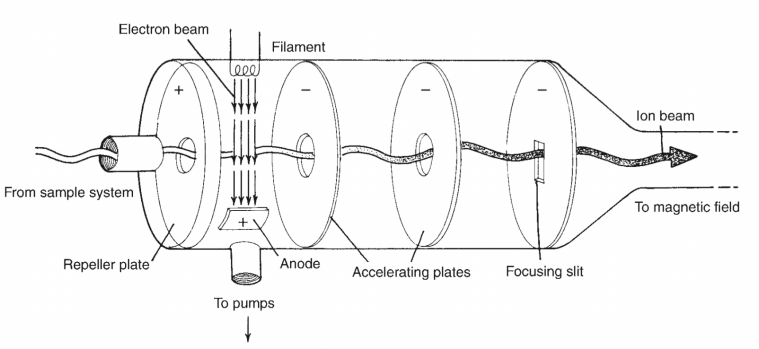

Figure 3.12: Illustration of the electron ionization chamber. Illustration is taken directly from (12).

ionization chamber can be seen in Figure 3.12, and the illustration is taken directly from (12). EI as ionization method leads to fragmentation patterns that can be typical for certain functional groups, something that is very useful in structural elucidation.

3.4.3 Liquid Chromatography - Mass Spectrometry, LC-MS

Liquid Chromatography - Mass Spectrometry, LC-MS, is a technique for separating compounds in a sample and analyzing the mass of the different compounds in the sample individually. The compounds in the sample are first separated using liquid chromatography, and then the compounds from the sample are directly introduced to the MS-instrument. By using this method one can get information about the amount of compounds present in the sample and their belonging masses, something that is very useful when doing experimental synthesis. Often it is possible to skip the LC compartment and perform direct injcetion, DI, of the sample.

3.4.4 Gas Chromatography - Mass Spectrometry, GC-MS

Gas Chromatography - Mass Spectrometry, GC-MS, is a technique for separating several compounds in a sample and analyzing the mass of the different compounds in the sample individually. In GC-MS, gas chromatography is the separation technique. This technique separates based on the boiling points of the compounds. The higher the boiling point of the compound, the longer the elution time for the compound will be. By using this method one can get information about the amount of compounds present in the sample and their belonging masses, something that is very useful when doing experimental synthesis.

3.4.5 Nuclear Magnetic Resonance, NMR

Nuclear magnetic resonance (NMR) spectroscopy is a technique that allows study of the behavior of atomic nuclei in a magnetic field and is one of the most useful tools for

analysis and structural elucidation of chemical species. When a sample is placed in a strong magnetic field and exposed to a specific frequency of electromagnetic radiation (radio waves), the nuclei in the sample will absorb energy from the radiation and become excited to a higher energy state. The amount of energy absorbed depends on the magnetic properties of the nuclei and their chemical environment. As the excited nuclei return to their original state, they emit radio waves that can be detected and analyzed to give information about the species chemical composition and molecular structure (32). Overall, NMR spectroscopy is a powerful tool to study the structure and properties of molecules.

In this thesis, the 1D experiments ^{1}H-NMR and ^{13}C-NMR are used, as well as 2D experiments such as ^{1}H-^{1}H COSY (correlation spectroscopy), ^{1}H-^{1}H NOESY (nuclear Overhauser effect spectroscopy), ^{1}H-^{13}C HMBC (heteronuclear multiple-bond correlation spectroscopy) and ^{1}H-^{13}C HSQC (Heteronuclear single-quantum correlation spectroscopy). COSY give information about which protons that are three bonds apart. NOESY give information about which protons that are close to each other in space. HMBC give information of heteroatoms two to four bonds apart. HSQC give information about which heteroatoms that are bonded to each other.

3.5 Optimization

3.5.1 Statistical Design of Experiments

Statistical design of experiments refers to the process of planning an experiment in a way that appropriate data that can be analyzed through statistical methods will be collected, resulting in valid and objective conclusions (33).

3.5.2 Factorial Design

As most experiments involve two factors or more, it is important to have a design that in a way can account for this. An efficient candidate for this is factorial design. Factorial design is when all possible levels (for example high and low level) of each factor is investigated. The effect of a factor, often referred to as a main effect, is the change in response, for example yield or purity, produced by a change in the level of a factor (34). A factorial design consists of n^x experiments, where n is the number of levels each factor is set to in the design, and x is the number of factors. For a 2^2 factorial design, 4 experiments are performed as in Table 3.1. It is important to randomize the order the experiments are performed in to avoid any bias.

Table 3.1: The 2^2 factorial design matrix.

Factor A	Factor B	Interaction between A and B	Mean	Measured response
-1	-1	1	1	Fill in
1	-1	-1	1	Fill in
-1	1	-1	1	Fill in
1	1	1	1	Fill in

To measure the effect each factor has on the response, each level for each factor is multiplied with the measured response for the experiment. These are summarized and divided by the number of experiments, which can be seen in Equation 3.7, where E_x is the effect of the factor x and n is the number of experiments (35).

$$E_x = \frac{\sum_i^n response * level}{n} \tag{3.7}$$

The effect of each factor can be put in a linear regression equation that to some extent can explain the response of the process based on the factors. The effect for each factor in the design is calculated, including the mean term and the interaction terms. These are all put together in an equation (36). For a $\mathbf{2^2}$ factorial design, it will look like Equation 3.8, where Y is the predicted response, $Mean$ is the mean effect, E_A is the effect of factor A, E_B is the effect of factor B and E_{AB} is the interaction effect of A and B and ε is the residual.

$$Y = Mean + E_A + E_B + E_{AB} + \varepsilon \tag{3.8}$$

It is important to remember that the results from the factorial design are only assumptions, and that the $\mathbf{2^2}$ factorial design only accounts for linear relationships. Reality is often more complex and sometimes more advanced designs need to be used to make a better fit. To account for polynomial relationships, designs such as Central Composite Design or optimization techniques such as the simplex method can be used.

3.5.3 The Simplex Method

A simplex is a geometric figure, more specifically a $(k+1)$-cornered figure where k is the number of variables in a k-dimensional space that is going to be investigated (36). In Figure 3.13 an optimization strategy using the simplex method when optimizing based on two variables can be seen. The simplex method is a step wise strategy for optimization, meaning that each experiment is done one by one, except from the $(k+1)$-starting experiments that generates the starting simplex. The response measured in each corner of the starting simplex decides in which direction the next experiment

should be done, and it is based on moving away from worst response in the factor space. There are three rules for optimizing with when using the simplex method:

Rule 1 Flip the simplex away from the corner with the coordinates that has the worst response. Do a new experiment where the factors are set to the coordinates of the new corner of simplex. The response is then measured in the new corner, and a new evaluation of the responses of each corner is done to decide where the new simplex should go. Continue doing this action until there no longer is improvement of the response (36).

Rule 2 If the response of the new corner does not show any improvement, flip the simplex away from the second worst corner from the previous simplex (36).

Rule 3 If the flipping of the simplex indicates that the new experiment should be done *outside* the experimental space, the new experiment's coordinates will be assigned an impossible low value, and the simplex should be flipped away from the second worst corner from the previous simplex (36).

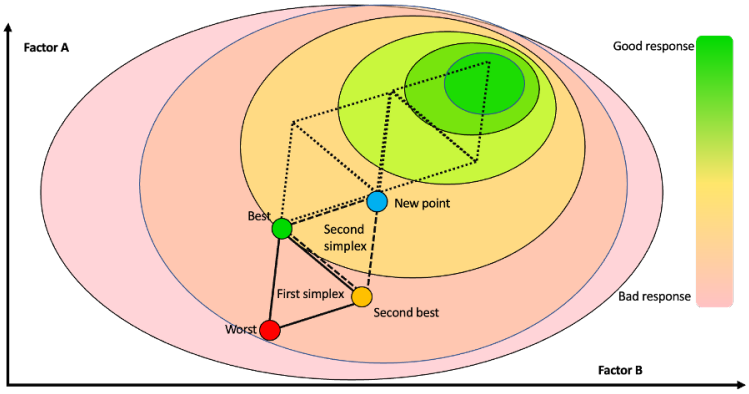

Figure 3.13: Illustration of how to use the simplex method when optimizing based on two factors.

After performing step wise experiments based on these three rules, one should ideally get a result where the simplex lastly circles around the optimum. A disadvantage using the simplex method, is that it does not consider that there could be more than one optimum.

3.5.4 Response Surface Methodology

Response Surface Methodology (RSM) explores the relationship between one or more factors and a response, introduced by George E. P. Box and K. B. Wilson in 1951. By performing factorial or reduced factorial design, one can achieve a first degree polynomial approximation that to some extent explains the relationship between the factors and the response. The factorial design will show which factors that is most important

for the response. When the most important factors are known, a more in-depth design or study of the response surface can be investigated through the use of a central composite design or through simplex optimization. Central composite design can present a second degree polynomial approximation that can be used to plot the response surface and further be used to optimize the response of the process. These are all just approximations, however, for practical purposes they are great for optimization.

Chapter 4

Results and Discussion

4.1 Precursor Synthesis Route 1

4.1.1 Planning of Synthesis Route 1

Using Google Scholar, a synthesis route for the production of Flumazenil was found (37). Replacing the starting material of step 1, ethyl 5-methyl-1H-imidazole-4-carboxylate, with 4-iodo-5-methyl-1H-imidazole **2**, the synthesis was pursued in the same way as in the work published by Donohue and Dannals in 2009 (37). The complete planned synthesis route can be viewed in Figure 4.1.

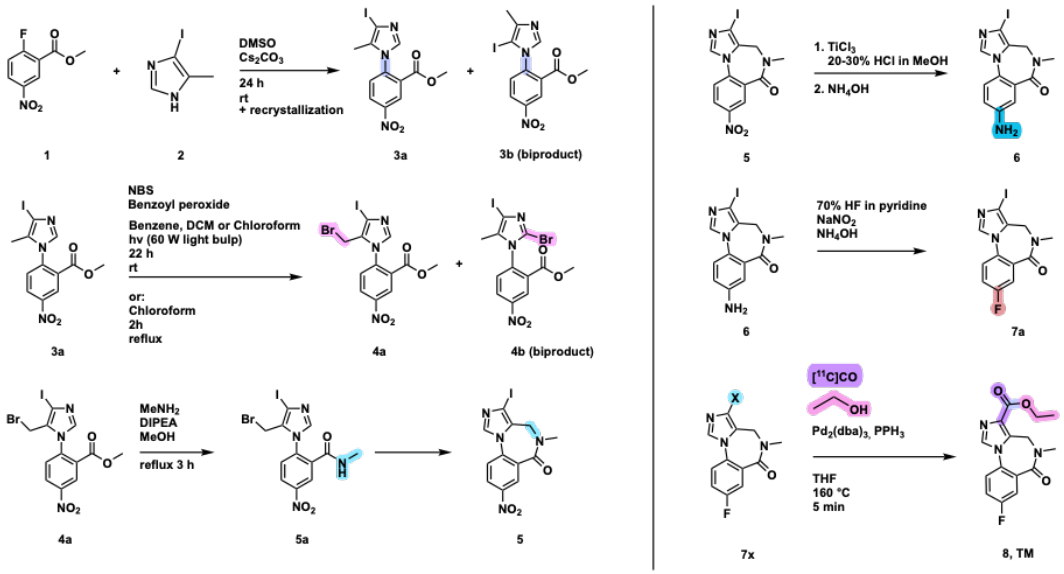

Figure 4.1: Synthesis route 1

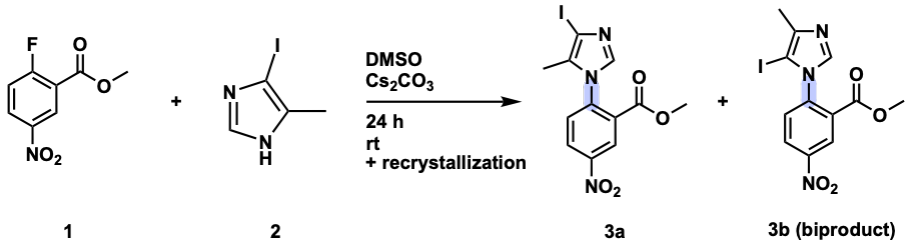

*Figure 4.2: Step 1: Synthesis of methyl 2-(4-iodo-5-methyl-1H-imidazol-1-yl)-5-nitrobenzoate **3a**.*

4.1.2 Step 1 - Nucleophilic Aromatic Subistitution through Meisenheimer Complex

The synthesis of **3a**, see Figure 4.2 and Table 4.1, was done twice with an average of 45 % isolated yield. Two species appeared in the lane upon TLC analysis of the crude crystals in pure ethyl acetate. By comparing this lane to the spots in the lanes for the starting materials **1** and **2**, it was confirmed that the crude did not contain any starting material, see Figure 4.3, pointing towards full conversion of the reactants. In Figure 4.5 the ^{1}H-NMR spectrum of the isolated product can be viewed, while in Figure 4.6 the ^{13}C-NMR spectrum can be viewed. The collected data from the two spectra can be viewed in Table 4.2 and 4.3, respectively. In Table 4.3 there is also information from 2D NMR experiments, ^{1}H-^{13}C HSQC and ^{1}H-^{13}C HMBC. The 2D experiments can be viewed in can be viewed in Appendix 7. The analysis indicates that **3a** was produced, and this is confirmed with a ^{1}H-^{1}H NOESY experiment (see Figure 7.6), showing that proton 3 can see proton number 6. If **3b** was produced, proton 3 would most likely not be able to see proton 6. The fact that **3a** is the isomer produced makes sense, since iodide occupies more space compared to a methyl group, and one can therefore argue that the molecule that has the iodide furthest away from the ester group of **2** will be the most stable and therefore most likely to be produced.

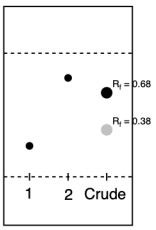

Figure 4.3: TLC analysis in pure ethyl acetate of the starting materials 1, 2 and the crude.

Exp	Crude yield [%]	Isolated yield [%]
1	59	36
2	75	53
mean	67	45

*Table 4.1: Yields for the synthesis of **3a**.*

*Table 4.2: Tabulated data from the ^{1}H-NMR spectrum of **3a***

Chemical environment	Chemical shift (ppm)	Signal type (multiplicity)	Coupling constant (Hz)	Integration value
1	8.65, 8.65	d	0	1
2	8.51,8.51, 8.52,8.53	dd	7.5, 5	1
3	7.78,7.80	d	10	1
4	7.74	s	-	1
5	3.68	s	-	3
6	1.89	s	-	3
			Total	10

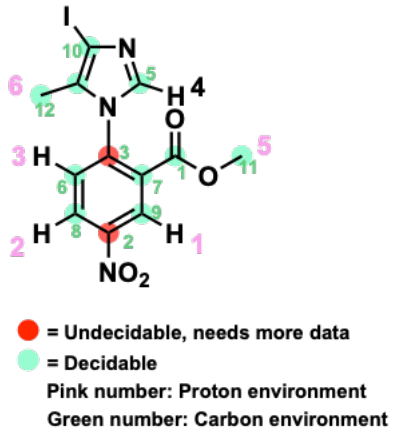

*Figure 4.4: Assignment of chemical environments of **3a***

Name	Shift	H's	HSQC	HMBC
1	163.26	Even	-	1,3,5
2	147.99	Even	-	1,2,3
3	140.49	Even	-	1,2,3
4	137.88	Odd	4	
5	131.58	Even	-	4,6
6	130.38	Odd	3	6
7	130.31	Even	-	1
8	127.63	Odd	2	-
9	127.00	Odd	1	2,3
10	84.33	Even	-	4,6
11	53.42	Odd	5	-
12	10.62	Odd	6	-

*Table 4.3: Tabulated data from the ^{13}C-NMR spectrum of **3a** as well ass information from the ^{1}H-^{13}C HSQC and ^{1}H-^{13}C HMBC 2D experiments.*

In figure 7.7, 7.8 and 7.9 in Appendix 7 the TIC graph and the belonging mass spectra from a GC-MS analysis of crude **3a** can be viewed. The second peak in the TIC graph is very large and has in its mass spectrum a very strong intensity peak of the molecular ion, $m/z = 387$, and also a peak of $M - M_{iodide}$. The first peak in the TIC graph is much smaller and show the same two peaks in its mass spectrum as for

the second peak. However, the intensity of $M - M_{iodide}$ is much stronger than for the second peak in the TIC graph, and the molecular ion peak has a low intensity. These results indicate two isomers with the same mass being present in the crude, most likely **3a** and **3b**, where **3a** belongs to the largest peak in the TIC graph.

To summarize, **3a** was successfully produced and isolated from its isomer **3b** in an average yield of 45 %.

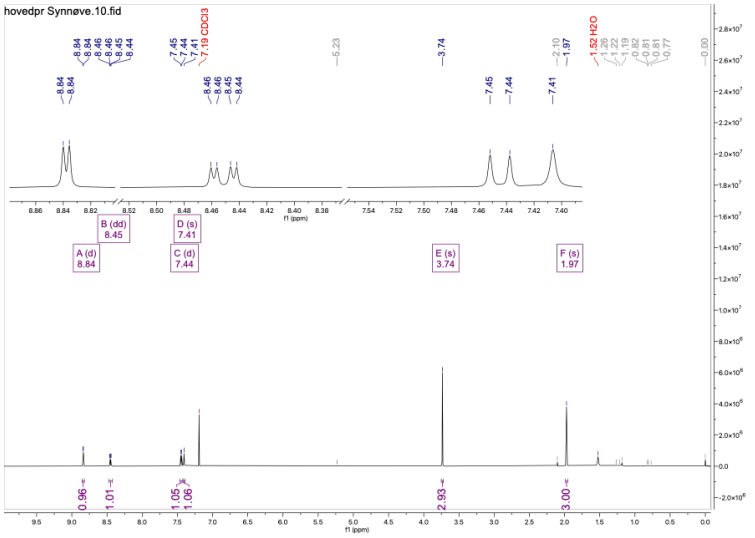

*Figure 4.5: ^{1}H-NMR spectrum of **3a**.*

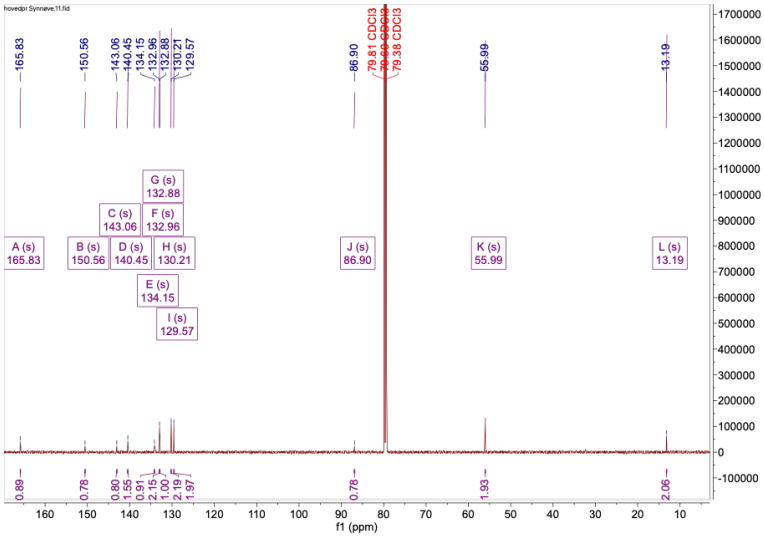

*Figure 4.6: ^{13}C-NMR spectrum of **3a**.*

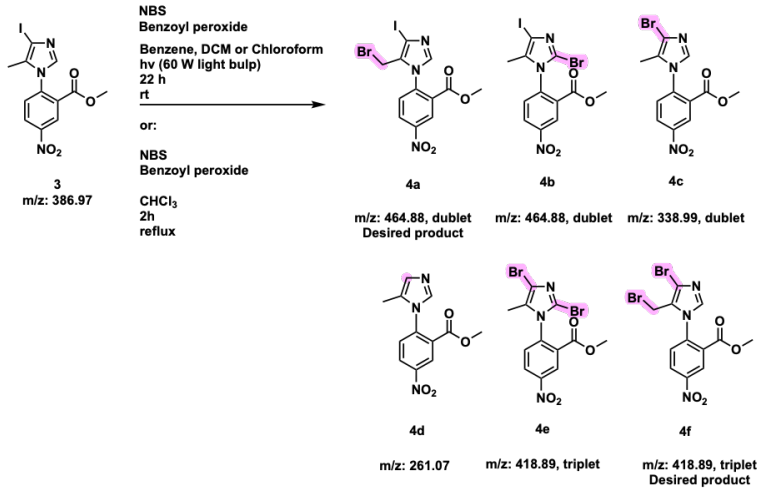

*Figure 4.7: Step 2: The attempted synthesis of **4a** methyl 2-(5-(bromomethyl)-4-iodo-1H-imidazol-1-yl)-5-nitrobenzoate or **4f** methyl 2-(4-bromo-5-(bromomethyl)-1H-imidazol-1-yl)-5-nitrobenzoate and suggested biproducts*

4.1.3 Step 2 - Attempt of a Wohl-Ziegler Reaction

Step 2, see figure 4.7, was unsuccessfully conducted 8 times using different types of solvents and energy sources, see table 4.4.

The first two experiments of step 2 were continued straight forward to step 3 (see Figure 4.1), like it was done by Donohue and Dannals (37). However, this was unsuccessful, and the desired products in step 2 and 3 were not found using LC-MS analysis. Step 2 was therefore pursued using different types of solvents as described in Table 4.4 with a 60 W light bulb for 22 hours. These experiments were unsuccessful according to LC-MS analysis, therefore reflux was used as an energy source for the reaction for the following three experiments which is also noted in Table 4.4. In Table 4.5 one can see an overview of LC-MS analysis of experiment 3 to 7 of step 2. The species in the crude of experiment 7 was separated using column chromatography, which is also stated in the table (exp no 7.1, 7.2 and 7.3). The crude of 8 was separated using semi-preparative HPLC, however only ^{1}H-NMR was used to analyze the fractions, therefore experiment 8 is not noted in the table. The table has an overview of the mass of compounds that theoretically can be made in the reaction as one can see in Figure 4.7, and it is noted if any of the molecular ions they potentially can generate was found using LC-MS analysis. LC-MS ESI analysis was the preferred method as it shows the molecular ion without fragmentation. In the table one can see that the experiments 3 to 5 utilizing a 60W light bulb as an energy source had very low to no amounts of the target compounds **4a** and **4b**. The experiments number 6 to 8 had very strong MS signals indicating the presence of **4a** and/or **4b** as well as **4e** and/or **4f**. Fraction 2 of experiment 7 indicates that

an iodide-bromide exchange occurred as the mass of **4c** was present. Fraction 2 of experiment 7 also had a mass peak of the starting material **3a**, indicating towards not full conversion. Experiment 6 also had a low intensity mass peak of the starting material. It is clear from this analysis that reflux is the preferred method for activating the radical bromination that happens in the reaction. LC-MS analysis do not give sufficient information for structural elucidation, and the NMR analysis in the following section was done in order to get sufficient information.

*Table 4.4: Data from the eight different experiments of step 2. *SFRC: Solvent Free Reaction Conditions. **No molecular mass of interest found in LC-MS, therefore crude was not weighed. a: 60 W light bulb for 22 hours, b: Reflux for 2 hours.*

Entry	Crude 3a, weight [g], amount [mmol]	NBS, weight [g], amount [mmol]	Benzoyl Peroxide, weight [g], amount [mmol]	Type of solvent, ammount [mL]	Energy source, reaction time [h]	Weight of crude [g]	Weight of isolated compound[g], if isolated
1	0.208 0.537	0.098 0.551	0.038 0.157	Toluene 21	a	0.170	
2	0.876 2.26	0.626 3.51	0.060 0.248	Toluene 80	a	1.08	
3	0.218 0.563	0.200 1.12	0.040 0.165	SFRC*, then DCM 10	a	- - **	
4	0.139 0.359	0.144 0.809	0.040 0.165	CHCl3 10	a	- -**	
5	0.117 0.302	0.120 0.674	0.08 0.330	Benzene 10	a	- -**	
6	0.097 0.25	0.108 0.607	0.05 0.206	CHCl3 10	b	0.129	
7	0.723 1.870	0.488 2.74	0.022 0.091	CHCl3 10	b	0.916	0.279
8	0.116 0.300	0.054 0.303	0.022 0.091	CHCl3 10	b	0.163	

*Table 4.5: LC-MS analysis of experiment 3 to 8 of step 2 of synthesis route 1. The table indicates the compounds in Figure 4.7 and their belonging possible ESI + ions. *Not sure if a triplet or a merge of two peaks **Two different peaks on LC indicating two different species even though very similar mass, ***Low intensity*

Compound	4a and 4b	4e and 4f	4c	4d	3a
Exp no					
3	466 *	418 *			
4					
5					
6	464*	419.9, 420**			388***
7.1	465.9, 488, 954.8	419.9			
7.2			340, 362		388, 410
7.3			362.0*		

NMR analyses of the fractions of experiment 7, and the different fractions of experiment 8 was conducted for structural elucidation.

In Figure 4.10 and Figure 4.11 the ^{1}H-NMR spectrum and the ^{13}C-NMR spectrum for fraction 1 of experiment 7 can be viewed, respectively. In Table 4.6 the data from the ^{1}H-NMR analysis can be viewed along with information from a ^{1}H- ^{1}H-COSY 2D NMR experiment. In Table 4.7 the data from the ^{13}C-NMR analysis along with information from ^{1}H- ^{13}C-HMBC and ^{1}H- ^{13}C-HSQC 2D NMR experiments can be viewed. The 2D NMR experiments can be viewed in appendix 8. The NMR analyses indicates that **4b** and **4e**, the undesired products were produced. There is no indication of **4a** and **4f** being produced. This is because the ^{1}H-NMR spectrum shows 3 aromatic signals with one proton each and two CH_3 proton environments. If **4a** or **4f** had been produced, it should be 4 aromatic signals with one proton each, one CH_3 environment and one CH_2 environment. There is an excess carbon peak, indicating that the fraction is a merge of signals from **4b** and **4e**, see Figure 4.8. This is also why the aromatic signals in the ^{1}H-NMR are not symmetrical and the remaining CH_3 peaks are are unsymmetrical doublets and multiplets instead of singlets as one can see in Figure 4.10. This is also confirmed in the LC-MS analysis where both of the masses of **4b** and **4e** are present, see Figure 4.9.

The semi-preparative HPLC of experiment 8 was run with the intention to find out if the desired products **4a** or **4f** were produced and could be isolated from **4b** or **3e**. There were 5 collected fractions that were of interest from the semi-preparative HPLC. ^{1}H-NMR spectra of fractions can be viewed in appendix 8. Fraction 1 (Figure 8.7) and 3 (Figure 8.11) of interest in experiment 8 could indicate the desired product being

formed, as they have 4 single aromatic proton signals, one CH_3 group and one CH_2 group. However, this would result in a yield of 5 % for fraction 1 and 4 % for fraction 3, and it was decided that this reaction should not be investigated any further.

To summarize, the synthesis was unsuccessful only producing the undesired bi products **4b**, **4e** or **4c** and possibly 1-5 % of the desired products **4a** and **4f**. It was decided not to go any further with synthesis route 2.

*Table 4.6: Tabulated ^{1}H-NMR data of **4b/4e***

Name	Shift	H's	Class	J's	COSY
A	8.71	1	dd	2.69, 5.33	
B	8.60	1	td	2.70, 8.43, 8.50	C
C	7.90	1	m		B
D	3.71	3	d	7.77	
E	1.87	3	d	9.12	

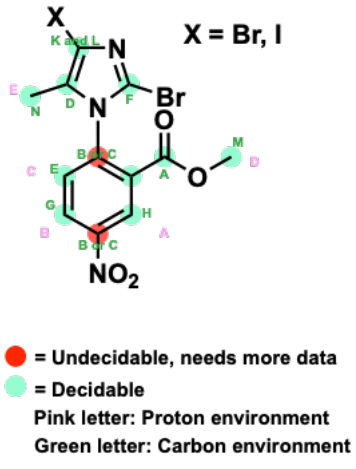

*Figure 4.8: Assignment of chemical environments of **4b/4e***

Name	Shift	H's	HSQC	HMBC
A (s)	163.03	-1		A, C, D
B (s)	148.66	-1		A,B,C,
C (d)	139.80	-1		A,B,C
D (s)	135.33	-1		E
E (s)	132.86	2	C	
F (s)	130.15	-1		C, E
G (s)	129.09	3	B	A
H (s)	126.72	3	A	B
K (s)	113.26	0		E
L (s)	83.86	1		E
M (s)	53.76	-3	D	
N (s)	11.89	0	E	E

*Table 4.7: Tabulated data from the ^{13}C-NMR spectrum of **4b/4e** as well ass information from the ^{1}H-^{13}C HSQC and ^{1}H-^{13}C HMBC 2D experiments.*

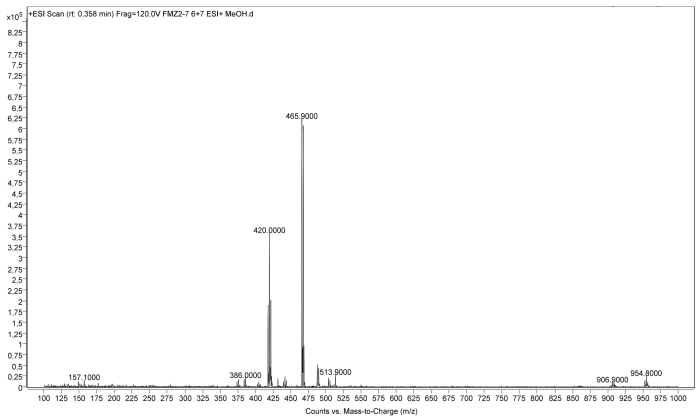

*Figure 4.9: Positive ESI MS spectrum of **4b/4e**.*

*Figure 4.10: ^{1}H-NMR spectrum of **4b/4e**.*

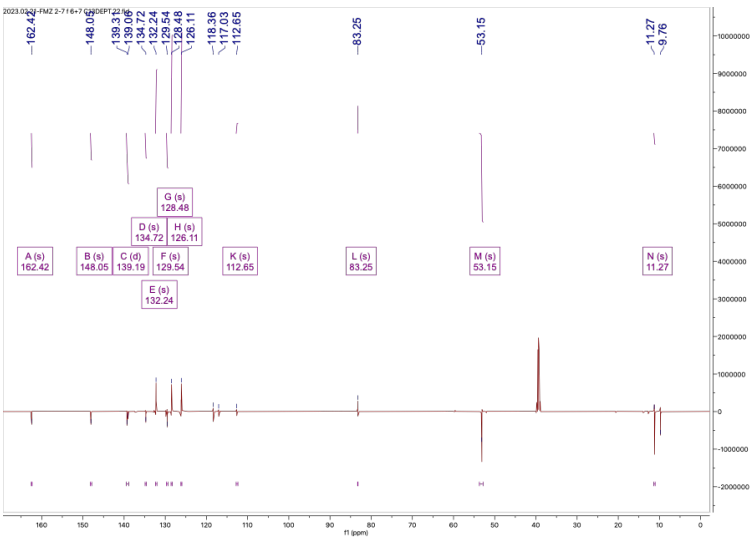

*Figure 4.11: ^{13}C-NMR spectrum of **4b/4e**.*

4.2 Precursor Synthesis Route 2

4.2.1 Planning of Synthesis Route 2

As synthesis route 1 was unsuccessful, a new synthesis route was planned, this time with Flumazenil as starting material. Synthesis route 2 was planned using SciFinder^n. Preparation 31 in a patent done by Jones et al in 2008 gives an example of an ester group on an imidazole ring being converted into an iodide group through two steps, and were the inspiration for synthesis route 2, see Figure 4.12 (8).

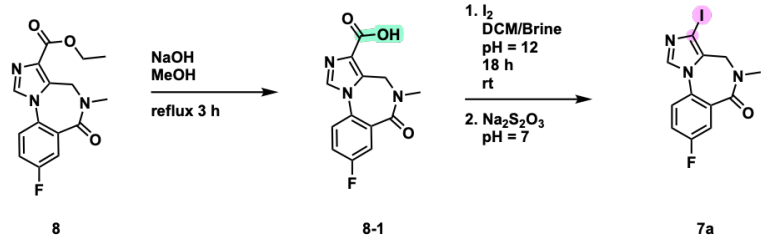

Figure 4.12: Planned synthesis route 2

4.2.2 Step 1 - Hydrolysis of Flumazenil

Hydrolysis of the ester group in Flumazenil **8** was done three times with full conversion, see Figure 4.13.

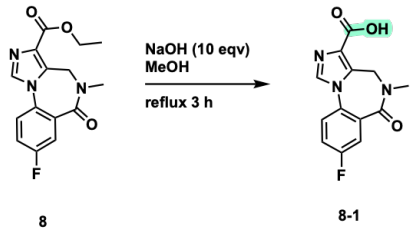

*Figure 4.13: Step 1: Hydrolysis of the ester group in Flumazenil, generating Flumazenil Acid, **8-1***

LC-MS analysis show the molecular ion with a mass of 276 (M^+), 298 (M + Na^+) and 573 (M^+ + Na^+ + M^+), which is expected with positive ESI. The mass spectrum can be seen in Figure 9.3 in Appendix 9. There are no signs of molecular ions originating from Flumazenil, however there are some other peaks that points towards bi products. None of the potential products are not visible on TLC analysis in 10:90 MeOH:DCM. The crude was never properly dried due to some technical issues with the rotavapor, therefore yield for this reaction is not presented, as the weight indicated a yield of 300 %. In Figure 4.14 the ^{1}H-NMR spectrum of the crude can be seen, along side with the tabulated NMR data in Table 4.8 . There are some other, quite pure, low intensity peaks, which also indicates formation of a bi-product, see Figure 9.2 in the Appendix 9. There are no peaks indicating the presence of Flumazenil, also pointing towards a full conversion.

*Table 4.8: Tabulated ^{1}H-NMR data for Flumazenil Acid **8-1**.*

Name	Shift	H's	Class	J
D	7,51	1	td	2.98, 7.79, 8.96
A	8,07	1	s	-
B	7,67	1	m	3.12, 6.01
C	7,65	1	m	-
G	3,20	3	s	
E	5,16	1	d	15.83
F	4,47	1	d	15.83

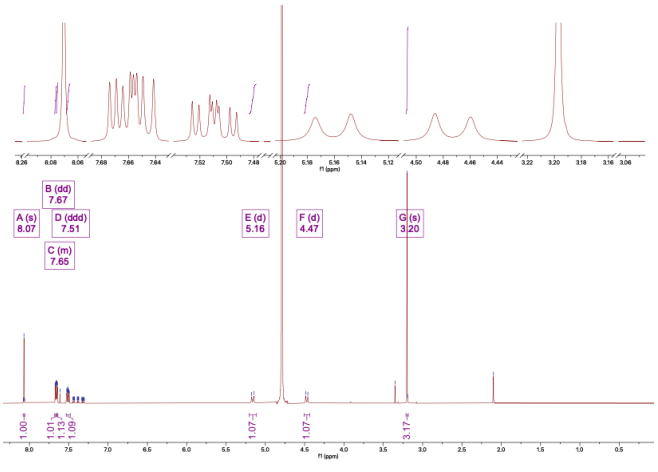

*Figure 4.14: Step 1: ^{1}H-NMR spectrum sof Flumazenil Acid **8-1**.*

4.2.3 Step 2-1 - Decarboxylative Iodation of Flumazenil Acid

The reaction in Figure 4.15 was attempted three times with no conversion. The synthesis was done twice in the biphasic DCM/Brine system at pH 12. The reason why this did not work could have something to do with the solubility of the reactants and the product in the two phases being different from the species in the patent where the procedure was taken from. Therefore, the reaction was also pursued in a one phase methanol solution at pH 12 without any yield. Methanol was chosen as solvent because I_2 is soluble in it, and because it was known that Flumazenil Acid was soluble in methanol from step 1.

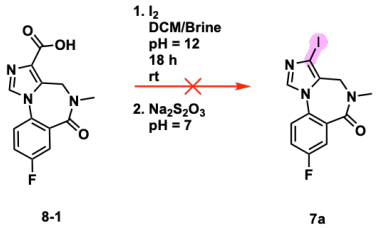

*Figure 4.15: Step 2-1: Attempt of decarboxylative iodation of Flumazenil Acid **8-1**.*

4.2.4 Step 2-2 - Protodecarboxylation of Flumazenil Acid, Oil Bath Assisted Heating

As step 2-1 was unsuccessful, other ways towards the target molecule were investigated. Inspired by the article by Lu et al 2009, protodecarboxylation of Flumazenil Acid mediated by Silver Carbonate in DMSO and acetic acid at 120 °C was pursued, see Figure 4.16 (4). This was done at a very low scale (0.031 g, 0.113 mmol of starting material) and only qualitative measurements were obtained. LC-MS analysis of the crude indicated towards not full conversion as notable amounts of the starting material were still present (m/z = 276), however sufficient amounts of the desired molecule (m/z = 232) **9** were obtained. The ESI MS spectrum can be viewed in Figure 10.1 in Appendix 10

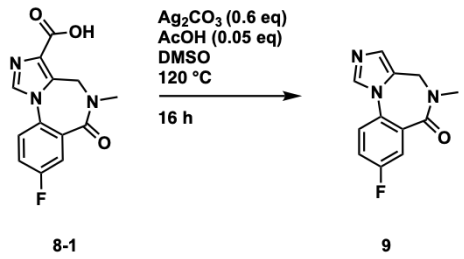

*Figure 4.16: Step 2-2: Ag_2CO_3 catalyzed Protodecarboxylation of Flumazenil Acid **8-1** in DMSO.*

4.2.5 Step 2-3 - Protodecarboxylation of Flumazenil Acid, Microwave Assisted Heating

As the protodecarboxylation of Flumazenil Acid **8-1** had shown to be successful in step 2-2, it was decided to investigate the reaction further using different silver salts and water as solvent. As the results described by Lu et al 2009 worked best using acetic acid as a co-catalyst for the silver salts, drops of acetic acid were also used (4). In the article by Lu et al 2009 it is not quite clear what re-generates the silver catalyst, therefore it was decided to use equivalent amounts of silver salt to achieve better conversion. This was done in hopes of finding a re-generator for the catalyst later. The reactions were performed in a microwave reactor, providing more efficient, stable and even heating of the reaction mixture than an oil bath.

To summarize step 2-3: Silver mediated protodecarboxylation of the carboxyilc group on the imidazole ring of Flumazenil Acid **8-1** was performed using three different silver salts in water, see Figure 4.17. All reactions had a full conversion and around 74 % isolated yield, see Table 4.9. The crude containing silver was vacuum filtrated and the isolated product was qualitatively analyzed using GC-MS, see Figure 10.3, 10.4

and 10.2 in Appendix 10. These results show that different silver salts can be used for silver-catalyzed protodecarboxylation of heteroaromatic carboxylic acids in water at 120 °C and microwaves as a source of heating.

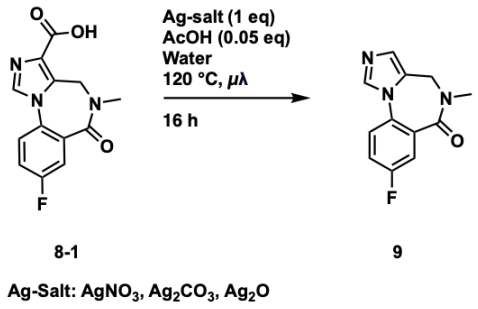

*Figure 4.17: Step 2-2: Ag_2CO_3 catalyzed protodecarboxylation of Flumazenil Acid **8-1** in water.*

Entry	AgX	Yield [%]
1	Ag_2CO_3	76
2	$AgNO_3$	71
3	Ag_2O	75
	Mean	74

*Table 4.9: Yields for silver catalyzed protodecarboxylation of Flumazenil Acid **8-1**.*

4.2.6 Step 3-1 - Attempt of Halogenation of Protodecarboxylated Flumazenil using DIH in Mild Conditions

Mono-iodation and di-iodation of imidazole using N,N'-Dichloro-5,5-dimethyl hydantoin, DIH, have been published by Sandtorv in 2013 (5). For the mono-iodation "mild" conditions were used with a 0.24 equivalent of DIH, while for the di-iodation "harsh" conditions with 1.5 equivalent of DIH were performed. Inspired by this, the mild conditions were pursued in the attempt to halogenate decarboxylated Flumazenil **9** with no yield, see Figure 4.18

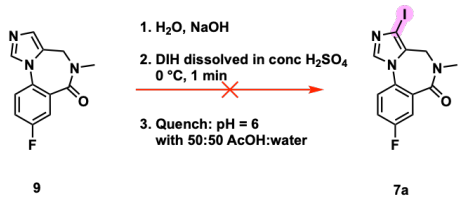

*Figure 4.18: Step 3-1: Iodation of **9** with DIH in mild condtitions.*

4.2.7 Step 3-2 - Attempt of Halogenation of Protodecarboxylated Flumazenil using DIH in Harsh Conditions

Even though the harsh conditions should yield di-iodated imidazole, the conditions only iodate in the 4 and 5 position on the imidazole ring, not the 3 position (5). As **9** already have something attached to the 4 position, the harsh conditions were pursued,

see Figure 4.19. Direct injection-MS analysis only indicated the starting material from step 2-3, the synthesis was therefore concluded unsuccessful.

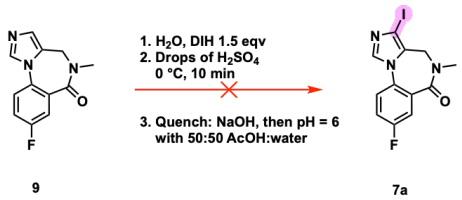

*Figure 4.19: Step 3-2: Iodation of **9** with DIH in harsh conditions.*

4.2.8 Step 2-4: Decarboxylative Halogenation of Flumazenil Acid

Three different reaction conditions were pursued in order to perform decarboxylative halogenation of Flumazenil acid, see Figure 4.20, all being unsuccsessfull. LC-MS analysis show that a) had a lot of the starting material, flumazenil acid, present (m/z = 276). The analyisis also showed a very small amount of **9** (m/z = 232), indicating small amounts of decarboxylation taking place. LC-MS analysis of b) and c) did not have any indication of the starting material, pointing towards full conversion. However, the mass of the desired molecule was not found (m/z = 358), and a), b) and c) were concluded unsuccessful.

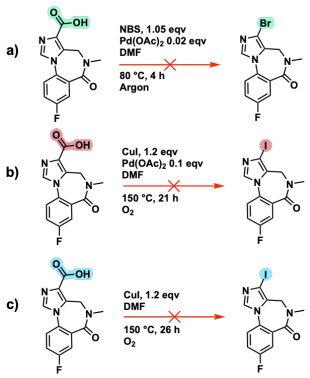

*Figure 4.20: Different approaches for performing decarboxylative halogenation of Flumazenil acid **8-1**.*

4.2.9 Step 2-5: Decarboxylative Halogenation of Flumazenil Acid using Silver Nitrate and a Source of Halogen Radical

As the experiments in step 2-4 was unsuccessful, other methods were investigated. As the protodecarboxylation using silver salts in water was successful, it was hypothesized that if Flumazenil Acid **8-1** is decarboxylated through a radical mechanism, then the presence of a radical halogen in the reaction mixture could potentially lead to a selective halogenation, yielding the desired product, **7x**, See Figure 4.21. The reaction should theoretically lead to six radicals that can produce either the protodecarboxylated product, R-H, the halogenated decarboxylated product, R-X, and some other undesired bi products.

To test this hyptohesis, two reactions were planned. The first reaction, a), was with silver nitrate for decarboxylation and NBS as the source of radical halogen. The second reaction, b), was with silver nitrate for decarboxylation and I_2 as the source of radical

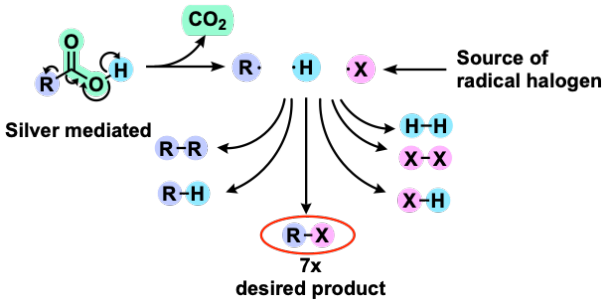

Figure 4.21: Hypothesized products of step 2-5

halogen. Both of the reactions were planned to be done in DMSO, as DMSO previously has been used as a solvent for decarboxylation, and as I_2 and NBS are soluble in it. AcOH was not added to the reaction mixture as in step 2-2 and 2-3 to minimize the presence of protons in the mixture. The two reactions can be viewed in Figure 4.22.

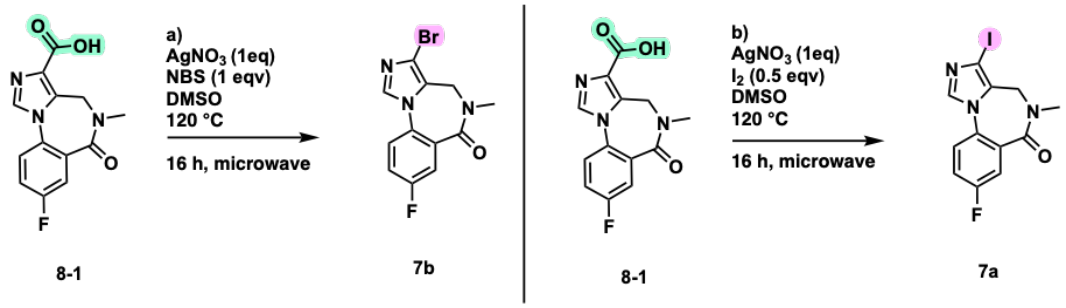

*Figure 4.22: Two approaches for decarboxylative halogenation of Flumazenil Acid **8-1** using silver nitrate and a source of halogen radical*

Reaction a) generated so much pressure that the micro wave reactor vial broke, probably through the generation of bromine or hydrogen gas in addition to the carbon dioxide gas that was generated in the decarboxylation. However, the pressure that made the vial break was very sudden, which could indicate some very sudden and exothermic reactions taking place. This reaction should therefore never be done in a sealed vial, and if done using an oil bath, one should take caution. The broken pieces of the reaction vial was washed with acetone and water, dried off. ^{1}H-NMR analysis revealed nothing of interest. Reaction b) was in the queue after reaction a) and was therefore never started. Surprisingly, after 72 hours and no stirring, the reaction mixture for reaction b) had switch color from orange to clear, see-through solution with white/bright yellow precipitation, indicating that something had happened. However, upon DI-MS postive ESI analysis, only Flumazenil Acid **8-1** was present. The switch in color of the reaction mixture can probably be attributed to the formation of silver iodide salt, AgI, although this was never confirmed through analysis.

4.3 Establishing a Process for [^{11}C]-Methylation of Flumazenil and Optimizing the Steps in the Process

A process for [^{11}C]-methylation of Flumazenil was to be established and optimized at the PET centre at Haukeland University Hospital in Bergen using a Synthra MeI Plus Research module. In order to perform the process, the following steps had to be established:

1. Establish a QC method for [^{11}C]-methylated Flumazenil using an analytical radio HPLC system.
2. Establish a chromatographic separation method using the semi-preparative radio HPLC system on the Synhtra MeI Plus Research Module.
3. Establish a stable, reproducible production of the primary synthon [^{11}C]-MeI that ends with sufficient trapping of [^{11}C]-MeI in an aprotic solvent such as DMF or DMSO.

Further, the established steps were to be optimized. The QC method was to be optimized based on resolution between Flumazenil and N-desmethyl Flumazenil, and desirably with a relatively short retention time. The knowledge from the optimization of the QC method were to be used for the establishment of the chromatographic separation method, as the same solvent for the mobile phase was planned to be used in both methods. The chromatographic separation method were then to be further optimized based on resolution and retention time. Optimization of the production of [^{11}C]-MeI was not planned to be optimized, however the trapping of [^{11}C]-MeI in the reaction vial was to be optimized based on the type of solvent, amount of solvent, and temperature of solvent. Lastly, the trapping of [^{11}C]-MeI were to be compared to the trapping of [^{11}C]-MeOTf. It was also to be investigated if the use of [^{11}C]-MeOTf could improve the yield, as OTf^- should act as a better leaving group than I^-.

4.3.1 QC method, 2^2 Factorial Design

It was desired to have a QC method for the production of ^{11}C-methylation of Flumazenil that could elute Flumazenil within maximum a time frame of 10 minutes, preferably less, and to also have a good resolution between Flumazenil and N-desmethyl so that it could be verified if the chromatographic separation method after the production had successfully separated the two species. The basis for the developement of the QC method was taken from Cleij et al 2009, where they used a flow rate of 1.3 mL/min and a 15:85 EtOH:H_2O mobile phase and UV detecting at 245 nm (38).

Table 4.10: 2^2 factorial design matrix with flow rate as factor A, level of EtOH in the mobile phase as factor B, and the measured resolution as the response.

					Resolution			
Entry	A	B	AB	Mean	Replica 1	Replica 2	Replica 2	Mean
1	-1	-1	1	1	0.86	0.80	0.76	0.81
2	1	-1	-1	1	0.87	1.27	0.79	0.97
3	-1	1	-1	1	0.54	0.61	0.62	0.59
4	1	1	1	1	0.69	0.65	0.62	0.65

The results for the three conducted replicates of the 2^2 factorial design for the resolution of Flumazenil and N-desmethyl Flumazenil in the QC method with an EtOH:H_2O mobile phase can be viewed in Table 4.10. Factor A is the flow rate varied between 0.9 and 1.3 mL/min. Factor B is the percentage of EtOH in the EtOH:H_2O mobile phase varied between 10 and 20%. The replicates were done to check if the results were reproducible. The only data point that seemed off was entry 2 in replica 2, which can indicate towards the system being a bit unstable at times. A mean of all the replicates were calculated, and the linear regression model was based on this. The model equation can be seen in Equation 4.1.

$$y = 0.756 + 0.059A - 0.136B + 0.028AB + \varepsilon \tag{4.1}$$

The equation shows that the most important factor for the resolution between of N-desmethyl Flumazenil and Flumazenil is factor B, the percentage of EtOH in the mobile phase. The equation shows that the less EtOH, the better resolution. Factor A, the flow rate, is also important for the resolution, however, to a less degree than factor B. An increased flow rate will lead to a better resolution. The correlation effect between factor A and B is quite low. There is a balance between lowering the levels of EtOH to yield a good enough resolution for its purpose and saving time, especially when dealing with carbon-11. The higher the levels of EtOH, the quicker the analytes elute. The optimal conditions are when the EtOH level is lowered so that a very good and reproducible resolution is obtained, while still allowing the analytes to elute within the time frame of 10 minutes, preferably less.

4.3.2 QC Method, Simplex Optimization

To get more certainty about which conditions that give the best resolution within a time frame of 10 minutes, a simplex optimization was done. This was done to learn about what factors that are important for a good resolution in order to apply this knowledge

to the chromatographic separation method on the semi-preparative radio HPLC, and to get some training in optimization.

The two data points in entry 1 and 2 in Table 4.10 of replicate 1 of the factorial design were chosen as two of the corners of the starting simplex. As entry 3 and 4 in Table 4.10 were of lower resolution, the last corner of the starting simplex was a triangle flip away from the average flow rate between entry 3 and 4. From the starting simplex, the rules explained in Subsection 3.5.3 of Chapter 2 were used to find the best resolution for the method, which was obtained at 1.1 mL/min flow rate and 8 % EtOH. The steps for the simplex optimization and a response surface plot can be seen in Figure 4.23 and Figure 4.24. In the simplex plot, p_n is the data point number n where the resolution of the data point is noted next to it. The response surface plot uses the data collected during the simplex optimization and the factorial design. The color bar in the response surface plot indicates the resolution from low (0.2) to high (1.6).

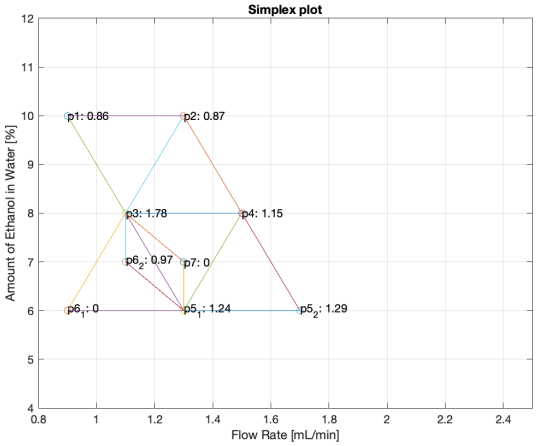

Figure 4.23: Simplex steps for the resolution in the QC method.

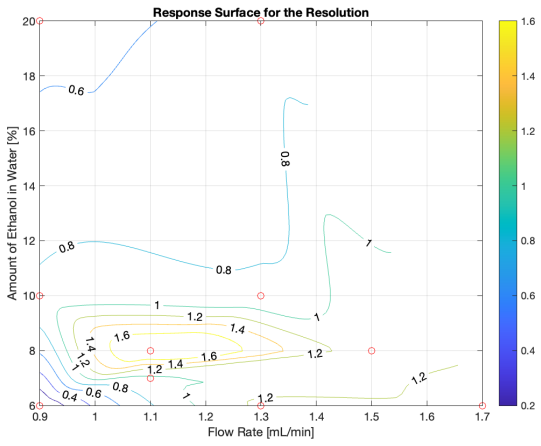

Figure 4.24: Response surface for the resolution in the QC method.

4.3.3 Chromatographic Separation of Flumazenil from N-Desmethyl Flumazenil

The same approach for optimization was as for the QC method supposed to be used for the chromatographic separation of Flumazenil from N-desmethyl Flumazenil using a semi-preparative radio HPLC. However, the UV-detector of the system broke, making this impossible to accomplish. Fortunately, some previous experiments with a standard solution of Flumazenil and N-desmethyl Flumazenil had been done early on in the

project, where one of the experiments gave an acceptable resolution at a flow rate of 4.75 mL/min in a 50:50 EtOH:H_2O mobile phase, see Figure 4.25. Another experiment where the flow rate was set to 4.6 mL/min in stead of 4.75 mL/min, the separation was no longer acceptable, see Figure 4.26. This indicates that a higher flow rate gives a better resolution, as was found for QC method. The flow rate cannot be set higher than 4.75 when using 50:50 EtOH:H_2O, as the pressure limit of 300 bar is almost reached. Lowering the percentage of EtOH level while trying to push the flow rate up towards the pressure limit of the system will probably result in a much better resolution. However, the amount of EtOH effects the retention time of Flumazenil and its precursor to a larger extent than the flow rate does, and there is a balance between getting a good resolution and loosing too much activity during the separation due to a slow retention time. A flow rate of (5 $\pm$ 0.2) mL/min and an EtOH percentage of (40 $\pm$ 5) % will probably give a much better resolution than what can be seen in Figure 4.75, while still eluting the analytes within an acceptable time frame. [^{11}C]MeI must also be taken into account in the separation, however, the work of Cleij et al in 2009 indicates that [^{11}C]MeI will elute earlier than Flumazenil and its precursor in a EtOH:H_2O mobile phase (38), therefore this was thought not to be an issue.

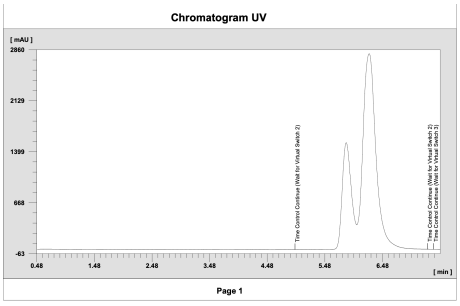

Figure 4.25: 4.75 mL/min 50:50 EtOH:H_2O

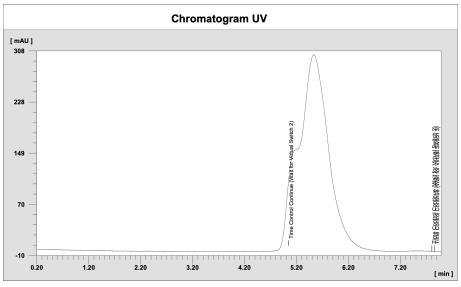

Figure 4.26: 4.6 mL/min 50:50 EtOH:H_2O

4.3.4 Trapping [^{11}C]-MeI in DMF in the Reaction Vial

Before producing [^{11}C]-methylated Flumazenil, some test runs were done to see how much [^{11}C]-MeI that was possible to trap in the reaction vial, and how much activity that was necessary to produce in the cyclotron in order to generate sufficient amounts of [^{11}C]-MeI. In Table 4.11 three different test runs are shown, all using 1 mL of DMF in the reaction vial. A test run means only trapping of [^{11}C]-MeI without having the precursor in the reaction vial. The data from the production runs of [^{11}C]-methylated

Flumazenil are also shown, however, in P2 only 0.2 mL of DMF was used. The table shows how much activity that was sent from the cyclotron, and how much activity that was obtained in the different traps of the system. It also shows the overall loss of activity from the $[^{11}C]CO_2$ production in the cyclotron to what was obtained in the reaction vial. In the script for the production of $[^{11}C]$-MeI, one has to manually push

Activity	T1		T2		T3		P1		P2	
	GBq	%	GBq	%	GBq	%	GBq	%	GBq	%
Sent from cyclotron	12	-	12.5	-	58	-	52	-	50	-
CO_2 trapping	8.3	69	8.6	69	33	57	10*	19*	19	38
Left after CO_2 desorption	-	-	-	-	10	-	2	-	4	-
Porapak trap	3.4	41	3.8	44	18	54	4	40	7	37
Reaction vial	2.3	68	1.2	32	12	67	1.1	28	5	71
Overall loss of activity (%)	81		90		79		98		90	
DMF used (mL)	1		1		1		0.2		1	

*Table 4.11: Table showing the amounts of activity reaching the reactor vial during a production. T: test, P: production, %: percentage from previous measured step, *Valve from target gas closed too early by mistake*

a button when the graph of the activity in the trap flattens out and one assumes that a peak in activity has been reached, before the system proceeds to the next step in the production. This allows for operator "errors", as one can see in T2 and P2 in the table. T1 and T3 has very similar values and an overall loss of activity of approximately 80 %. T2 is quite similar to T1, however the bubbling of $[^{11}C]$-MeI with Helium in to the DMF in the reaction vial, was probably not done long enough by the operator. The same kind of problem happened during P1, where the operator pushed the button that starts the desorption of CO_2 before all of the target gas has flowed through the cooled trap. These examples show that the process is fragile towards operator errors. However, if an experienced operator is operating the system, then one can expect to trap $[^{11}C]$-MeI with approximately 10-20 % of the activity produced in the cyclotron in 1 mL DMF. The results indicates (not surprisingly) that the more DMF that is in the reaction vial, the more MeI can be trapped, as P1 had the overall lowest trapping compared to the activity in the Porapak trap. It would therefore be advantageous to have as much DMF as possible in the vial for trapping as much MeI as possible. However, the reaction vial is not very large (3 mL) and there is only space for 1.5 mL in the load position of the semi-preparative HPLC system that is to be used post reaction. As 0.4 mL of buffer and EtOH was used to quench the reaction, and 60 μL of KOH was added, this left a space of $(1.5 - 0.460)mL = 1.04mL$ for the precursor dissolved in DMF. This lead to the decision of using more DMF for production P2 even though the precursor would be more diluted, in hopes to increase the amount of $[^{11}C]$MeI trapped in the reaction vial.

The reaction kinetics were already very fast (1-10 minutes reaction time), therefore it was not of concern that the dilution should effect the reaction drastically.

4.3.5 Establishing a Process for [^{11}C]-Methylation of Flumazenil, including QC

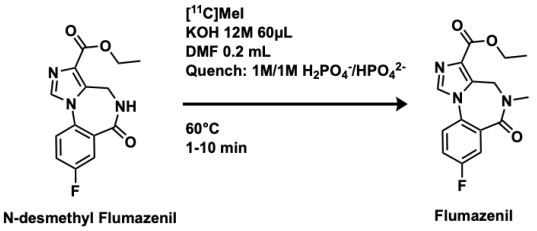

Figure 4.27: [^{11}C]-methylation of Flumazenil

As the UV detector of the semi-preparative radio-HPLC system broke and was not operational until the 30th of May, the planned optimization could not be accomplished. Fortunately, when using the chromatographic method for the separation described in the previous section (4.75 mL/min flow rate and 50:50 EtOH:H_2O), it was assumed that Flumazenil could be "blindly" be collected at the expected eluting time of 5 minutes and 40 seconds of the chromatographic separation method which can be seen in Figure 4.25. The production could then be verified using the QC method. This was not optimal at all, however, it could prove that the process can be used and further optimized with a functioning UV lamp.

First production, P1 The first production was to some extent successful, as there was activity at the expected eluting time of Flumazenil in the QC method, see Figure 4.28. The activity was, however, **very** low (27 Bq), and the UV detector in the QC method was not able to detect at this concentration. This hindered measuring different parameters such as SA, and only allowed for a qualitative verification that Flumazenil was radiolabeled. Therefore in the next run, the dilution with saline was not done in order to concentrate the sample more for the QC. The formulation of the product with saline can be established at a later point once the UV lamp is operational.

Second production, P2 For the second production, 0.8 mL more DMF was used in the reaction vial than in production 1 in the hopes of trapping more [^{11}C]-MeI, something that was successful, as 71 % of the activity from the Porapak was transferred to the reaction vial, compared to the 28 % in P1, see Table 4.11. The flow rate of the QC method was also switched to 1.5 mL/min as this would make the analytes elute quicker while maintaining a sufficient resolution. Suddenly, when using the chromatographic separation method, the UV-lamp started working again, for no apparent reason,

see Figure 4.30. The UV signal and the counter show that everything elutes after approximately 3 minutes instead of the 5 minutes and 40 seconds that was expected with the developed chromatographic method (see Figure 4.25). This could indicate that the DMF in the reaction mixture changes the properties of the mobile phase, making it more polar. This would make the analytes elute much quicker than when the standards were dissolved in 50:50 EtOH:H_2O and were injected manually as in Figure 4.25. If this is the case, the chromatographic method should be developed further with this in mind, injecting the standards dissolved in the same solvent with the same conditions that is used in the reaction when producing Flumazenil. The addition of KOH and buffer to the reaction mixture could also effect the pH of the system, something the column could be very sensitive towards. Therefore this should also be considered while developing the chromatographic method. As one can see in 4.30, the separation was unsuccessful. In Figure 4.29 one can see the QC, showing all reactants present: to the left most likely [^{11}C]-MeI, in the middle N-desmethyl Flumazenil and lastly [^{11}C]-Flumazenil/Flumazenil. There is an uncertainty of whether the first eluting peak is [^{11}C]-MeI or not, as the UV detector is measuring at 245 nm. MeI has absorption in the gas phase from 160 to 335 nm, and from 330 to 400 nm in liquid state (39). If the peak does not belong to MeI, then it is an unknown radioactive specie. The specie also seems to be present in Figure 4.28 without activity. A suggestion to what it could be if the peak does not belong to [^{11}C]-MeI is [^{11}C]-methylated Flumazenil Acid, as hydrolysis of Flumazenil is possible when being heated in a basic environment. This could make sense as the acid group makes the analyte much more polar compared to Flumazenil and N-desmethyl Flumazenil. Another thing to consider, is that the UV signal of the chromatographic separation came very sudden after 3 minutes compared to what was expected from the chromatographic method. Therefore, the collection of the product did not start until about one third into the UV-peak. There is therefore a possibility that there is more product than what was shown in the QC. No parameters such as SA, RCY and RCP were calculated as the production process was unsuccessful with regard to separation. These results also show why very little Flumazenil was collected in production 1, as the product was collected after approximately 5 minutes in stead of

3 minutes in production 1.

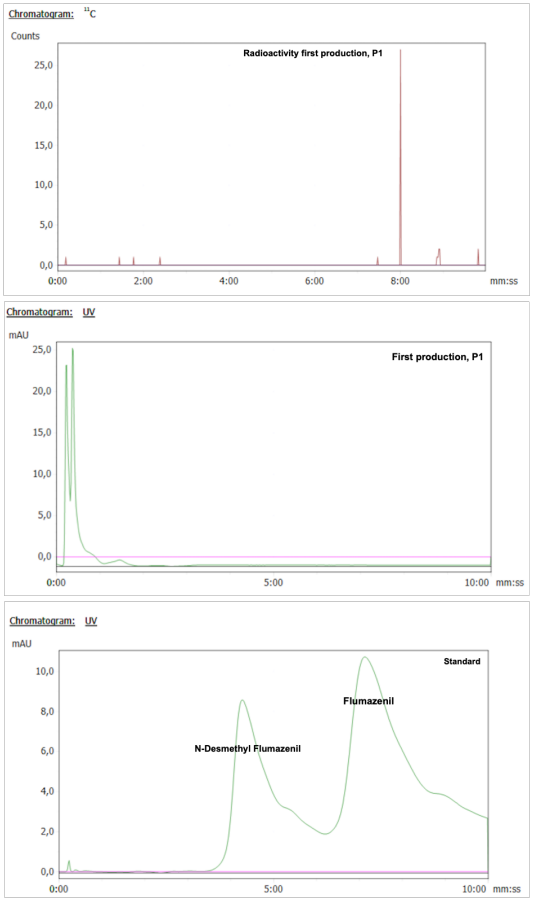

Figure 4.28: QC of the first production with the standard on the bottom.

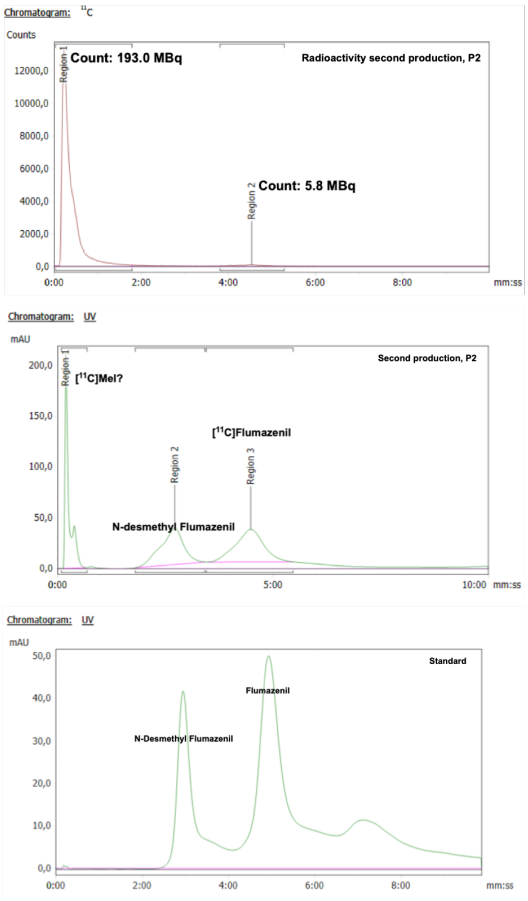

Figure 4.29: QC of the second production with the standard on the bottom.

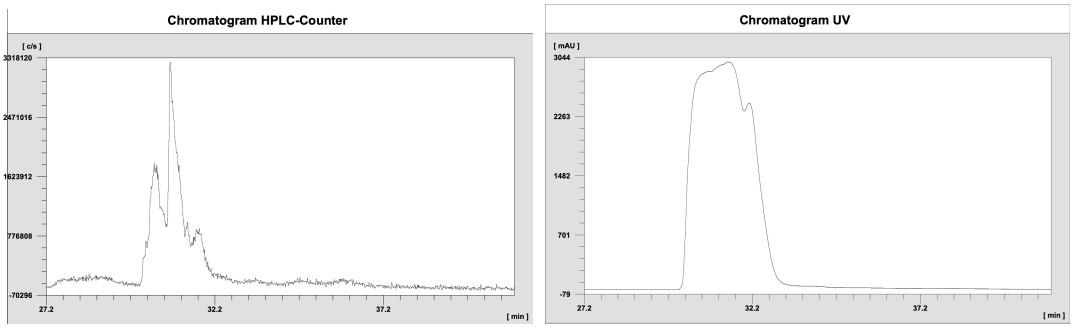

Figure 4.30: Second production, counter to the left and UV signal to the right

4.4 Discussion

4.4.1 Synhtesis Route 1

The first step of synthesis route 1 worked nicely with an average isolated yield of 45 %. The structural elucidation was challenging but was clarified using ^{1}H-^{1}H NOESY. The reason why the reaction worked so well can probably be attributed to the nitrogroup at methyl 2-fluoro-5-nitrobenzoate **1**, facilitating for the nucleophilic aromatic substitution proceeding through a Meisenheimer complex. The column chromatography method developed for this step, described in experimental section, was very time consuming, and the product and bi product partly overlapped. If this step is improved, then the isolated yield is likely to be better.

Step 2 in synthesis route 1 was reported successful in the work of Donohue and Dannals in 2009, when an ester group was at the starting material **2** instead of iodide (37). In this work, when iodide took place instead of the ester group, only the undesired bi product with a bromide in the 2-position of the imidazole ring was made. A reason for this could be that iodide is a very large atom, and the repulsive forces could be too large for bromide to be stable on the methyl group, see Figure 4.31 and therefore only yielding the undesired bi product. Suggestions on how to work around this problem are listed:

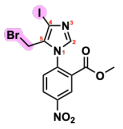

Figure 4.31: The desired product of step 2 in synthesis route 1

- Introduce iodide in the 4-position of the imidazole ring at a later stage in the synthesis, starting with plane imidazole in step 1 (See Figure 4.1). However, in synthesis route 2, it was very challenging to introduce a halogen in the 4-position of the imidazole ring, so this might not be the best strategy.
- If the size and the repulsive forces between iodide and bromide is the problem, leading bromide in the wrong positions, then perhaps another halogen could be used, starting with 4-bromo-5-methyl-*1H*-imidazole or 4-chloro-5-methyl-*1H*-imidazole in step 1 (See Figure 4.1).
- The reaction conditions at step 2 could also have been modified, perhaps use another source of bromide that have been reported to be able to brominate on a methyl group attached to an aromatic ring. Perhaps one could also try to use another halogen instead of bromide at this step. Again, if the size of iodide is he issue, perhaps chloride could be used instead of bromide, even though chloride is a worse leaving group for the next step i synthesis route 1 (See Figure 4.1).

- A protecting group could also be put in the 2-position on the imidazole-ring, hindering the bromination in this position. However, this would lead to two additional steps in the overall synthesis, making it a more demanding and less green synthesis than what it already is.

Either way, terminating synthesis route 1 at this stage was probably the wisest thing to do, as the overall goal was to perform ^{11}CO carbonylation of Flumazenil, not to get stuck on structural elucidation and complicated synthesis techniques. Synthesis route 2 is much simpler than synthesis route 1 and can much quicker be used to achieve the overall goal of radiolabeling Flumazenil with carbon-11 in the carbonyl position of the ester group. If the goal would have been achieved, then one could go back to synthesis route 1 and develop and optimize this if one wishes to have a production from scratch.

In the work of synthesis route 1, structural elucidation using NMR was emphasized much more than in synthesis route 2. This is because in synthesis route 1 small building blocks of Flumazenil were put together, allowing for different compositions and isomers taking place. While in synthesis route 2, only small bits of Flumazenil was removed, and therefore MS analysis could to a much larger extent be trusted.

4.4.2 Synthesis Route 2

Step 1 of synthesis route 2, the hydrolysis of Flumazenil **8** worked very well with full conversion to Flumazenil Acid **8-1**. This is not very surprising as hydrolysis of esters is a very common reaction and one of the main metabolic pathways of Flumazenil, see Figure 2.9. There was a concern that the very basic conditions (10 eqv of NaOH) could lead to an unintentional hydrolysis of the amide group as well, however, this did not happen. The reaction conditions of step 1 were never optimized as it worked very well the first time, however there are absolutely possibilities for improvement. It is probably not necessary to use that much base (10 eqv), and the solvent does not necessarily need to be methanol, although experimentally it was nice for analysis purposes, as methanol vaporize quickly compared to for example water. Which solvent that is best to use depends on the following step. If for example water is used in the next step, it would be advantageous and greener to use water for step 1 of synthesis route 2, because then the synthesis could be continued straight forward to the next step, minimizing the use of time, energy and waste of solvents.

Step 2-3 was a very straight forward, successful protodecarboxylation of Flumazenil Acid **8-1** in good yields (74%) and with a full conversion, proving that the discoveries of Lu et al 2009 works very well for carboxylic acids on aromatic rings next to a

heteroatom (4). The reason why the yields are not higher, is probably due to the loss of product during vacuum filtration. Also, a lot of the reduced silver was stuck on the walls of the microwave reactor vials, likely holding some of the product. The only way to remove the silver was by putting it in an acid bath, so the product that potentially was trapped in the silver depositions could not be revived. A solution to this problem is to use catalytic amounts of silver. For this to be possible, a re-generator for the silver salt would also need to be added to the reaction mixture. The step has not been optimized, and it is likely that it does not need the full 16 hours reaction time, at least not when using stochiometric amounts of silver. Or, perhaps the full 16 hours reaction time actually is necessary when using catalytical amounts of silver. It was also very nice that the reaction could be performed using water instead of DMSO. As mentioned for the discussion of step 1, this means that one could go straight forward with the solvents from step 1 if water was to used be there. Step 2-3 could be of precursor inspiration for other already established drugs that could be candidates for radiolabeling. If there are drugs with an ester or carboxylic group next to a heteroatom on an aromatic ring, then all that needs to be done is hydrolysis, selective protodecarboxylation mediated by silver (I) salts and lastly a selective halogenation, and then one would have a precursor that can participate in [^{11}CO]-carbonylation. A safety-note to this reaction is that is was done in a sealed vial. In the prodotdecarboxylation, CO_2 gas is developed. When performing at larger scale, this could perhaps not be safe any longer as one would have a risk of the sealed microwave reactor vial exploding if much larger amounts of CO_2 is generated.

After the successful protodecarboxylation of step 2-3, halogenation was attempted using DIH in mild and harsh reaction conditions. This step would also only use water as a solvent, something that would make the synthesis an easy, and to some extent green, route. It is strange why this did not work, as it works so well on plane imidazole with both mild and harsh conditions (5). One could probably have investigated the reaction more by varying the reaction conditions and trying with DBH or DCH as sources of halogen, however, there was not that much starting material left, and from step 2 from synthesis route 1 it was experienced that it could be smarter to try new approaches instead of trying to force through a reaction that does not appear to take place. Reasons for why the halogenation works well on plane imidazole and not for **9** could have something to do with the structure of **9**. **9** is conjugately linked to a benzene ring which again is conjugately linked to a carbonyl group. Perhaps this withdraws electrons away from the imidazole ring, which results in some kind of effect on the halogenation of the imidazole ring.

Other conditions were attempted in the pursuit of halogenating in the 4-position of the imidazole ring on Flumazenil Acid **8-1** through a 1-step decarboxylative halogenation. Attempt 2-4a consisted of using Palladium Acetate for decarboxylation, while trying to get bromide to replace the carboxylic group using NBS as a source of the bromine radical. This was unsuccessful, with low conversion of Flumazenil Acid **8-1**. This indicates that Palladium Acetate under inert conditions in DMF at 80 °C is not able to decarboxylate Flumazenil Acid **8-1**. There were some traces in LC-MS indicating that a small amount of **9** had been made, however this was very low amounts. Perhaps if the temperature was increased to 120 °C as was done in step 2-3, one would see larger formations of **9** and maybe also the desired product **7b**. Attempt 2-4b consisted of using Palladium Acetate for decarboxylation and getting iodide in CuI to replace the carboxylic group. This was also unsuccessful, however there was a full conversion of Flumazenil Acid **8-1**. As palladium acetate did not convert Flumazenil Acid **8-1** in step 2-4a, the conversion in step 2-4b can probably be attributed to CuI, as there was also a full conversion in step 2-4c, where palladium acetate was not used. However, one cannot tell for sure since the reaction conditions were different compared to 2-4a, using DMSO at 150 °C in aerobic conditions. This indicates that either CuI interacts with Flumazenil Acid **8-1** in some way, or it could be that the high reaction temperature resulted in the decomposition of Flumazenil Acid **8-1**. Attempt 2-4c consisted of using only CuI for both the decarboxylation and the source of halogen. Here, there was also a full conversion of Flumazenil Acid **8-1**, also indicating that either CuI interacts with Flumazenil Acid **8-1** in some way, or it could be that the high reaction temperature resulted in the decomposition of Flumazenil Acid **8-1**. It would be interesting to perform step 2-4b and 2-4c at 120 °C. If there would still be a full conversion of Flumazenil Acid that did not lead to **9** or **7a**, then it can be concluded that CuI interacts/decomposes Flumazenil Acid **8-1**.

As CuI can be used both as a decarboxylating agent and a source of iodide (7), it was also hypothesized that AgI could function in the same way. Different, insoluble silver salts (Ag_2O, Ag_2CO_3) had shown to be able to decarboxylate Flumazenil Acid **8-1**, therefore there is no apparent reason for why AgI should not be able to do so. Hopefully, I^- could be a source of iodide. One could also add KI to have an excess of iodide in the reaction mixture. This idea came very late in the master's project, and there was unfortunately not enough time to buy new reagents, therefore this reaction was never attempted.

None of the reactions in 2-4 where able to produce decarboxylated Flumazenil **9**, however silver(I) salts were able to do this. The decarboxylation most likely proceeds

through a radical mechanism, as described in step 2-5, see Figure 4.21, and by having a halogen radical present in the reaction mixture, it is likely to produce the desired product **7x**. This was attempted in step 2-5, however, due to the breakage of the sealed micro wave reactor vial when using $AgNO_3$ and NBS, there was a safety concern that there was an unexpected exothermic reaction after a couple of hours, causing a safety hazard, especially upon heating to 120 °C. Ways to work around this could be to perform the reaction in flow. Performing reactions in flow can lead to better heat transfer, enhanced control of the process, lower concentration and minimizing the chance of hot spots or localized high temperatures that could lead to undesired reactions or thermal runaway. However, the formation of solids from the silver being reduced in flow would be an obvious obstacle. This issue could be overcome by having a re-generator of the silver(I) salts or by having in-line filtration.

4.4.3 Optimization of Steps in the [^{11}C]-Methylation of Flumazenil

QC Method When reflecting upon the optimization of the analytical HPLC method (CQ method), one could argue that there has been spent too much time on optimizing something that early on gave a sufficient resolution. However, the skills acquired while doing this would have been of great help in the optimization of the semi-prep method and optimization of the [^{11}C]-methylation of Flumazenil. Scripts in MATLAB were also developed and would be ready for use later. It was also nice to have a good resolution, ensuring good quality control and making sure that there is no precursor left in the sample after producing [^{11}C]-Flumazenil.

In the factorial design, the high and low levels of ethanol was based on 15 % ethanol. The level was increased up to 20 % or decreased down to 10 %, which is an increase or decrease of $5/15x100\% = 33\%$. The levels of the flow rate was based on a flow rate of 1.3 mL/min. If the same relative increase or decrease should have been done for the flow rate, then the flow rates should have been set to $1.3mL/min + 0.33x1.3mL/min = 1.7mL/min$ for the high level and $1.3mL/min - 0.33x1.3mL/min = 0.9mL/min$ for the low level. However, the EtOH:H_2O mobile phase generated a lot of backpressure, resulting in a system limit of approximately 1.3 mL/min when having a 20 % EtOH level in the mobile phase. This could have an effect on the model equation 4.1, making it seem like the EtOH level i more important for the resolution than what it actually is. This could have been fixed by lowering the increase and decrease in the high an low levels of EtOH, however this was not done.

For the Simplex optimization of the analytical HPLC method, the starting simplex should have been different. As two of the first corners of the starting simplex were set

at the same EtOH level, less information is collected than if all the corners were set to different levels both for the EtOH level and for the flow rate. However, these were simple and cheap experiments taking only 10 minutes per experiment, therefore it was not problematic to do more experiments.

The results from the optimization of the QC method also points towards other settings for the flow rate and level of EtOH than what was described by Cleij et al in 2007 (38). They used 15:85 EtOH:H_2O and a flow rate of 1.1 mL/min, while the data presented in this thesis point towards the most optimal resolution occurring at a 8:92 EtOH:H_2O mobile phase and a flow rate of 1.1 mL/min. However, the optimal conditions will of course vary from system to system and from column to column.

Chromatographic Separation Method It was very unfortunate that the UV-lamp in the semi-preparative HPLC system broke, hindering further optimization of the synthesis of [^{11}C]-methylated Flumazenil. Luckily, some separation runs of Flumazenil and N-desmethyl Flumazenil on the semi-preparative HPLC had been investigated early on in the project, and one of these experiments had shown a sufficient separation. In this method, the settings were set to 4.75 mL/min and 50:50 EtOH:H_2O. The level of EtOH needed for a good separation was a lot higher than anticipated from the gained knowledge from the analytical HPLC. This shows that it is necessary to to optimize, or at least do some screening experiments, on analytical methods for in house production of radio pharmaceuticals and not copy the settings that are noted in the literature, as the optimal settings will vary from laboratory to laboratory as one often operates with different columns and different systems. After the second production, when the UV lamp was functioning again, it was revealed that developing the method with the standards dissolved in the mobile phase prior to injection, was not ideal, and misleading. The chromatographic method should be developed with the standards dissolved in the components of the reaction mixture: DMF, KOH, 1M/1M aqueous phosphate buffer solution and EtOH.

4.4.4 Establishing a Process of [^{11}C]-Methylation of Flumazenil

The fact that the UV-lamp in the semi-preparative HPLC system broke and did not function until the 30th of May, lead to it being impossible to establish a very well and consistent process for the [^{11}C]-methylation of Flumazenil, as the product was collected "blindly" without any UV signal. [^{11}C]-Flumazenil was in the first production attempted collected at the time where it was shown to elute in the developed chromatographic separation method, however, the chromatographic method was developed based on standards of N-desmethyl Flumazenil and Flumazenil. In the established pro-

cess, the precursor is dissolved in DMF and quite basic conditions before the reaction, and the reaction is quenched with a buffer after the reaction. In the second production, it was shown that this had an effect on the eluting time and resolution of N-desmethyl Flumazenil and Flumazenil. There was, however, not enough time to improve the chromatographic method. Yet, a process for producing [^{11}C]-methylated Flumazenil was partly established and will be functioning well once the chromatographic method has been further developed.

4.4.5 Overall Discussion of the Work

Even though the aim of the study, making a precursor for palladium mediated [^{11}CO]-carbonylation of Flumazenil, was not achieved, a very nice 3 or 4 step synthesis strategy that could be applicable to a lot of other pharmaceuticals with an ester next to a heteroatom on a heteroaromatic ring was developed, see Figure 4.32. All one would need to do is buy the pharmaceutical and perform these simple steps. The establishment of a process for [^{11}C]-methylation of Flumazenil was partly successful, and the skills obtained during the optimization of the QC method would have allowed for quick and efficient optimization of the steps in the production of [^{11}C]-methylated Flumazenil, such as the chromatographic separation method on the semi-preparative HPLC system. However this was not possible due to the technical issues.

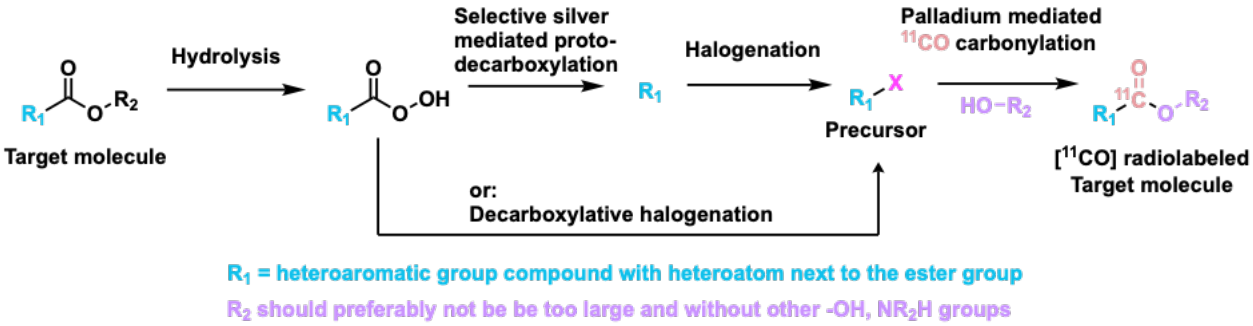

Figure 4.32: The developed ^{11}CO-precursor synthesis strategy.

Final, overall thoughts of this project, is that the main intention was to do carbon-11 chemistry. When finding a target drug that one wants to radiolabel, one should firstly have the target in mind, then find the tools for radiolabeling. However, when I found the target drug Flumazenil, I found it based on the fact that I could perform carbon-11 chemistry and not based on the target. This resulted in spending large amounts of time compared to what was anticipated in a regular organic synthesis laboratory trying to generate a precursor for carbonylation in stead of spending time actually performing carbon-11 chemistry. In retrospect, if the overall goal was to perform carbon-11

chemistry, then more simpler reactions where the precursors could have been bought commercially should have been done in stead. Suggestions for how this could be done is described further in future work in Chapter 5.

Even though the overall goals of this project was not achieved in the way that was anticipated, this thesis can hopefully be of inspiration to upcoming radiochemistry students, especially the ones doing their master's thesis at the University of Bergen. In further work I have suggested some approaches for finishing and optimizing synthesis route 2, some simple reactions that can be used to learn more about carbonylation chemistry, and I have also listed some drugs that are selective towards certain types of receptors in the brain that has not been radiolabeled for PET yet. I have also suggested strategies for radiolabeling them with carbon-11.

Chapter 5

Conclusions and Future Work

5.1 Conclusion

In this work, two synthesis routes towards a precursor for radiolabeling Flumazenil with carbon-11 in the carbonyl position of the ester group were attempted without success. A 3(4) step synthesis strategy for generating precursors that can be radiolabeled in the carbonyl position of an ester group next to heteroatoms on heteroaromatic rings was developed, see Figure 4.32. A process for [^{11}C]-MeI methylation of Flumazenil was partly established at the PET centre at Haukeland University Hospital, using a Synhtra MeI Plus Research module for the process and an analytical radio HPLC for QC.

5.2 Future Work

5.2.1 Finishing and Optimizing the Synthesis of the Precursor for Producing [^{11}CO]-carbonylated Flumazenil

Further work involves finishing the synthesis of the precursor for producing ^{11}CO carbonylated Flumazenil. The most promising way of doing this is through performing decarboxylation of Flumazenil Acid **8-1** while simultaneously having a source of a halogen radical present. If this is not possible, a clever way of halogenating in the correct position after silver mediated protodecarboxylation of Flumazenil Acid **8-1** should be developed. The use of AgI as both a decarboxylative agent as well as a source of iodide should also be investigated. All of the reactions in step 2-4 of synthesis route 2 should also be pursued at 120 °C.

If the synthesis is successfully carried out, optimization of the synthesis can be done. Firstly, the hydrolysis reaction of turning Flumazenil into Flumazenil Acid **8-1**, can be adjusted to less basic conditions, and the reaction time probably does not

need to be 3 hours long. Different solvents can also be tested as well as the reaction temperature. Secondly, for the silver mediated decarboxylation of Flumazenil Acid **8-1**, a re-generator for making the silver salt function as a catalyst can be investigated. Lastly, a work up and purification for the last step of the synthesis needs to be explored. Perhaps all the synthesis steps could be conducted in flow, although, the generation of solids from the silver mediated decarboxylation would be an obvious obstacle for this.

5.2.2 Alternative Way of Performing [^{11}CO]-Carbonylation of Flumazenil

An alternative way of perform carbonylation on Flumazenil could be to make the precursor in Figure 5.1 and try to do [^{11}CO]-carbonylation of Flumazenil. Although, it is not sure if the iodide and the amine will unintentionally react in a aryl amination reaction.

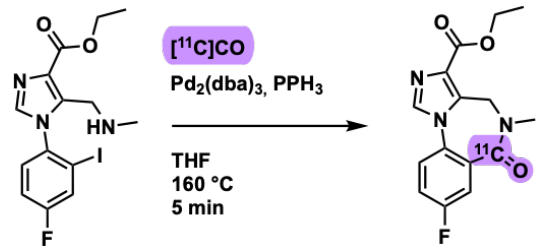

Figure 5.1: Alternative way to perform [^{11}CO]-carbonylation of Flumazenil

5.2.3 Establishing the Process of [^{11}C]-Methylation of Flumazenil

The process of [^{11}C]-methylation was established, however, as the UV lamp of the separation system did not work until the 30th of May, a very consistent, optimal and certain process was not achieved. Further work would be to finish the establishment of the process properly and verify the chromatographic separation method of Flumazenil and N-desmethyl Flumazenil. A calibration curve for the quantification of Flumazenil on the analytical radio HPLC system also needs to be established. The chromatographic separation method on the semi-preparative radio HPLC should be developed with the standards dissolved in the components of the reaction mixture: DMF, KOH, 1M/1M aqueous phosphate buffer solution and EtOH.

5.2.4 The Synhtra Module

Per now, the Synhtra module at the PET center at Haukeland University Hospital is only set up for methylation. Future work would be to set it up for carbonylation and try to use the strategy as described in 2.7 where the oxygen percentage in the target gas in the cyclotron is set to a low level of 0.1 % to avoid destroying the zinc column. This should be tried first with a very simple reaction with reactants that can be bought

commercially. An example of this is the carbonylation of iodobenzene together with ethanol, described in Figure 5.2.

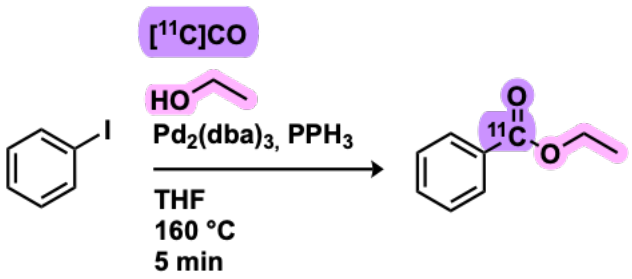

Figure 5.2: A simple carbonylation of ethyl benzoate using commercially available reagents

In future work, if there is no specific target of interest, but one wants to learn about the carbonylation chemistry, one could perform it on different commercially available substrates such as in 5.2 and vary the reaction conditions. The products of the reactions should ideally be possible to buy commercially or very easily synthesized in order to use them as standards for analysis. Different substrates for the reaction could for example be different positions of the imidazole ring, see figure 5.3. Other substrates could be halogenated pyridine, benzimidazole, quinoline, isoquinoline, thiazole, oxazole. These are of interest because they are often building blocks in pharmaceutical species. One can also vary the halogen between iodide, bromide, chloride and triflate. It would also be interesting to vary the nucleophilic coupling partner in the reactions from for example ethanol to water, amines or alcohols that also has an amine group etc.

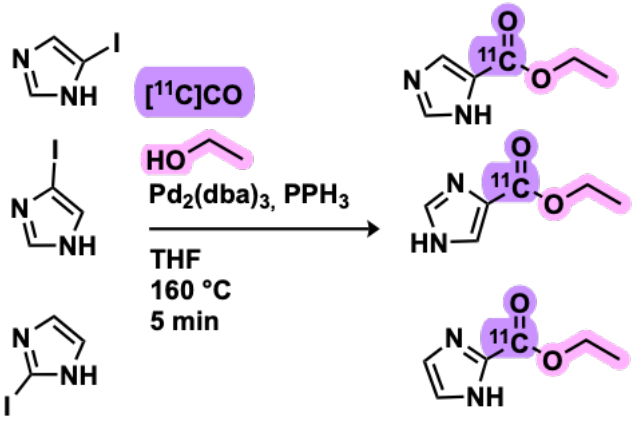

Figure 5.3: [^{11}C]CO-Carbonylation of iodo-imidazole derivates

5.2.5 Future Targets for Radiolabeling with Carbon-11

Obviously, if the synthesis of the precursor for producing ^{11}CO carbonylated Flumazenil is successfully produced, then this should be attempted radiolabeled.

If any new targets for radiolabeling are found, beare in mind that methylation is almost always the preferred method for radiolabeling as it is simple and robust, and that methyl groups attached to for example oxygen or nitrogen are often metabolized very early, leading to no radiolabeled metabolites of the drug, which is important. If the methylation is not possible, then one can look towards other labeling methods. However, other methods such as carbonylation can also be useful when the goal is to investigate metabolism of a drug, as the carbonyl group often is very stable towards metabolism. Throughout the work on this thesis, ideas for radiolabeling of drugs with high selectivity towards certain receptors in the brain that has not yet been radiolabeled for PET have been developed. In the following subsections these ideas are listed with a short description of the candidates.

Baclofen

Baclofen is a selective and therapeutically available $GABA_B$ receptor agonist (40). In 2016 Chow et al showed that [^{11}CO]-carbonylations could be done on non-activated β-hydride containing substrates through thermally initiated radical carbonylations (41). Baclofen could participate in this type of reaction with water functioning as a nucleophile, see Figure 5.4. This radiolabeling can be attempted if the precursor in the reaction were to be developed, see Figure 5.4. However, water has shown to be a bad nucleophile in this type of reaction, only yielding trace amounts, and the reaction conditions would have to be improved. The best approach would be to first verify that this type of reaction can be done with water as a nucleophile by the use of commercially available reagents. If this is confirmed, then the precursor could be developed and pursued radiolabeled.

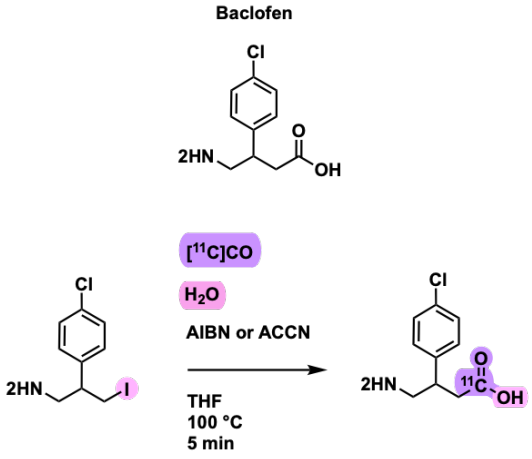

Figure 5.4: Suggestion for how to radiolabel Baclofen

Dexmedetomidine

Dexmedetomidine is a selective alpha-2 adrenergic agonist with a high affinity and selectivity for the alpha-2 adrenergic receptors in the brain (42). By specifically activating these receptors, dexmedetomidine produces a sedative, anxiolytic, and analgesic effects (42). The drug has not yet been radiolabeled for PET. If the precursor in Figure 5.5 is to be made, then a palladium mediated Stille Reaction with [^{11}C]MeI could be investigated. One should bear in mind that there are some complications with using organostannane and toxicity, therefore work up and quality control would be an important focus when developing the process for this reaction.

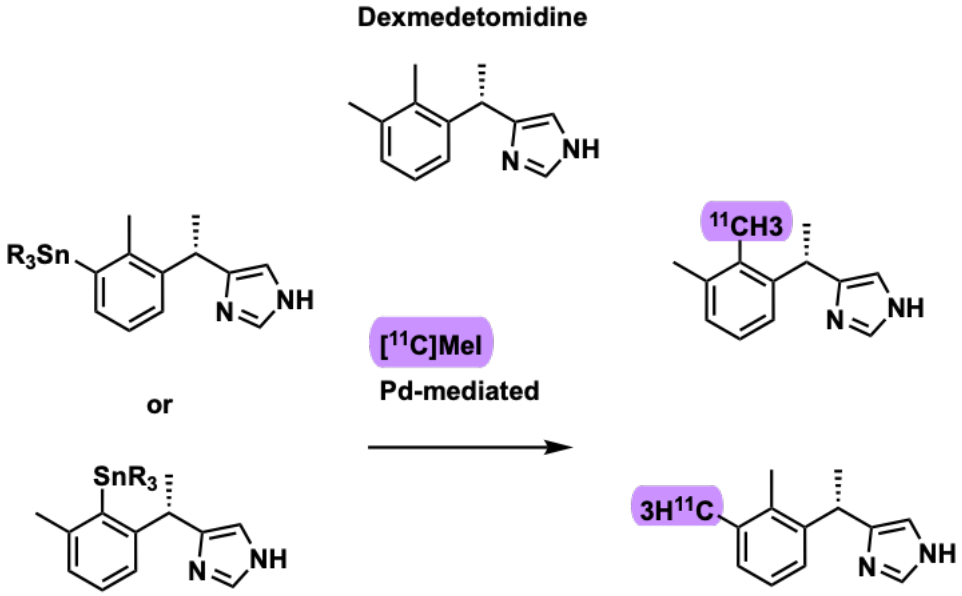

Figure 5.5: Stille Reaction for ^{11}C radiolabeling of Dexmedetomidine

5.2.6 Trapping of MeI or [^{11}C]-MeI or [^{11}C]-MeOTf in Different Solvents

Other work that could be done in regards to methylation, could be to test how much [^{11}C]-MeI or [^{11}C]-MeOTf that is possible to trap in DMSO or DMF and compare which solvents that are best to use. This is typical information that is known by pioneers in the field, however it is not noted anywhere in the literature. Therefore it could be nice to report these experiments as a simple, educational graph that others can use.

Chapter 6

Experimental

6.1 General Methods

6.1.1 Chemicals

All of the chemicals used were purchased commercially and used as received.

6.1.2 Experimental Description

TLC analyses were performed on coated alumina foils embedded with fluorescent indicator 254 nm. The mobile phase used consisted of various mixtures of hexane and ethyl acetate or DCM and MeOH. Manual flash chromatography was performed using silica gel as stationary phase and with various mobile phases. Semi Prep HPLC was done using Thermo Fisher Scientific UltiMate 3000 with a YMC-Actus Triart Phenyl 250 x 20 mml.D. S-5mikrom, 12 nm TPH12S05-2520WX Ser.No. 129XB10001 column.

6.1.3 Spectroscopic Descriptions

NMR spectra were obtained on Bruker BioSpin AVANCE NEO 600 MHz (500 MHz for 1H, 125 MHz for 13C). Chemical shifts are reported in ppm relative to the signal of the remaining protons of the deuterated solvent used. Coupling constants are given in Hz and the multiplicity is reported as singlet (s), doublet (d), triplet (t), quartet (qt), doublet of doublets (dd), triplet of doublets (td), doublet of triplets or multiplet (m). GC-MS analyses were performed on a capillary gas chromatograph with a fused silica column and helium as the carrier gas. Gas chromatography was done using Agilent Technology 7890A GC system, which was connected to a mass spectrometer , Agilent Technologies 5977A MSD, using electron ionization (EI) as ionization source. LC-MS analysis were performed on an Aglient 6420A triple quadrupole (QqQ configuration) mass analyzer using electrospray ionization (ESI). It is connected to an Agilent 1200 series LC module (binary pump, column compartment/oven and autosampler). The

column used was Agilent Eclipse Plus C18 RRHD 1.8 mikrometer 2.1 x50 mm 959757 USDAY 58154 B19306. HPLC analysis was done with an Agilent 1260 Infinity II using a YMC-Triart Phenyl 250 x 5.6 mm.D. S-5mikrom, 12 nm TPH12S05-2546PTH Ser.No. 126HB10054 column

6.2 Precurors Synthesis Route 1

6.2.1 Step 1 - Nucleophilic Aromatic Subistitution through Meisenheimer Complex

5-iodo-4-methyl-imidazole **1** (5.978 g, 24.41 mmol), methyl 2-fluoro-5-nitrobenzoate **2** (4.901 g, 24.61 mmol) and CsCO3 (10.42 g, 31.27 mmol) was added to a round bottom flask and dissolved in DMSO (25 mL) and stirred at rt for 25 hours. The color of the reaction mixture started as yellow, then turned orange and eventually dark red as the CsCO3 dissolved. The reaction mixture was then poured into ice water, precipitating creamy-beige crystals that were left in the water for 2 hours. The crystals were then filtrated using vacuum filtration. The crude crystals were then weighed (7.087 g). TLC analysis in pure EtOAc showed two spots, indicating two species, something that was confirmed with GC-MS. The two species were then separated using flash chromatography. Since the reaction was done at a relatively large scale, only 2.5 g of the crude was purified. The eluent system for the flash chromatography was a gradient, starting with pure hexane and increasing the amount of EtOAc until the first spot appeared on TLC analysis at around 50:50 EtOAc:Hexane. The eluent composition was held at 50:50 until the spot disappeared. The column was then flushed with MeOH to collect the remaining bi product. The fractions for each specie were then pooled and solvents removed under reduced pressure. The isolated **3a** was weighed (2.037 g, 5.26 mmol) and some of it dissolved in deuterated DMSO to perform NMR-analysis. If all of the crude were to be purified using this method for flash chromatography, the total yield would be (5.032, 13.00 mmol 53%). The isolated bi product **3b** was also weighed (0.534 g, 1.38 mmol) and and some of it dissolved in deuterated DMSO to perform NMR-analysis. **3a**: 1H NMR (600 MHz, CDCl3) δ 8.84 (d, J = 2.6 Hz, 1H), 8.45 (dd, J = 8.5, 2.6 Hz, 1H), 7.44 (d, J = 8.6 Hz, 1H), 7.41 (s, 1H), 3.74 (s, 3H), 1.97 (s, 3H). **3b**: 1H NMR (600 MHz, CDCl3) δ 8.87 (d, J = 2.6 Hz, 1H), 8.45 (dd, J = 8.6, 2.6 Hz, 1H), 7.76 (s, 1H), 7.47 (d, J = 8.5 Hz, 1H), 3.74 (s, 3H), 2.28 (s, 3H). DI-MS ESI was also performed $m/z = 387,796$.

6.2.2 Step 2 - Attempt of a Wohl-Ziegler Reaction

Crude Methyl 2-(4-iodo-5-methyl-1H-imidazol-1-yl)-5-nitrobenzoate **3a** (0.723 g, 1.87 mmol), NBS (0.488 g, 2.74 mmol), benzoyl peroxide (0.022 g, 0.091 mmol) was added to a round bottom flask and dissolved in 25 mL CHC3. The reaction was heated at reflux using an oil bath for 2 hours. The reaction mixture was yellow with a hint of orange at the beginning and quickly shifted to dark red after being heated. The crude reaction mixture was washed with brine x3. TLC analysis of the crude in 10:90 EtOAc:Hexane showed four different species present, which were separated using column chromatography, starting with 20:80 EtOAc:Hexane and gradually increasing the amount of EtOAc. The collected fractions were dissolved in deuterated DMSO to perform NMR-analysis. The first eluting specie was the undesired product with bromo in the 2 position, **4b**, while the other eluting species were not of interest. NMR analyisis of **4b/4e**: 1H NMR (600 MHz, DMSO) δ 8.71 (dd, J = 5.3, 2.7 Hz, 1H), 8.60 (td, J = 8.4, 2.7 Hz, 1H), 7.94 – 7.82 (m, 1H), 3.71 (d, J = 7.8 Hz, 3H), 1.87 (d, J = 9.1 Hz, 3H). DI-MS ESI was also performed ($m/z = 420,466$).

6.3 Precursor Synthesis route 2

6.3.1 Step 1 - Hydrolysis of Flumazenil

Flumazenil (0.196 g, 0.646 mmol) was dissolved in 25 mL MeOH in a round bottom flask and 10 equivalents (4M, 1.6 mL, 6.4 mmol) of NaOH was added. The mixture was heated to reflux for 3 hours using an oil bath. The reaction mixture was cooled to room temperature and solvents were dried off using a stream of N_2. The crude was then weighed, however it never dried and therefore the weight indicated more than a 100 % yield (therefore weight is not noted), and a fraction was dissolved in deuterated water to perform NMR-analysis. A sample was also concentrated to 50 μg/mL and analyzed with LC-MS ESI. $m/z = 276,298,551,573$. 1H NMR (600 MHz, D2O) δ 8.07 (s, 1H), 7.67 (dd, J = 6.0, 3.1 Hz, 1H), 7.66 – 7.64 (m, 1H), 7.51 (ddd, J = 9.0, 7.8, 3.0 Hz, 1H), 5.16 (d, J = 15.8 Hz, 1H), 4.47 (d, J = 15.8 Hz, 1H), 3.20 (s, 3H).

6.3.2 Step 2-1 - Attempt of Decarboxylative Iodation of Flumazenil Acid

Flumazenil acid **8-1** (0.196 g, 0.712 mmol) was dissolved with a solution of DCM (34 mL) and brine (32 mL). The pH was adjusted to pH = 12 with NaOH (4M) and HCl (2M). I2 (0.259 g, 1.02 mmol) was dissovled in DCM (14 mL) and added dropwise to the vigorously stirred reaction mixture, while the pH was remained at pH = 12 by periodic addition of NaOH whenever the reaction mixture turned sour. This was

monitored using pH paper. The reaction mixture was stirred for 18 hours at rt, before being quenched with 10 % Na2S2O3x2O and neutralizing by addition of HCl (2M until pH = 7) The organic layer was separated and the aqueous layer was pursued extracted with DCM. However, TLC analysis of the water phase and the organic phase only revealed the starting material, **8-1**, which was also confirmed using LC-MS ESI, $m/z = 276, 298, 551, 573$.

The same procedure was attempted using only MeOH in stead of DCM/brine. However this was also unsuccessful.

6.3.3 Step 2-2: Protodecarboxylation of Flumazenil Acid, Oil Bath Assisted Heating

Flumazenil acid **8-1** (0.031 g, 0.112 mmol), $Ag2CO_3$ (0.018 g, 0.065 mmol) was added to a 5 mL micro reactor vial and dissolved in DMSO (2 mL). A tiny drop of AcOH from the tip of a syringe was added to the solution. The reactor vial was sealed and heated (16 hours, 120 °C) by the means of an oil bath. The solution was white/grey in the beginning and dark brown with grey precipitates at the end. The reaction was quenched with 2 M HCl (2 mL). The aqueous phase (DMSO and water) was extracted with EtOAc (5 × 5 mL) and the organic phase was washed with brine (2 × 25 mL), however this step was not necessary/it needs adjustments before being useful. There were a lot of silver particles in the crude, that came into both the organic and water phase, therefore it is probably better to filtrate the crude. The water phase and the organic phase were both analyzed with LC-MS ESI, showing that the product and the reactant were in both phases (hence the extraction and washing not necessary), and that there was not a full conversion. **8-1** $m/z = 276, 298, 551, 573$, **9** $m/z = 232, 254, 465, 487$.

6.3.4 Step 2-3 - Protodecarboxylation of Flumazenil Acid, Microwave Assisted Heating

Flumazenil acid **8-1** (0.032 g, 0.134 mmol), $AgNO_3$ (0.034 g, 0.200 mmol) was added to a 5 mL micro wave reactor vial and dissolved in water (2 mL). A tiny drop of AcOH from the tip of a syringe was added to the solution before the vial was sealed and put in the microwave reactor (16 hours, 120 °C). The solution was white/grey in the beginning and dark brown with grey precipitates at the end. The cap of the vial was bulped upwards, indicating the formation of CO2 gas. The grey precipitates were filtered of using vacuum filtration and the filtrate was evaporated and analyzed using GC-MS EI $m/z = 232(M^+), 203, 189, 147, 42$ and LC-MS ESI. A fraction of the dried filtrate was dissolved in deuterated water to perform NMR-analysis, however more work up and isolation is needed to achieve a useful spectrum. The filtrated crude was dried using N_2

flow over the weekend and weighed (0.032 g, 0.14 mmol, 76 %).

6.3.5 Step 3-1 - Attempt of Halogenation of Protodecarboxylated Flumazenil Acid using DIH in Mild Conditions

8-fluoro-5-methyl-4,5-dihydro-6H-benzo[f]imidazo[1,5-a][1,4]diazepin-6-one, **9** (0.032 g, 0.138 mmol) was added to a micro wave reactor vial and dissolved in 2 mL water and immersed in an ice-bath. The mixture was stirred until the solids were dissolved. NaOH (4M, 1.1 mL, 4.7 mmol) was then added. *N,N*'-diiodo-5,5-dimethyl hydantoin, DIH, (0.013 g, 0.035 mmol) was dissolved in conc H2SO4 (0.2 mL). This was then added drop wise to the reaction mixture over the course of 10 min. After this, the mixture was immediately neutralized with a 50:50 mixture of AcOH:H2O until pH = 6. The solution was saturated with NaCl and extracted with diethyl ether (3x5 mL). The organic phases were combined and extracted with 10 % HCl (3x5 mL). It was confirmed using TLC that there were no UV signal from the crude water phase and the organic phase, and that the compound was transferred to the acidic water phase. The water was evaporated using a flow of nitrogen gas over the course of a couple of days. It was confirmed by DI-MS with positive ESI that only the starting material **9** was present $m/z = 232, 254, 465, 487$ and therefore the synthesis was concluded unsuccessful.

6.3.6 Step 3-2 - Attempt of Halogenation of Protodecarboxylated Flumazenil Acid using DIH in Harsh Conditions

8-fluoro-5-methyl-4,5-dihydro-6H-benzo[f]imidazo[1,5-a][1,4]diazepin-6-one, **9** (0.038 g, 0.138 mmol), DIH (0.079 g, 0.208 mmol) and KI (0.245 g, 1.64 mmol) were transferred to a 15 mL micro wave reactor vial immersed in an ice bath. Water (2 mL) was added, and the mixtrue was stirred vigorously while adding conc H2SO4 (1 mL) over the course of 1 minute. After the addition, NaOH (1.9 mL, 4 M) was added. The solution was then immediately neutralized with a solution of 50/50 acetic acid and water to pH = 6. DI-MS with positive ESI analysis of the crude showed no sign of the desired product.

6.3.7 Step 2-4a - Attempt of Decarboxylative Bromination of Flumazenil Acid with NBS and $Pd(OAc)_2$ Under Inert Conditions

Flumazenil acid **8-1** (0.0541 g, 0.197 mmol), NBS (0.036 g, 0.202 mmol), Pd(OAc)2 (0.0064 g, 0.029 mmol) were transferred into a 5 mL pre-dried micro wave reactor vial, sealed and dried with vacuum and flushed with argon. Anhydrous DMF (1 mL) was then transferred inertly to the vial which was again flushed with argon. The reaction was stirred at 80 °C for 4 hours before being cooled to rt. The crude was yellow-orange with the typical succinimide layer on top. The crude was vacuum filtered with

celite and the DMF in the filtrate was dried off by the means of flushing with N2 over the weekend. The filtrate was analysed using LC-MS ESI. However, there were no indication of the desired product, only intense signals from the starting material **9** was present $m/z = 276$. The synthesis was therefore unsuccessful.

6.3.8 Step 2-4b - Attempt of Decarboxylative Iodation of Flumazenil Acid using CuI and $Pd(OAc)_2$ under Aerobic Conditions

Flumazenil acid **8-1** (0.0656 g, 0.238 mmol), CuI (0.0485 g, 0.255 mmol), $Pd(OAc)_2$ (0.0086 g, 0.024 mmol) were transferred into a 5 mL pre-dried micro wave reactor vial. The reaction vial was then sealed and dried with vacuum and flushed with argon. Anhydrous DMF (2 mL) was then transferred inertly to the vial which was again flushed with argon. A balloon was then filled with oxygen and attached to the reaction vial by the means of a syringe cut in half with a needle. Another syringe was then used to drag oxygen out of the balloon and into the reaction vial, creating aerobic reaction conditions. The reaction was stirred at 150 °C for 22 hours before being cooled to room temperature. The crude was vacuum filtered with celite and the DMF was dried off by the means of flushing with N_2 over the weekend. The crude appeared as brown and viscous. LC-MS ESI analysis revealed full conversion of the starting material, however, there was no indication of the desired product.

6.3.9 Step 2-4c - Attempt of Decarboxylative Iodation of Flumazenil Acid using CuI under Aerobic Conditions

Flumazenil acid **8-1** (0.0592 g, 0.215 mmol) and CuI (0.0459 g, 0.24 mmol) were transferred into a 5 mL pre-dried micro wave reactor vial. The reaction vial was then sealed and dried with vacuum and flushed with argon. Anhydrous DMF (2 mL) was then transferred inertly to the vial which was again flushed with argon. A balloon was then filled with oxygen and attached to the reaction vial by the means of a syringe. Another syringe was then used to drag oxygen out of the balloon and into the reaction vial, creating aerobic reaction conditions. The reaction was stirred at 150 °C for 28 hours before being cooled to room temperature. The crude was vacuum filtered with celite and the DMF was dried off by the means of flushing with N2 over the weekend. LC-MS ESI analysis revealed full conversion of the starting material, however, there was no indication of the desired product.

6.3.10 Step 2-5a - Attempt of Decarboxylative Bromination of Flumazenil Acid, Microwave Assisted Heating

Flumazenil acid **8-1** (0.0517 g, 0.188 mmol), $AgNO_3$ (0.0367 g, 0.216 mmol) and NBS (0.0334 g, 0.188 mmol) was added to a 20 mL micro wave reactor vial and dissolved

in DMSO (1 mL) and sealed. The reaction mixture was put in a microwave reactor (16 hours, 120 °C). This reaction lead to breakage of the reaction vial and the experiment was never analyzed properly.

6.3.11 Step 2-5b - Attempt of Decarboxylative Iodation of Flumazenil Acid, Microwave Assisted Heating

Flumazenil Acid **8-1** (0.0500 g, 0.182 mmol), $AgNO_3$ (0.0321 g, 0.189 mmol) was added to a 20 mL micro wave reactor vial. I_2 (0.0266 g, 0.105 mmol) was dissolved in DMSO (1 mL) and added to the reaction vial and sealed. The reaction mixture was supposed to be put in a microwave reactor (16 hours, 120 °C), however, due to the explosion of the reaction vial of step 2-5a, the reaction mixture was never heated, but left standing at room temperature without stirring for approximately 72 hours. The reaction mixture had during this time turned from a cloudy orange-red solution to a see through blank solvent with white and yellow particles lying on the bottom of the reaction vial, indicating iodine being consumed somehow. Upon DI-MS with positive ESI, Flumazenil Acid **8-1** was still present, and the change in color can probably be attributed to the formation of AgI salt, although this was never confirmed.

6.4 Optimization of the Process for [^{11}C]-Methylation of Flumazenil - QC Method

6.4.1 2^2 factorial design for the QC method

A $\mathbf{2}^2$ factorial design was made to see what effect the chosen factors had on the separation. The chosen factors were **A**: percentage of EtOH in the EtOH:Water eluent system and **B**: the flow rate. The high level for **A** was 20 % while the low level was 10 %. The high level for **B** was 1.3 mL/min while low level was 0.9 mL/min. A higher flow rate would be preferred, however the system could not sustain much higher pressure as there is a lot of back pressure using ethanol. A standard solution of Flumazenil (1.25 mg/mL) and N-Desmethyl Flumazenil (0.04 mg/mL) in 50:50 EtOH:Water was used for the experiments. The retention time and resolution were chosen as the responses to be measured. The four experiments in the $\mathbf{2}^2$ factorial design were measured and a total of 3 replicates of the design were done to check for stability. The resolution was measured using the software of the Agilent 1260 infinity HPLC system and time was measured at the right tale tip of the last eluting peak in the chromatogram.

6.5 Process for the Production of [^{11}C]-Methylated Flumazenil

6.5.1 Preparing HPLC Systems Prior to Production and Preparing the Work Station

First, EtOH and H2 was purged on the analytical HPLC. A a sample run with flow rate of 1.5 mL/min and 8:92 ethanol:water was put in the queue, ready to start analysis as soon as the production was finished. Ethanol and water was degassed in an ultrasonic bath and then purged on the semi-preparative HPLC. The settings were put to a 4.75 mL/min flow rate and 50:50 ethanol:water. The purge valve was then closed to check for a stable pressure in the range where it normally lies (ca. 280 bar). When checked, the flow rate was put to standby while conditioning the system. N-desmethyl Flumazenil (1 mg, 0.2 mL of 0.2 mg/mL in DMF) was transferred to the reaction vial. A 1M/1M $H_2PO_4^-$/HPO_4^{2-} buffer solution (0.2 mL) together with EtOH (0.2 mL) was put in a container in the automated system, ready to quench the reaction when the script tells it to. The EtOH was put there to minimize the disturbance of the polarity of the mobile phase when using the chromatographic method after the reaction. Saline (3 mL) was put in the product vial to dilute the product. Lead and wolfram equipment was put into the work station and made ready for handling the radioactivity safely when transporting for quality control.

6.5.2 Conditioning of the Synhtra System

Conditioning is very important as atmospheric CO_2 will dilute the [^{11}C]CO_2. Conditioning was done by filling the thermos with liquid nitrogen and then running the script "Conditioning MeI". What happens during this script is mainly heating the different traps (see Figure 2.4) and releasing all unwanted residues before filling the system with inert gas and cooling some of the traps so they are ready for production. It is important to do the conditioning right before the start of production, as there is not unlimited amounts of liquid nitrogen for cooling in the system, and the system starts with the CO_2 trap and the CH_4 trap cooled. If these traps are heated to rt between the conditioning and the production, there is no point to do conditioning.

6.5.3 Production of [^{11}C]CO_2

The production of [^{11}C]CO_2 was done in a GE PETtrace 800 cylcotron through a $^{14}N(p,\alpha)^{11}C$ nuclear reaction using a target gas consisting of N_2 with a quality of 6.0 and with 1% O_2 present.

6.5.4 Production of [^{11}C]-Flumazenil

The high temperature oven for converting methane to MeI was set to 730 °C. The CO_2 trap was set to -180°C. The methane trap was set to -50 °C. He and H_2 gas was verified connected to the system. The script "Flumazenil klar" was used to run the production. What the script does, is described in Chapter 2, and visualized in Figure 2.4. The script also includes the chromatographic separation method for the semi-preparative radio HPLC system using a RP C-18 column. The chromatographic method was 4.75 mL/min flow rate and 50:50 EtOH:H_2O. The product was then collected in a product vial where it was diluted with 3 mL saline. The system used for the production was a Synthra MeI Plus Research Module, see Figure 3.1.

6.5.5 Quality Control

A sample of the product (1 mL) was transferred to a sample glass and 20 μL were analyzed for quality control with an analytical radio HPLC system. Flow rate was set to 1.1 mL/min with a 8:92 EtOH:H_2O mobile phase. UV measuring at 245 nm. Analytical radio HPLC system: Agilent 1260 infinity and a radio HPLC detector LabLogic Posi RAM model-4 with a 00B-4435-B0 Gemini 5 micrometer C18 110 Å LC column 50x2mm.

6.5.6 Trapping of [^{11}C]-MeI in DMF in the Reaction Vial

The same was done here as for the process for the production of [^{11}C]-methylated Flumazenil, however the process was stopped before the chromatographic separation method on the semi-preparative radio HPLC.

Compound #	Structure	Compound #	Structure
3a	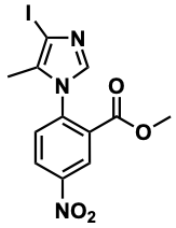	**3b**	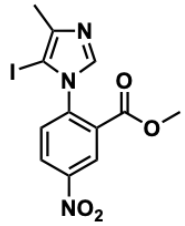
4a	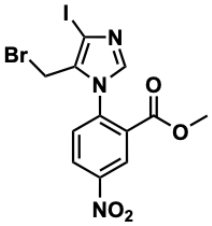	**4b**	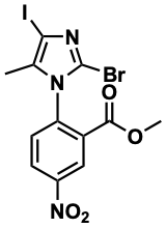
4e	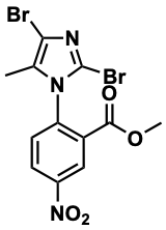	**4f**	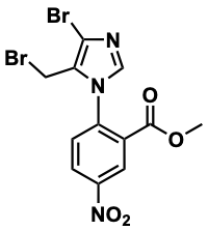
8	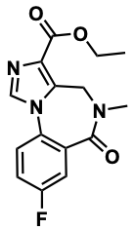	**8-1**	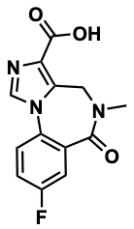
9	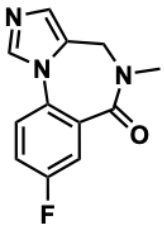	**7a**	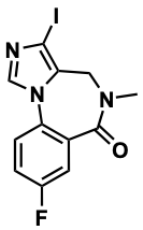
7b	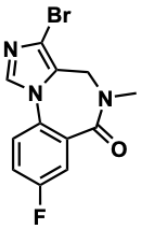	**7c**	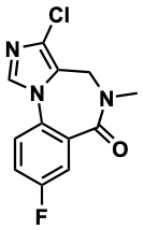

Table 6.1: Table of the most relevant compounds. 7x indicates either 7a, 7b or 7c.

Chapter 7

Appendix Synthesis 1 Step 1

7.1 Spectroscopic and Spectrometric Data from Step 1 of Synthesis Route 1

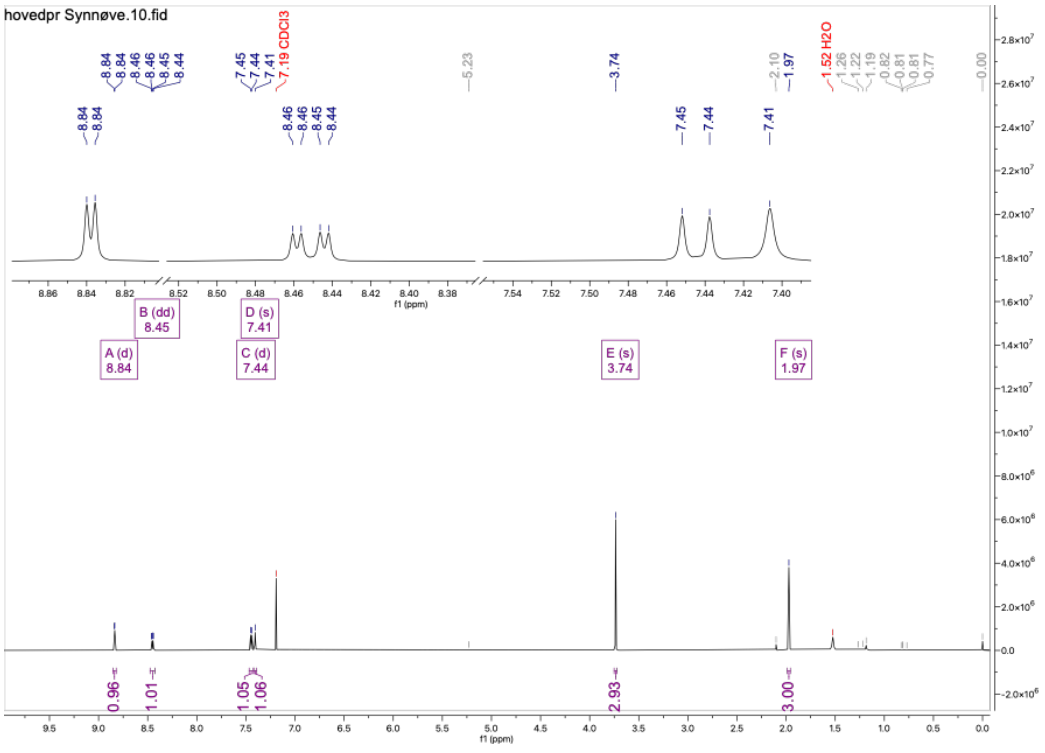

*Figure 7.1: ^{1}H-NMR spectrum of **3a***

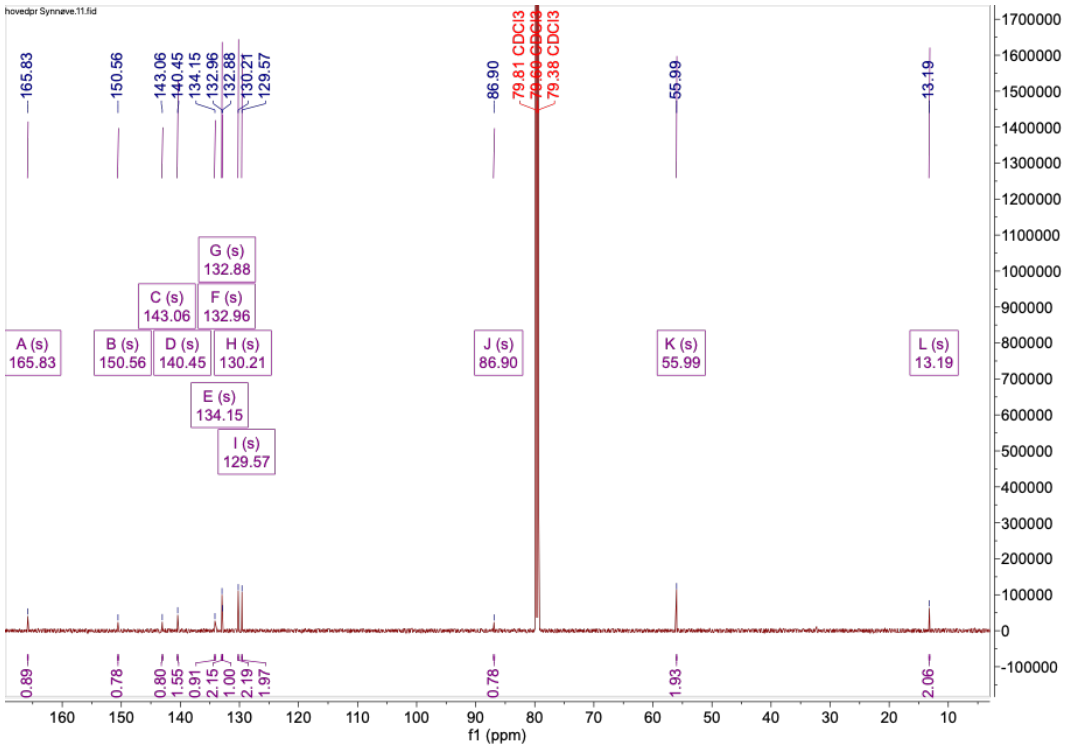

*Figure 7.2: ^{13}C-NMR spectrum of **3a***

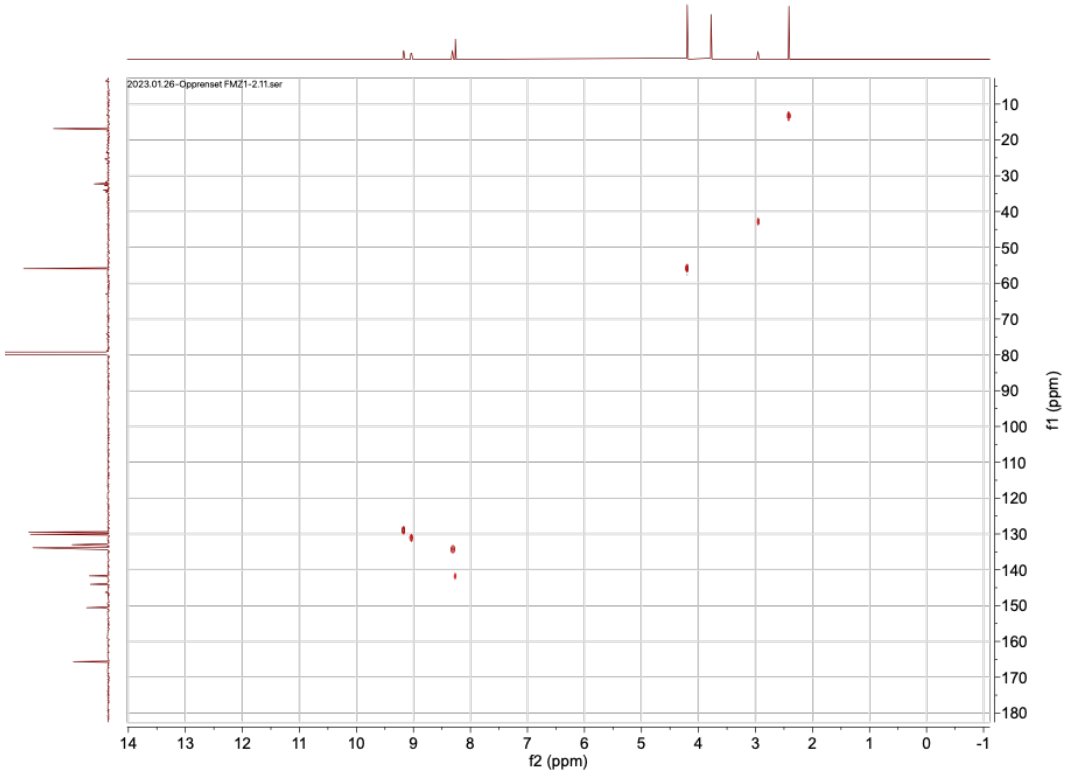

*Figure 7.3: ^{1}H-^{13}C HSQC 2D NMR experiment of **3a***

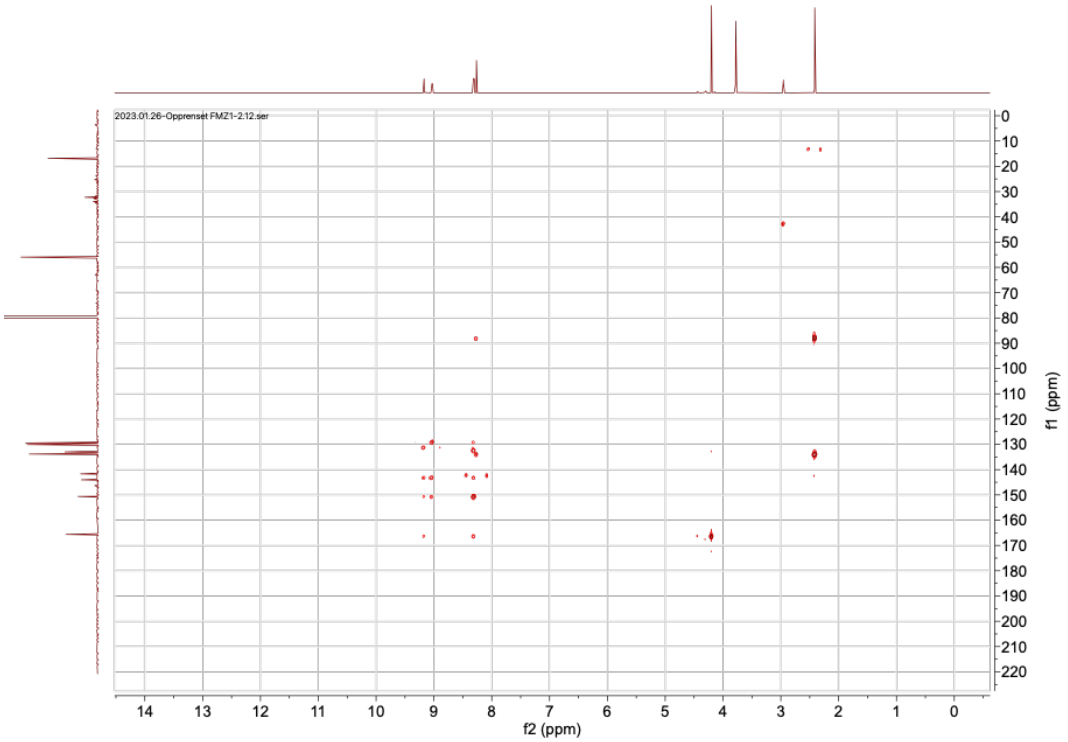

*Figure 7.4: ^{1}H-^{13}C HMBC 2D NMR experiment of **3a***

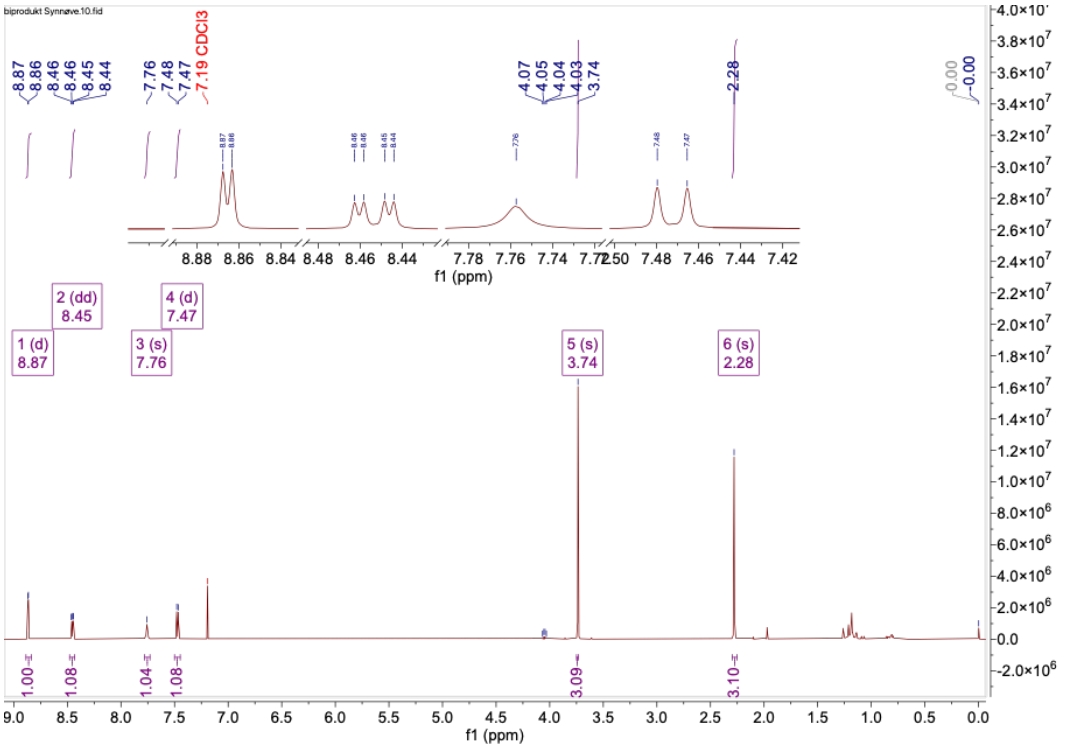

*Figure 7.5: ^{1}H-NMR spectrum of **3b***

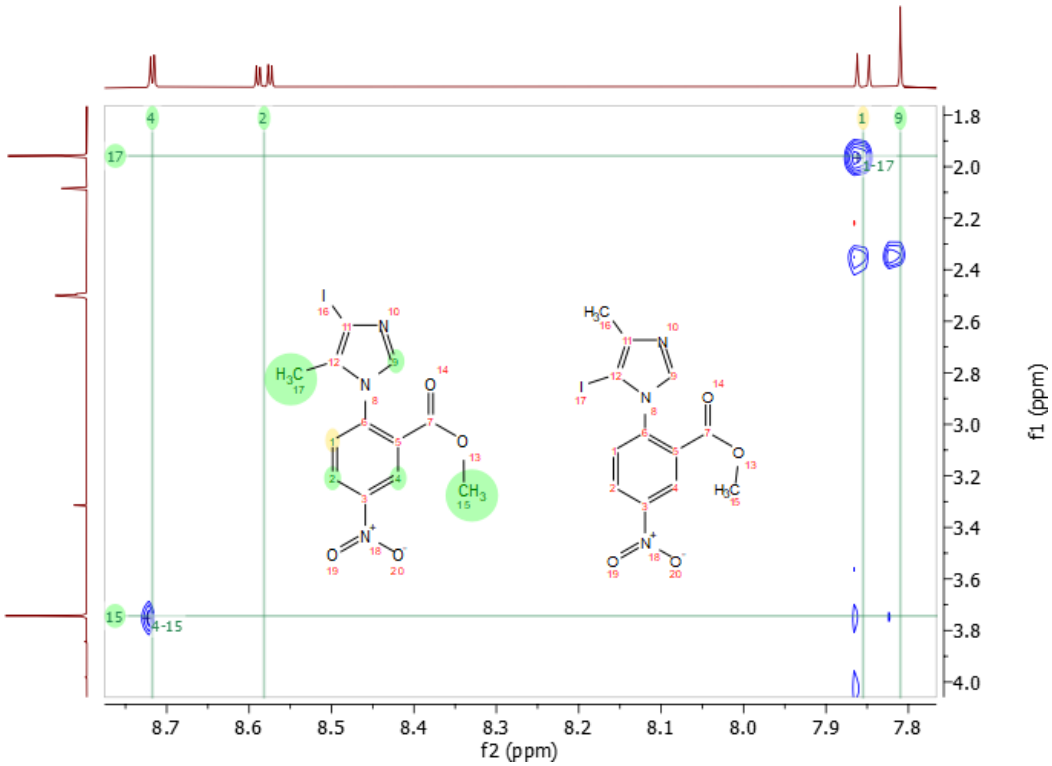

*Figure 7.6: ^{1}H-^{1}H-NOESY 2D experiment of **3a***

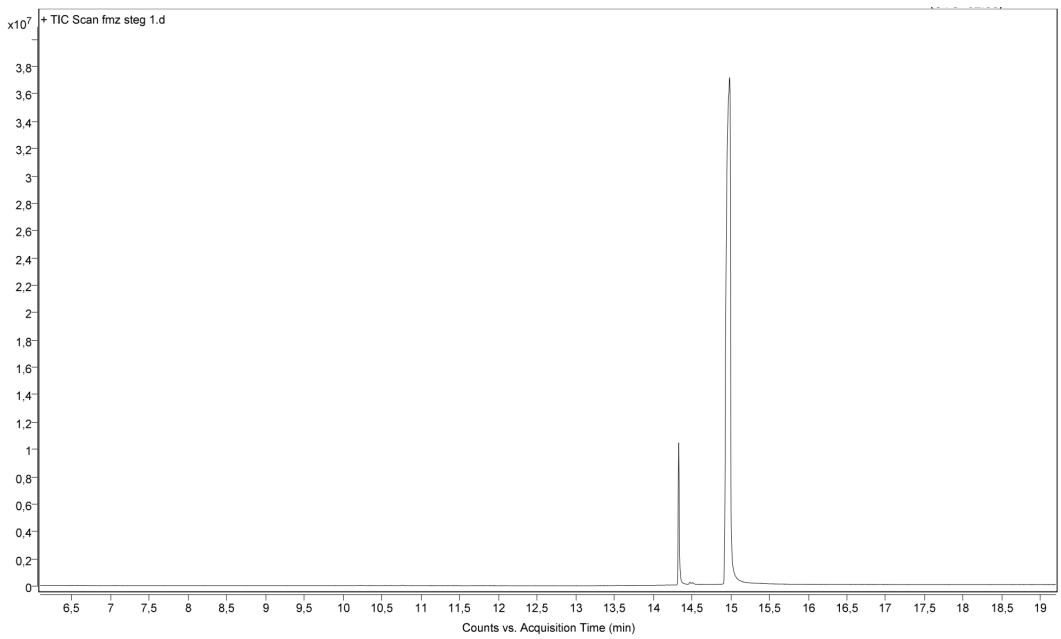

Figure 7.7: GC-MS TIC chromatogram for the crude of step 1 of synthesis route 1

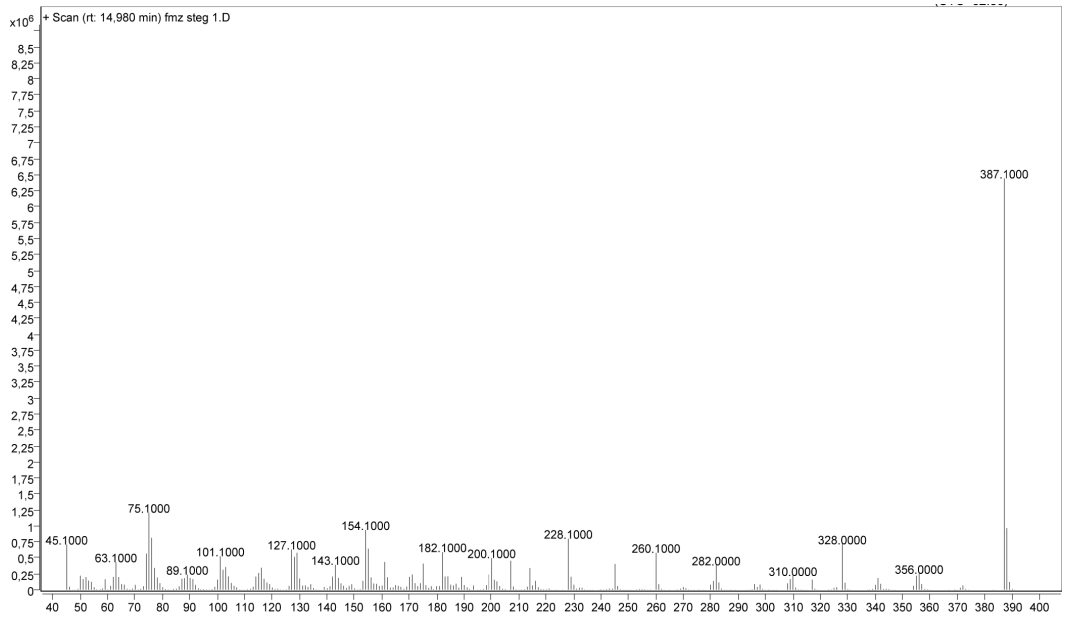

*Figure 7.8: EI MS spectrum of **3a**. Peak belongs to second peak in the TIC chromatogram in Figure 7.7.*

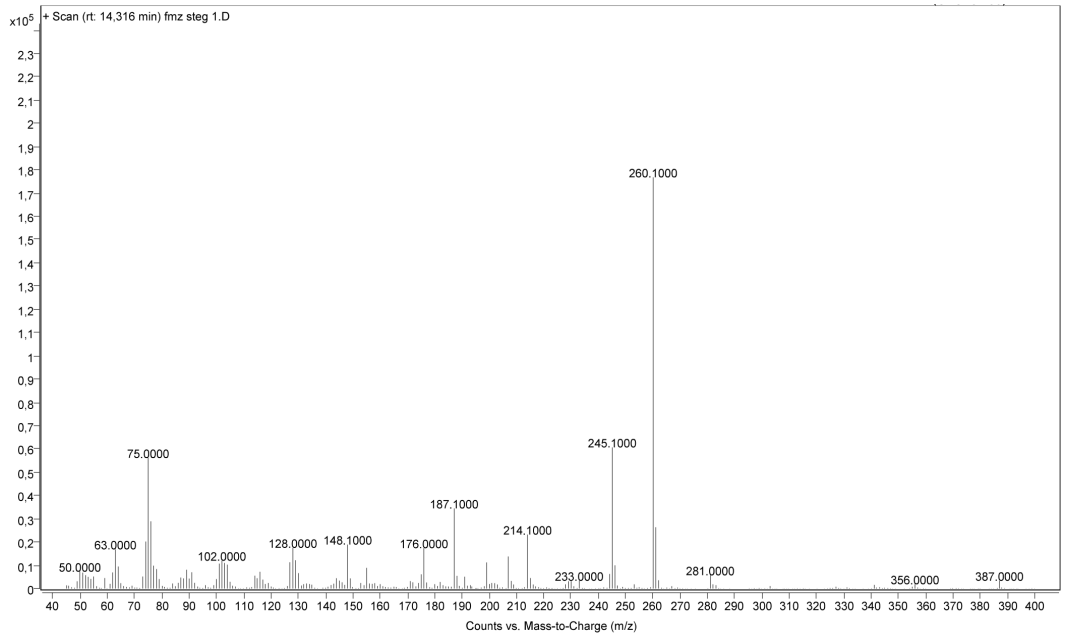

*Figure 7.9: EI MS spectrum of **3b**. Peak belongs to first peak in the TIC chromatogram in Figure 7.7.*

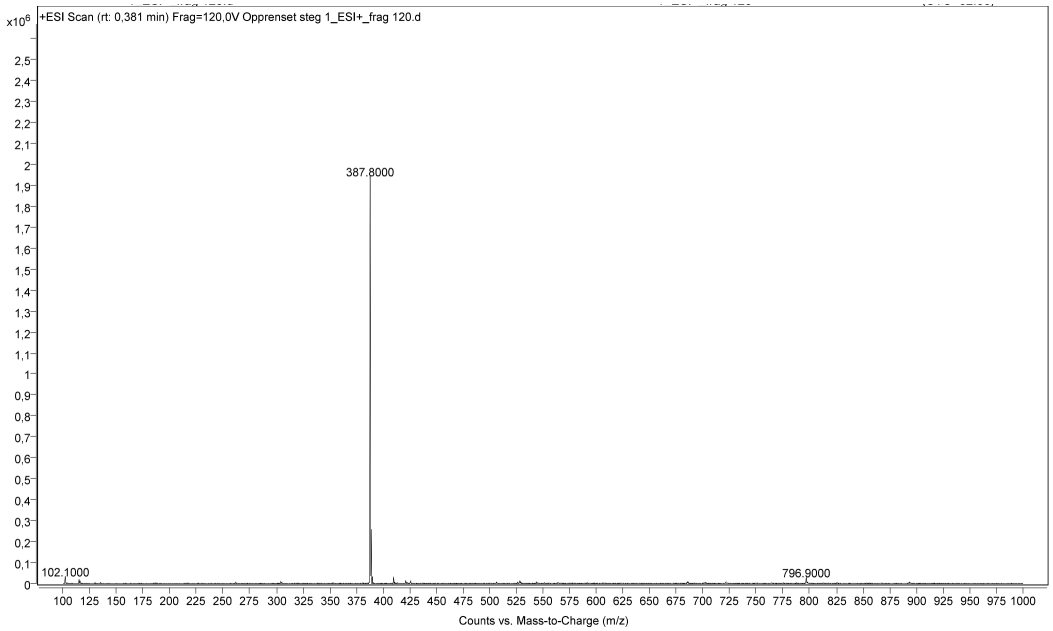

*Figure 7.10: ESI MS spectrum of isolated **3a***

Chapter 8

Appendix Synthesis 1 Step 2

8.1 Spectroscopic and Spectrometric Data for Step 2 of Synthesis Route 1, Experiment 7

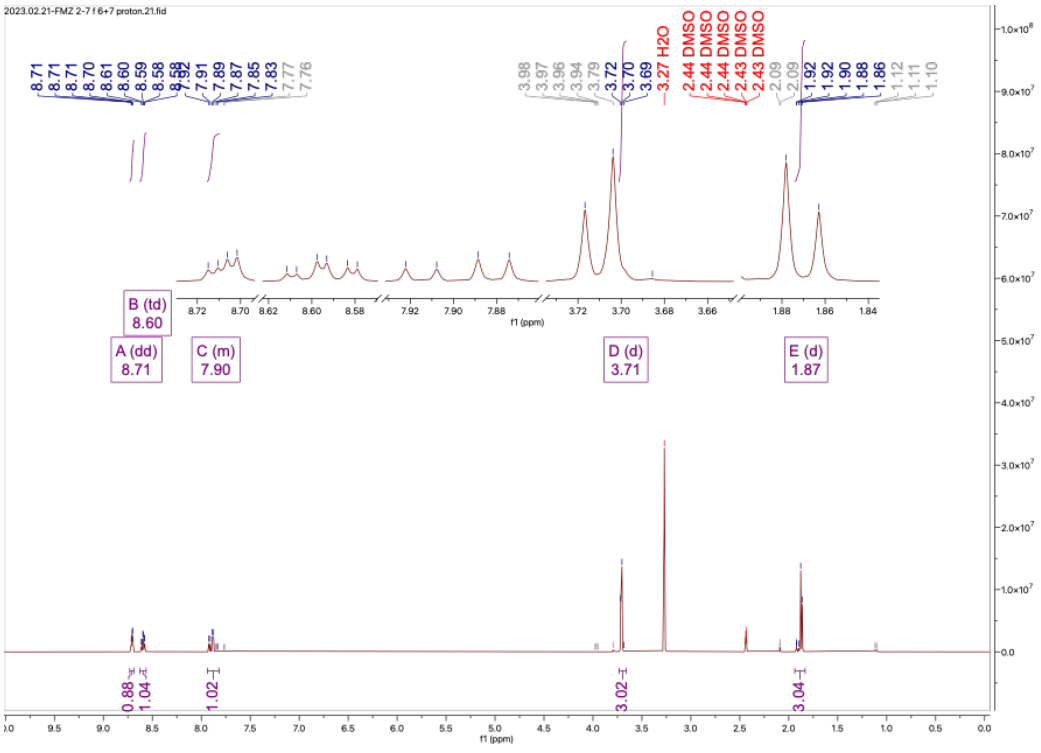

*Figure 8.1: ^{1}H-NMR spectrum **4b/4e***

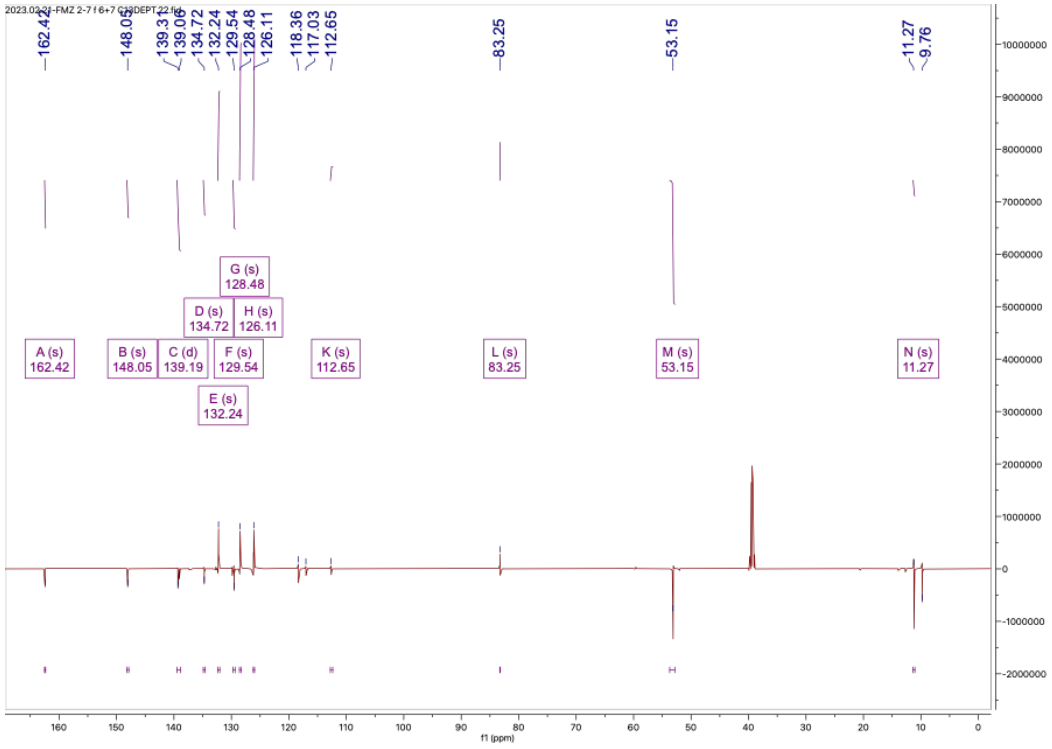

*Figure 8.2: ^{13}C-NMR spectrum **4b/4e***

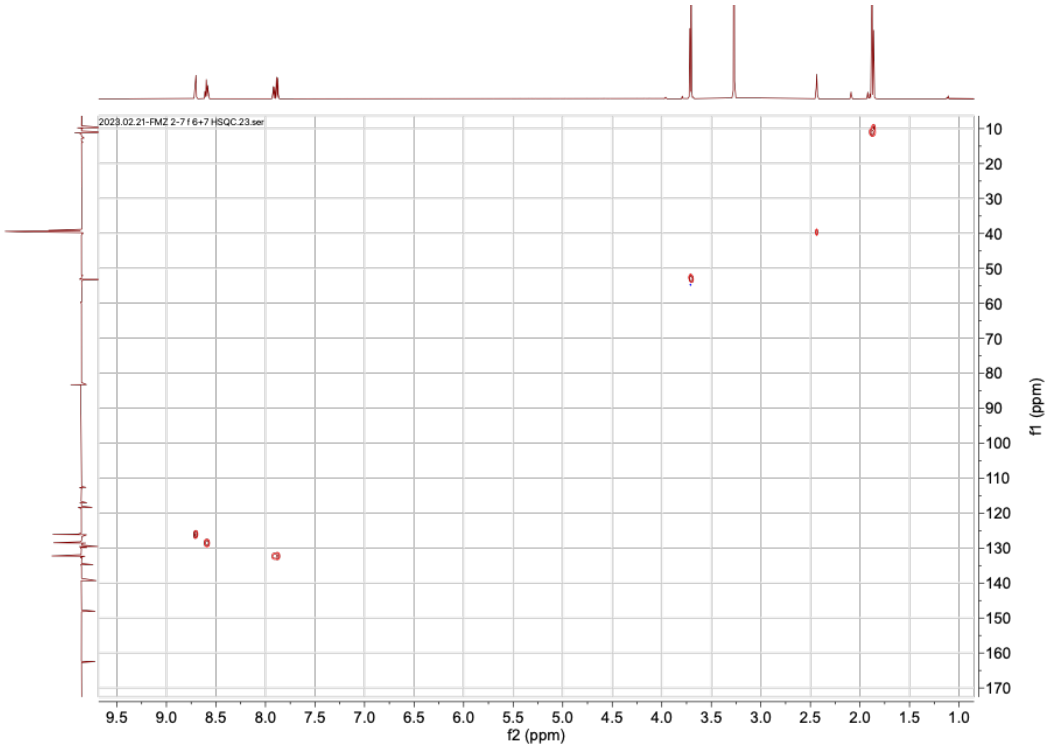

*Figure 8.3: ^{13}C-^{13}C HSQC 2D experiment of **4b/4e**.*

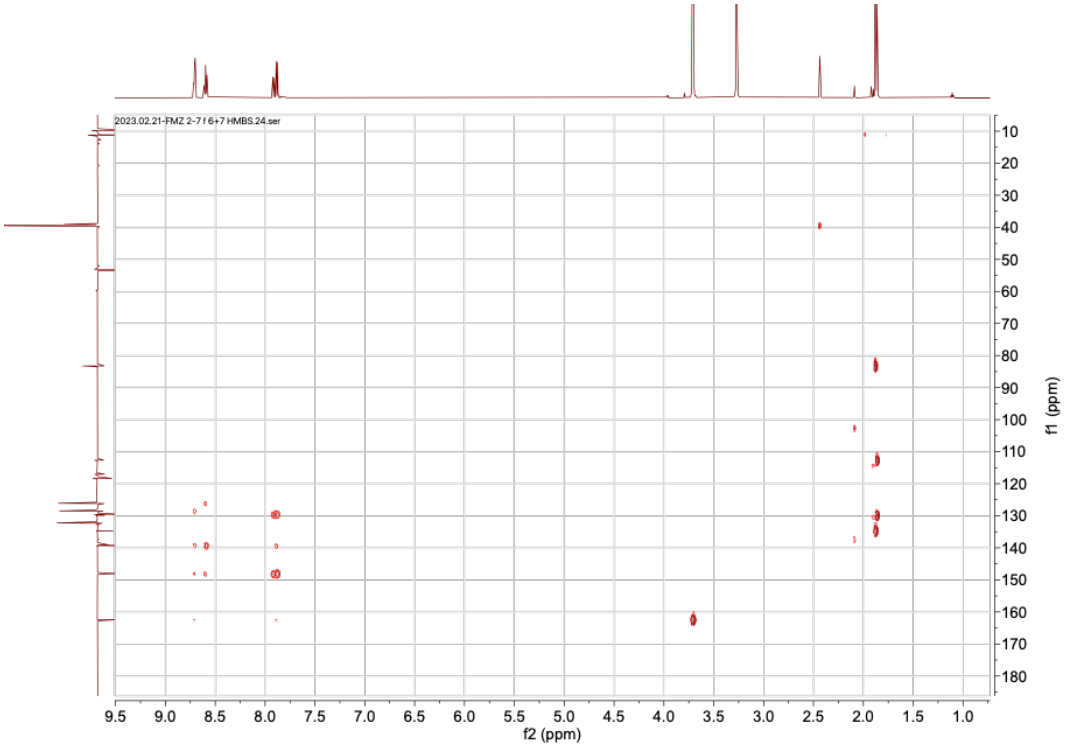

*Figure 8.4: ^{13}C-^{13}C HMBC 2D experiment of **4b/4e**.*

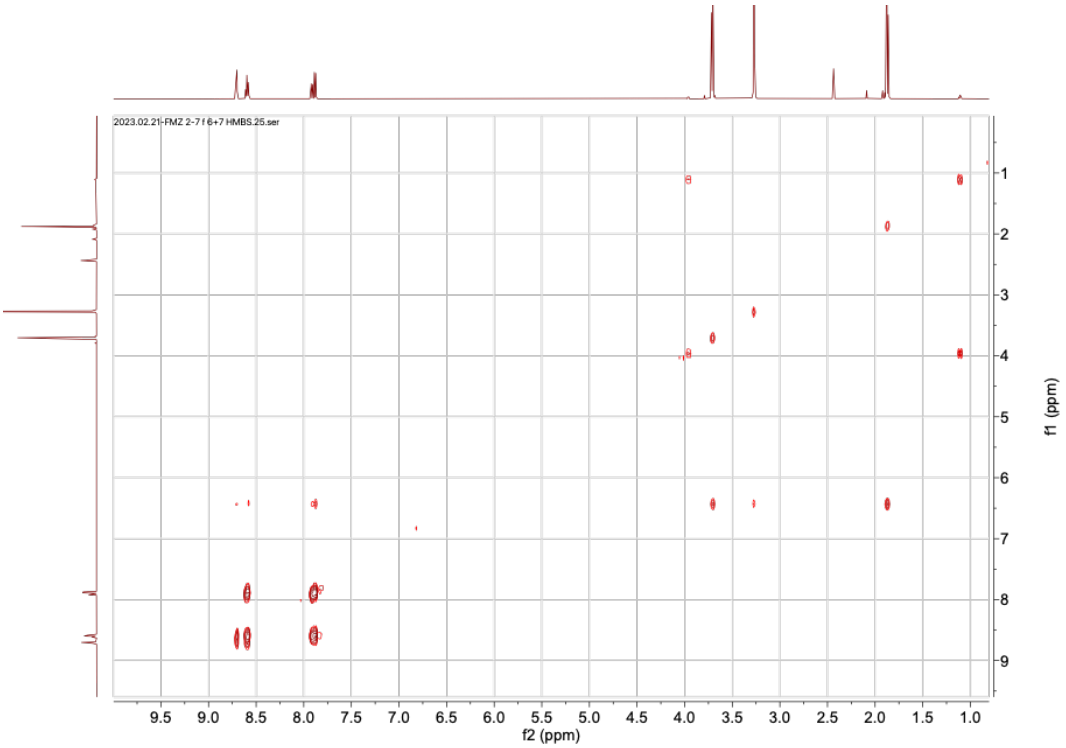

*Figure 8.5: ^{1}H-^{1}H-COSY 2D experiment of **4b/4e**.*

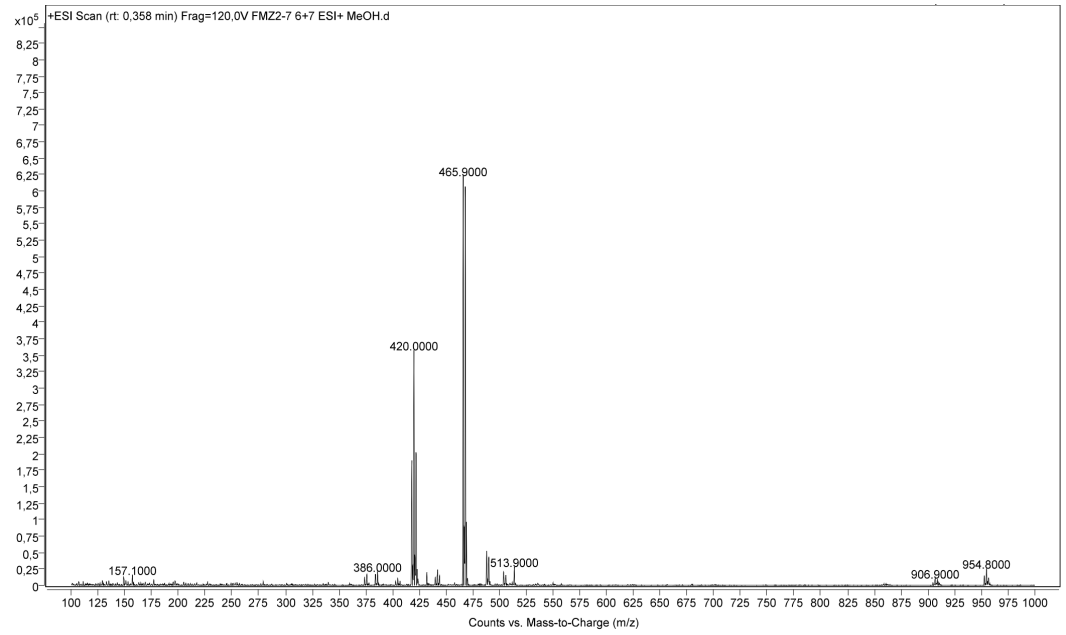

*Figure 8.6: ESI MS spectrum of **4b/4e***

8.2 Spectroscopic and Spectrometric data for Step 2 of Synthesis Route 1, Experiment 8

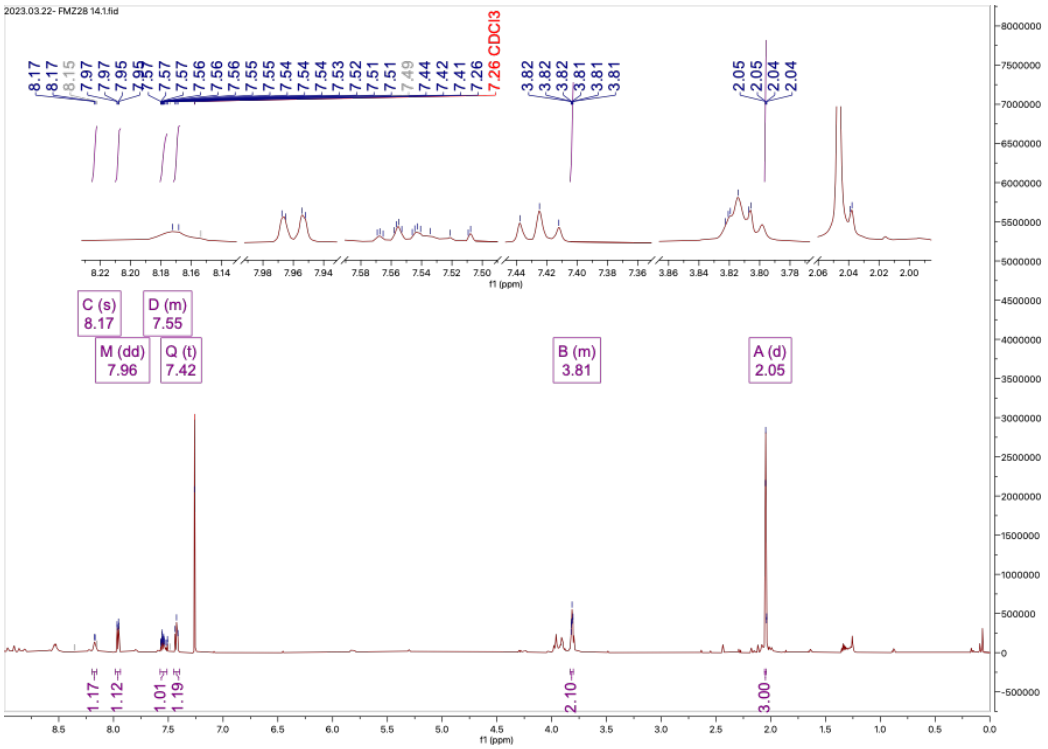

Figure 8.7: ^{1}H-NMR spectrum of fraction 1 of interest from experiment 8 of step 2

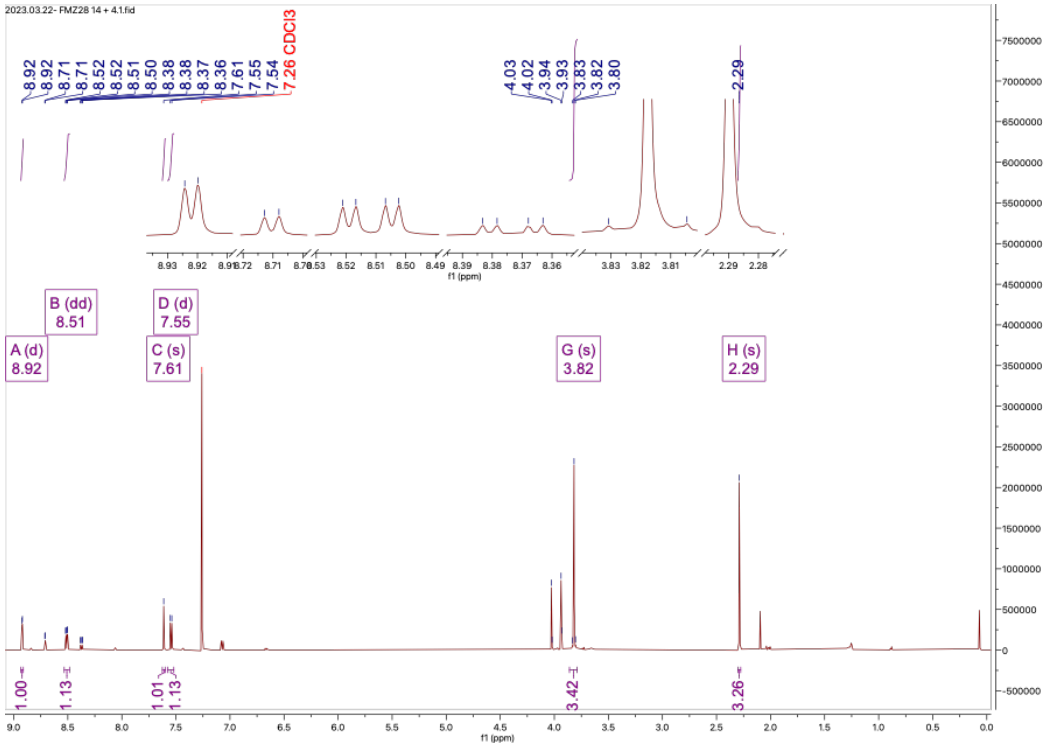

Figure 8.8: ^{1}H-NMR spectrum of fraction 2 of interest from experiment 8 of step 2

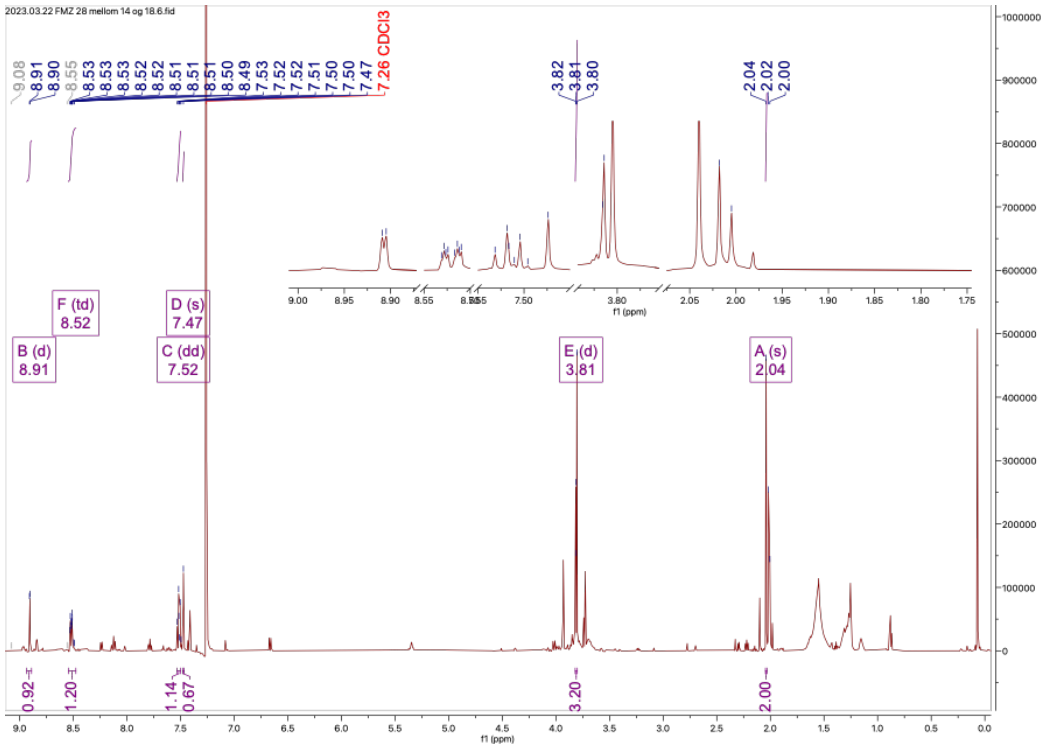

Figure 8.9: ^{1}H-NMR spectrum of fraction 3 of interest from experiment 8 of step 2

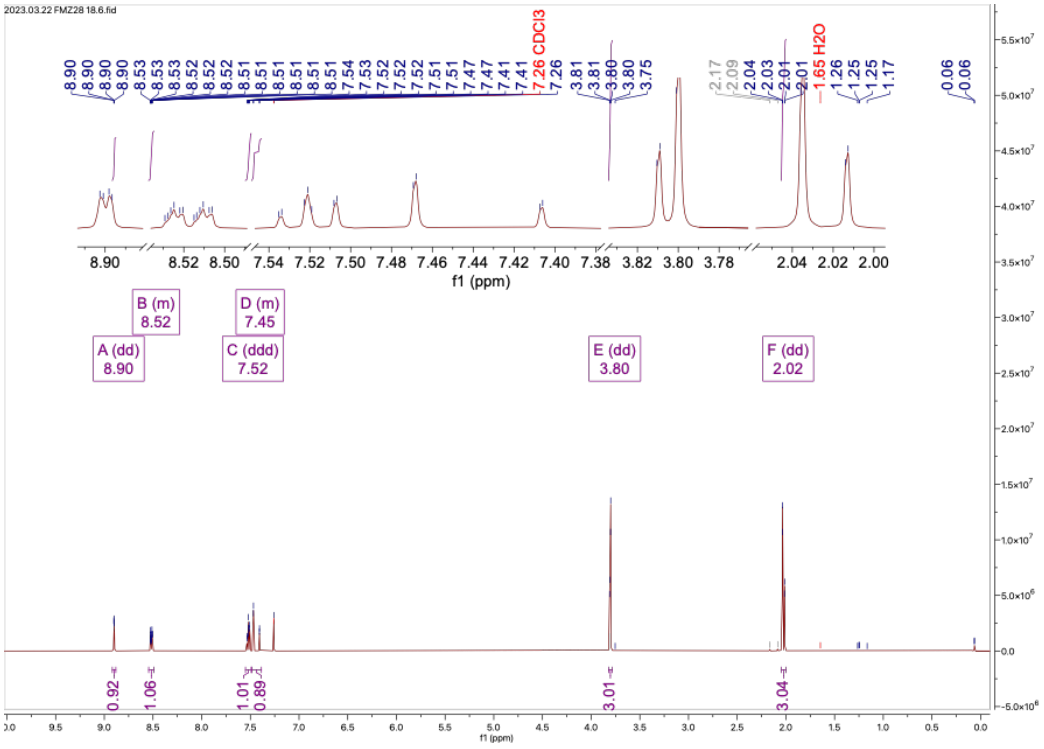

Figure 8.10: [1]H-NMR spectrum of fraction 4 of interest from experiment 8 of step 2

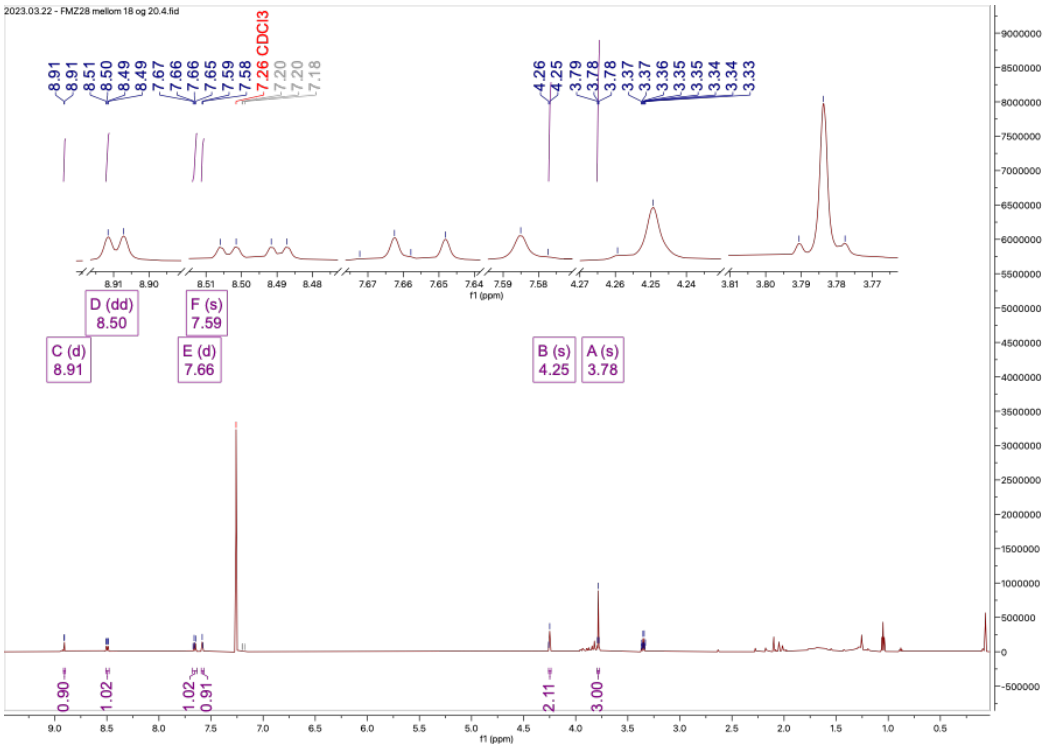

Figure 8.11: [1]H-NMR spectrum of fraction 5 of interest from experiment 8 of step 2

Chapter 9

Appendix Synthesis 2 Step 1

9.1 Spectrometric and Spectroscopic Data from Step 1 of Synthesis Route 2

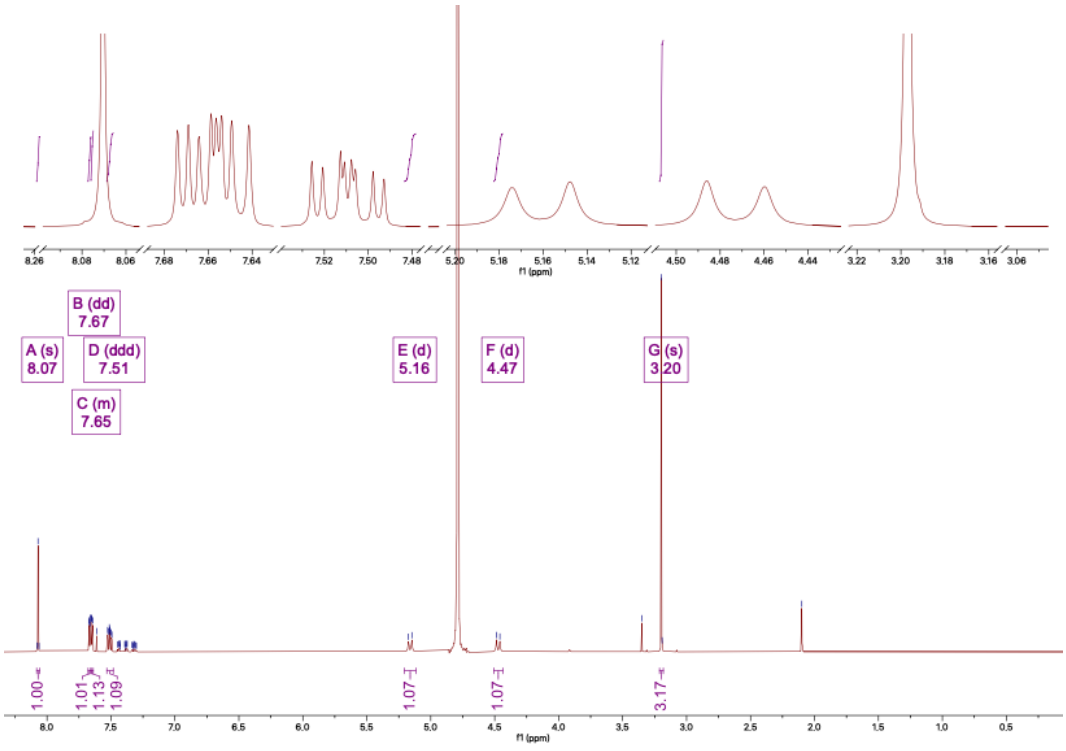

Figure 9.1: [1]H-NMR spectrum of Flumazenil Acid ***8-1***

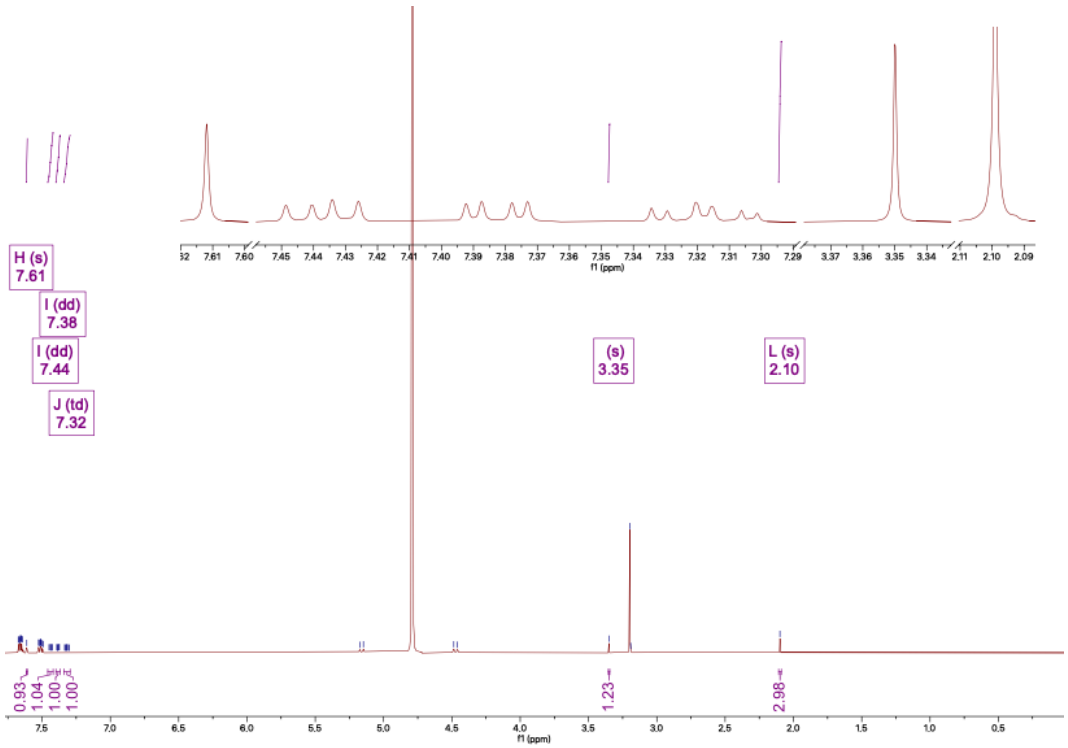

Figure 9.2: ^{1}H-NMR spectrum of the bi product in the hydrolysis of Flumazenil.

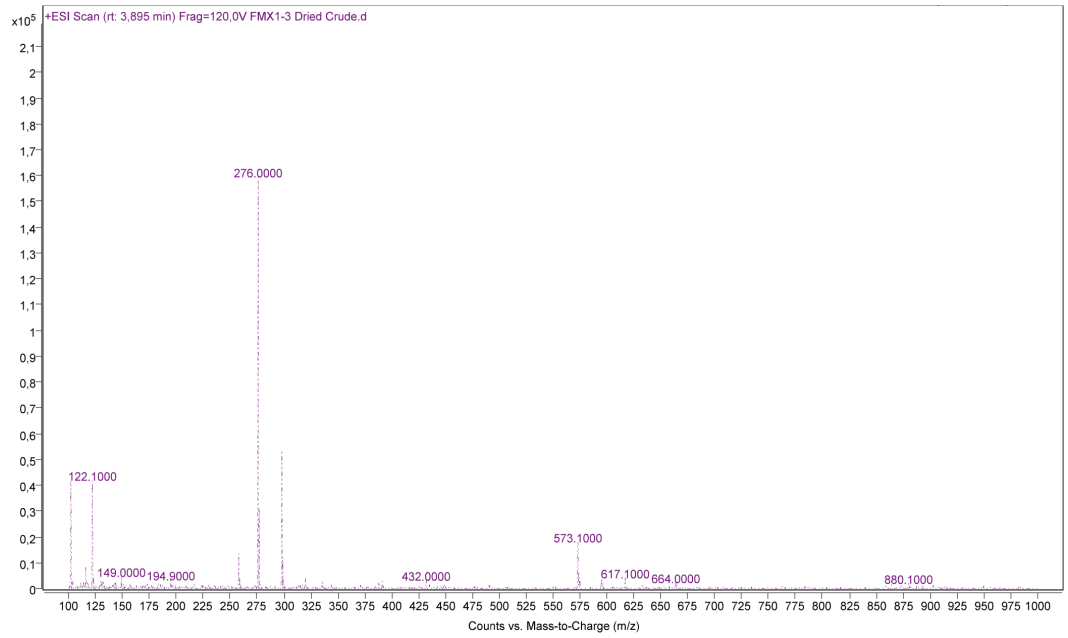

*Figure 9.3: ESI MS spectrum of Flumazenil Acid **8-1**.*

Chapter 10

Appendix Synthesis 2 Step 2-2 and 2-3

10.1 Spectrometric Data for Step 2-2 of Synthesis Route 2

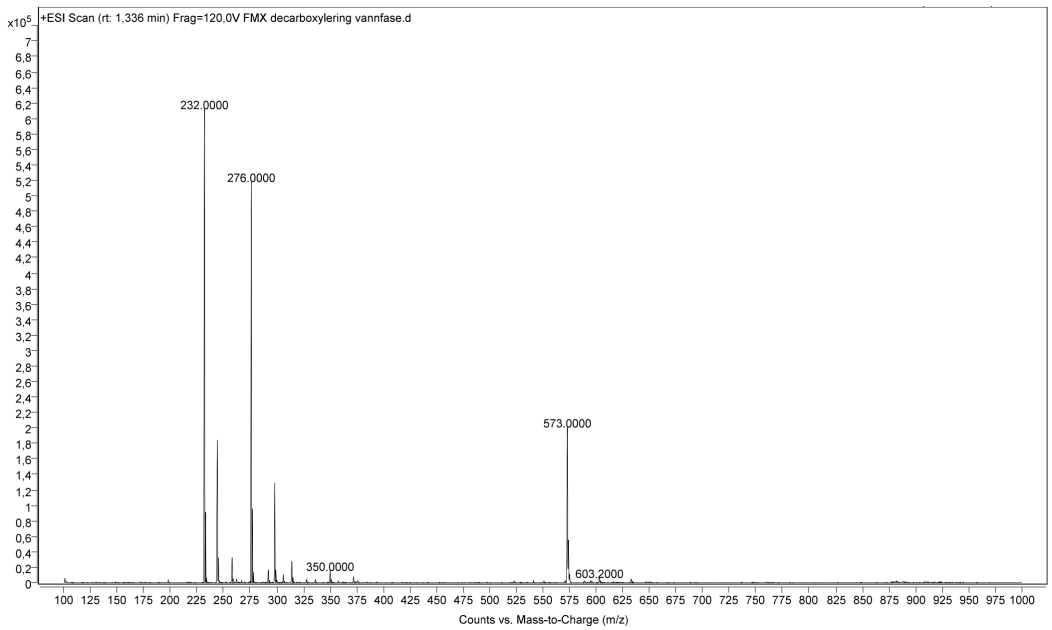

*Figure 10.1: ESI MS spectrum of **9** when using oil assisted heating.*

10.2 Spectrometric Data for Step 2-3 of Synthesis Route 2

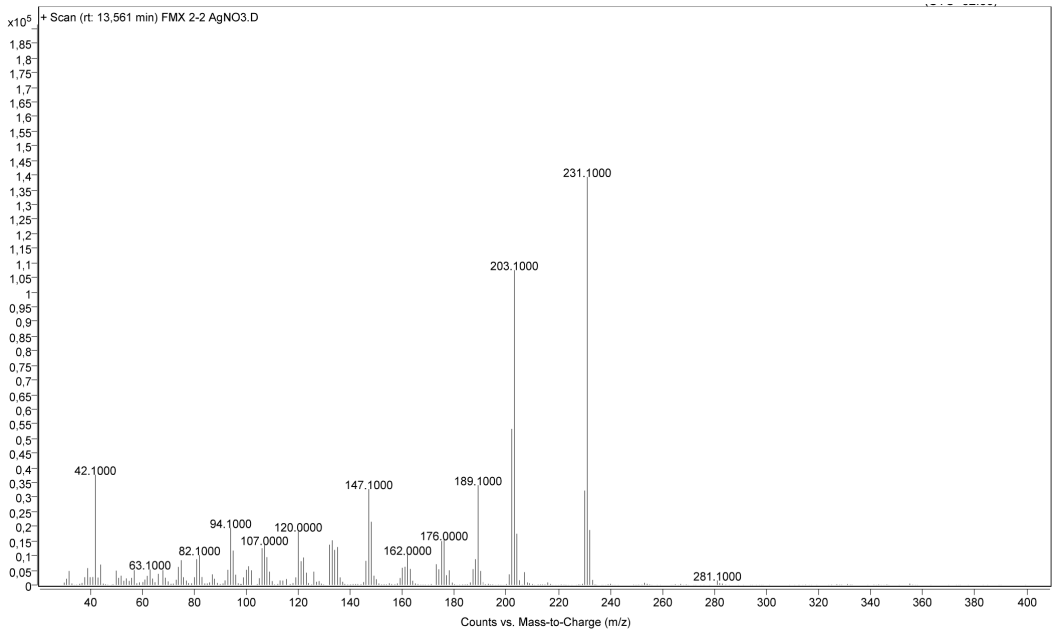

*Figure 10.2: EI MS spectrum of **9** when using $AgNO_3$*

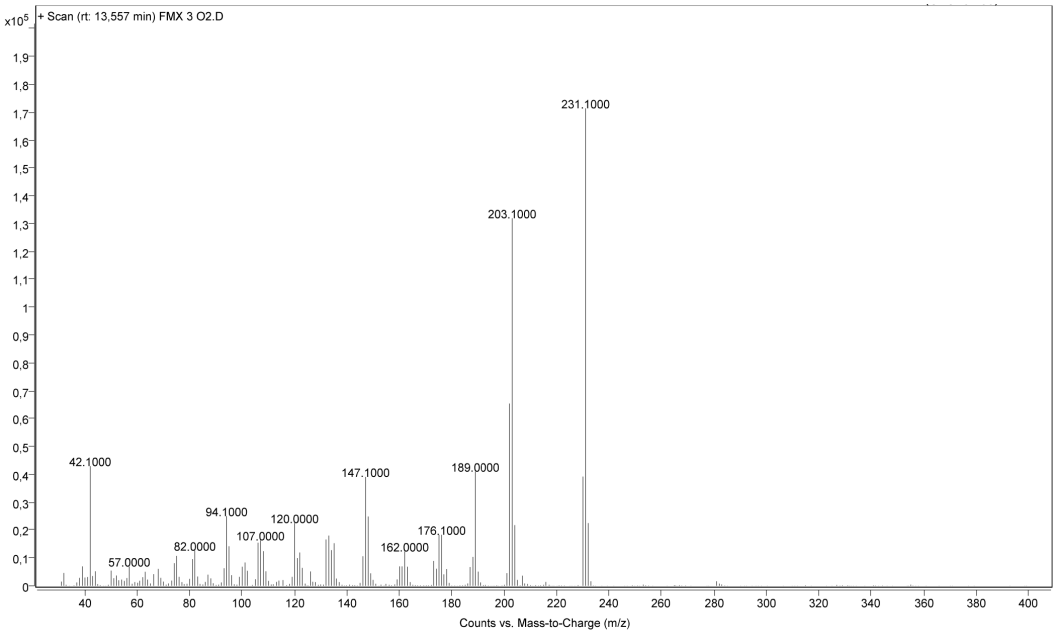

Figure 10.3: EI MS spectrum of in Figure 7.7. when using Ag_2O

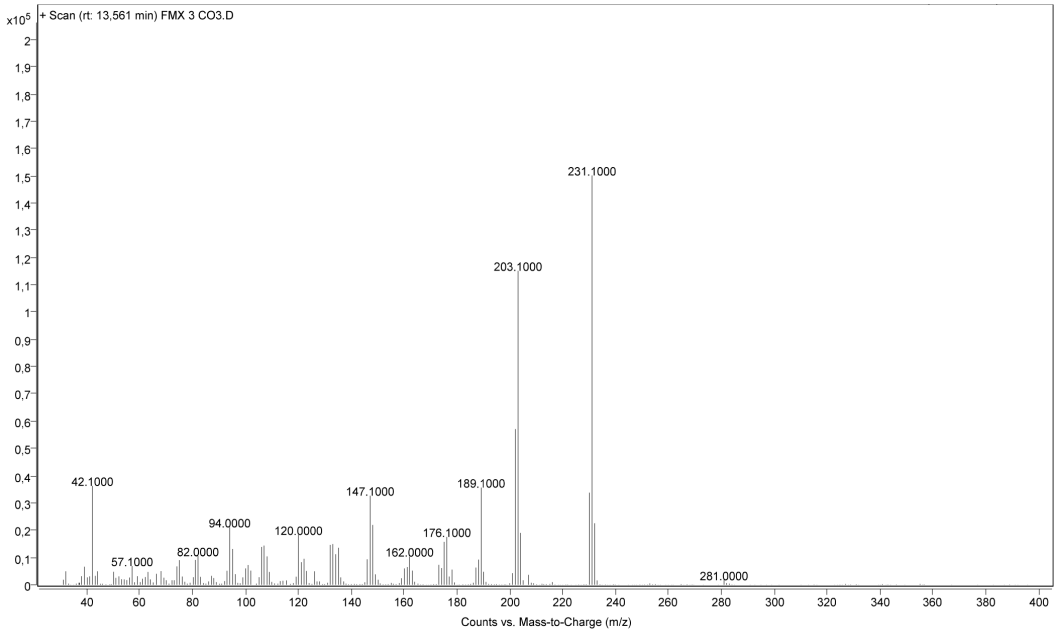

*Figure 10.4: EI MS spectrum of **9** when using Ag_2CO_3*

Chapter 11

Appendix Optimization

11.1 MATLAB Script for the Factorial Design

```
% This script should take inn a table from excel containing a 2D factorial
% design with measured response from the each experiments.
%The script should print the effects of each factor based on the factorial
%design and the response.
%Prints out:
%   The equation describing the response, contain the effects of each
%   factor and the effect of the correlation between the factors.
%   A normal plot of the response so that we can look for outliers
%

%%%%% Replicate 1 %%%%%


% With resolution as the response
% M1 = [xlsread('DoE av EtOH H2O.xlsx','DoE 1 Analytical column 2^2 ','C3:F6') xlsread('DoE av EtOH H2O.xlsx','DoE 1 Ana
% Resolution_1 = my_equation(M1)
Responses_1 = xlsread('DoE av EtOH H2O.xlsx','DoE 1 Analytical column 2^2 ','K3:K6');  %Collecting the responses for lat

%With residence time as response
%nexttile
%M2   = [xlsread('DoE av EtOH H2O.xlsx','DoE 1 Analytical column 2^2 ','C3:F6') xlsread('DoE av EtOH H2O.xlsx','DoE 1 An
%Time_1 = my_equation(M2)




%%%%% Replicate 2 %%%%%


% With resolution as the response
% M3 = [xlsread('DoE av EtOH H2O.xlsx','DoE 2 Analytical column 2^2','C3:F6') xlsread('DoE av EtOH H2O.xlsx','DoE 2 Anal
% Resolution_2 = my_equation(M3)
Responses_2 = xlsread('DoE av EtOH H2O.xlsx','DoE 2 Analytical column 2^2','K3:K6');%Collecting the responses for later

%With residence time as response
%nexttile
%M4   = [xlsread('DoE av EtOH H2O.xlsx','DoE 2 Analytical column 2^2','C3:F6') xlsread('DoE av EtOH H2O.xlsx','DoE 2 Ana
%Time_2 = my_equation(M4)




%%%%% Replicate 3 %%%%%

% With resolution as the response
%
% M5 = [xlsread('DoE av EtOH H2O.xlsx','DoE 3 Analytical column ','C3:F6') xlsread('DoE av EtOH H2O.xlsx','DoE 3 Analyti
% Resolution_3 = my_equation(M5)
Responses_3 = xlsread('DoE av EtOH H2O.xlsx','DoE 3 Analytical column ','K3:K6');%Collecting the responses for later


%With residence time as response
%nexttile

%M6   = [xlsread('DoE av EtOH H2O.xlsx','DoE 3 Analytical column ','C3:F6') xlsread('DoE av EtOH H2O.xlsx','DoE 3 Analyt
%Time_3 = my_equation(M6)


%Up until now the model equation has only been calculated for each replica
%alone.
%Here, the responses are collected for each replica an the mean is
%calculated for each experiment and the model equation is then based on
%this

All_responses = [Responses_1 Responses_2  Responses_3]; %collecting the responses
mean_responses = [];
for i = 1:4
    mean = (All_responses(i,1) + All_responses(i,2) + All_responses(i,3))/3; %taken the mean of each experiment
    mean_responses(i,1) = mean; %Adding the mean to a new list
end
mean_responses;


facmatrix = [-1 -1  1 1;
              1 -1 -1 1;
             -1 1 -1 1;
              1  1  1 1]; %We need the design matrix for 2^2 factorial design
```

```
Mean_factorial_design = [facmatrix mean_responses] %Combining the design matrix and the mean resolution
```

```
Mean_factorial_design = 4×5
   -1.0000   -1.0000    1.0000    1.0000    0.8051
    1.0000   -1.0000   -1.0000    1.0000    0.9798
   -1.0000    1.0000   -1.0000    1.0000    0.5890
    1.0000    1.0000    1.0000    1.0000    0.6511
```

```
Mean_Resolution_Equation = my_equation(Mean_factorial_design) %Collecting the equation and printing the normal prob plot
```

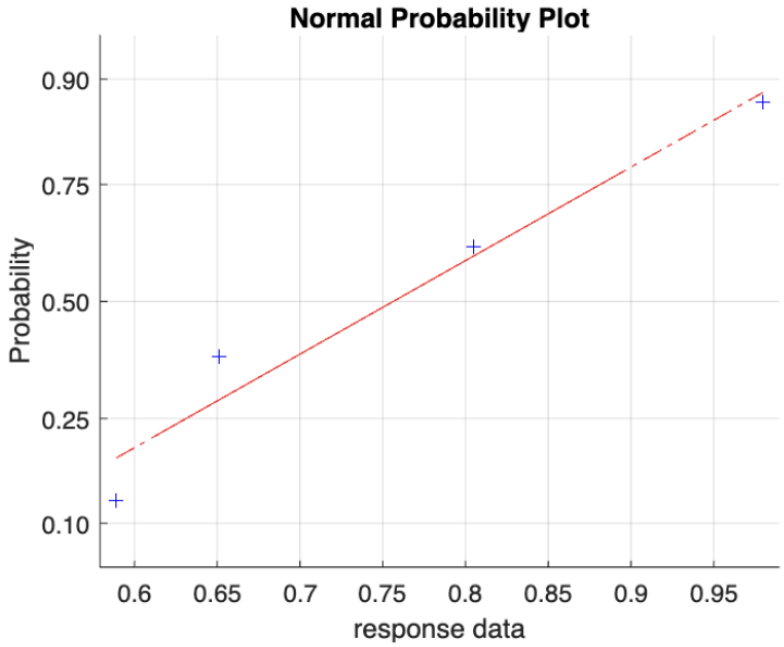


```
Mean_Resolution_Equation = 'y =  0.756 + 0.059A -0.136B -0.028AB + ε'
```

```
function equation = my_equation(num1)

%Presenting a normal plot of the respons for each experiment so we can
%access if there are any outliers
x = num1(:,5);
figure
normplot(x)
xlabel('response data')

%Finding the mean response for the linear regression
mean = 0;

for i = 1:size(num1,1)
    mean = mean + num1(i,4)*num1(i,5);
end
mean = mean/4;


%Finding the effects of each factor on the response:

%For factor A
A = 0;

for i = 1:size(num1,1)
    A = A + num1(i,1)*num1(i,5);
end
A = A/4;

%For factor B
B =  0;
for i = 1:size(num1,1)
    B = B + num1(i,2)*num1(i,5);
end
B = B/4;

%For the combination of A and B, AB
AB =  0;
```

```
for i = 1:size(num1,1)
    AB = AB + num1(i,3)*num1(i,5);
end
AB = AB/4;


%Printing the equation with the effects
eps  = char(949);
if B>0 & AB > 0
    str = sprintf('y = %.3f + %.3fA + %.3fB + %.3fAB + %s', mean, A, B, AB, eps);
end

if B>0 & AB < 0
    str = sprintf('y =  %.3f + %.3fA + %.3fB %.3fAB + %s', mean, A, B, AB, eps);
end

if B<0 & AB < 0
    str = sprintf('y =  %.3f + %.3fA %.3fB %.3fAB + %s', mean, A, B, AB, eps);
end

if B<0 & AB > 0
    str = sprintf('y =  %.3f + %.3fA %.3fB + %.3fAB + %s', mean, A, B, AB, eps);
end

equation = str;

end
```

Figure 11.1: Script for generating the model equation and making the normal probability plot

11.2 MATLAB Script for Response Surface

```
%The data points for the response surface goes in matrix M.
%The data is from the simplex optimization
%First column (X values) is the flow rate
%Second column (Y values) is the amount of ethanol in water
%Third column (X values) is the resulotion (The response)
M = [1.300    20.000     0.6900;
        0.9000   20.0000    0.5400;
        0.9000   10.0000    0.8600;
        1.3000   10.0000    0.8700;
        1.1000    8.0000    1.7800;
        1.5000    8.0000    1.1500;
        1.3000    6.0000    1.2400;
        1.7000    6.0000    1.2900;
        1.1000    7.0000    0.9700;
        0.9000    6.0000    0.0000;
        ]
```

```
M = 10×3
    1.3000   20.0000    0.6900
    0.9000   20.0000    0.5400
    0.9000   10.0000    0.8600
    1.3000   10.0000    0.8700
    1.1000    8.0000    1.7800
    1.5000    8.0000    1.1500
    1.3000    6.0000    1.2400
    1.7000    6.0000    1.2900
    1.1000    7.0000    0.9700
    0.9000    6.0000         0
```

```
X = M(:,1); %Collecting X values from matrix M
Y = M(:,2); %Collecting Y values from matrix M
Z = M(:,3); %Collecting Z values from matrix M
% Apply cubic interpolation
[xGrid,yGrid] = meshgrid(linspace(min(X),max(X)),linspace(min(Y),max(Y)));
zGrid = griddata(X(:),Y(:),Z(:),xGrid(:),yGrid(:),'cubic');
zGrid = reshape(zGrid,size(xGrid));
% Visualize the result
figure
contour(xGrid,yGrid,zGrid,'ShowText','on')
hold on
scatter(X,Y,'ro')
grid on
title("Response Surface for the Resolution")
xlabel("Flow Rate [mL/min]")
ylabel("Amount of Ethanol in Water [%]")
colorbar
```

Figure 11.2: Script for generating the response surface plot

11.3 MATLAB Script for Simplex Optimization

```
%%%%%% Script for the simplex method for the analytical HPLC %%%%%%

%%% This script contains functions that helps you perform the simplex
%%% method in a 2D space and also visualises in a 2D plot.

clear
clc

p1 = [0.9 10 0.86];
p2 = [1.3 10 0.87];
p3 = [1.1 8 1.78];

M  = [p1; p2; p3]; %Kanskje starte med


%Setting the limits based on the highest and lowest x and y value
graf = figure
```

```
graf =
  Figure (5) with properties:

      Number: 5
        Name: ''
       Color: [0.9400 0.9400 0.9400]
    Position: [440 278 560 420]
       Units: 'pixels'

  Show all properties
```

```


%plotting the datapoints in the 2d plot
label_1 = "p1: " + string(p1(3));
plot(p1(1),p1(2),'o')
text(p1(1),p1(2),label_1)
hold on
label_2 = "p2: " + string(p2(3));
plot(p2(1),p2(2),'o')
text(p2(1),p2(2),label_2)
hold on
label_3 = "p3: " + string(p3(3));
plot(p3(1),p3(2),'o')
text(p3(1),p3(2),label_3)
hold on

%Plotting the lines between them so we can visualise the triangle
plot([p1(1) p2(1)], [p1(2) p2(2)])
hold on
plot([p1(1) p3(1)], [p1(2) p3(2)])
hold on
plot([p2(1) p3(1)], [p2(2) p3(2)])
hold on


%Setting the limits based on the highest and lowest x and y value
grid on
xlabel('Flow Rate [mL/min]')
ylabel('Amount of Ethanol in Water [%]')
title('Simplex plot')
```

```
xlim([0.8  2.5])
ylim([4  12])

%print(graf)


%asking for a new datapoint using my_simplex
[p4, best1, best2] = my_simplex(p1,p2,p3);


%adding my new point to the plot, also adding what response it had

p4 = show_grapically(best1, best2, p4, 1.15, getVarName(p4));
M( end+1 , : ) = p4;

%asking for a new datapoint
[p5_1, best1, best2] = my_simplex(best1, best2, p4);
%The suggested point p5 has a too slow, flowrate, therefore I interfere and
%put the flow rate higher
p5_2  = p5_1;
p5_2(1) = 1.7;

p5_1 = show_grapically(best1, best2, p5_1, 1.24, getVarName(p5_1));

p5_2 = show_grapically(best2, p5_1, p5_2, 1.29, getVarName(p5_2));
M( end+1 , : ) = p5_1;
M( end+1 , : ) = p5_2;
%Next datapoint:
[p6_1, best1, best2] = my_simplex(p3, p5_1, p4);
p6_1 = show_grapically(best1, best2, p6_1, 0, getVarName(p6_1));

%I don't have faith in a flow rate this low, and will therefore adjust p6
p6_2(1) = 1.1;
p6_2(2) = 7;

p6_2 = show_grapically(best1, best2, p6_2, 0.97, getVarName(p6_2));
%print graf

[p7, best1, best2] = my_simplex(p6_2, p5_1, p3);
p7 = show_grapically(best1, best2, p7, 0, getVarName(p7));
```

```
%%% Showing the new simplex point graphically %%%

    %This is a way of turning the name of a variable into a string so that
    %it can be plotted.

    %It also adds the newly measured response to the new point.

    %The function takes in the two best points[vectors] and the new point[vector], the
    %value [float] for the response and the variable name [string].

    %The function plots the new point on top of the other points and makes
    %triangles. The function returns the new point with the respons added
    %to the vector
```

```
function [np]  = show_grapically(p1, p2, np, response, stringen)
np(3) = response;
label_x = (stringen + ": " + string(np(3)));
plot(np(1),np(2),'o')
text(np(1),np(2), label_x)
hold on
```

```
plot([p1(1) np(1)], [p1(2) np(2)])
hold on
plot([p2(1) np(1)], [p2(2) np(2)])
hold on
end
```

```
%%% Getting the variable name %%%

    %This is a way of turning the name of a variable into a string so that
    %it can be plotted.

function out = getVarName(var)
    out = inputname(1);
end
```

```
                    %%% Flipping the triangle %%%


    % This function take in three vectors that each contains the grid for an edge in a
    % triangle in a 2d plot. On the 2d plot we have one factor on each axis,
    % which you can define before calling the function.
    % Each vector should contain the factor grid and the beloning response in
    % that grid, like this: [ factor   factor  response ]

    % The fucntion will compare the three vectors based on their response. The vector
    % containing the worst response, should be the corner where the triangle
    % now is being flipped away from

    % The function should present the new corner of the triangle to the user,
    % It is important that the user verify that the new point makes sence
    % and is possible to perform in real life. If not, the user can simply
    % generate a new point manually

    % The function returns the new point and and the two that were best so
    % that they can be graphically displayed using "show graphically"

function [new_point,best1,best2] = my_simplex(p1, p2, p3)

%M  = [p1; p2; p3];
```

```
%Cheking which datapoint that has the worst response. Her må du sikkert
%legge på noe greier i tilfelle du får to like responser
for i = 3
    if p1(3) > p3(3) & p2(3) > p3(3)
        worst = p3;
        best1 = p1;
        best2 = p2;
    end

    if p3(3) > p1(3) & p2(3) > p1(3)
        worst = p1;
```

```
        best1 = p3;
        best2 = p2;

    end

    if p1(3) > p2(3) & p3(3) > p2(3)
        worst = p2;
        best1 = p1;
        best2 = p3;
    end

end

%I would now like to flip the triangle away from the worst point

%First I am turning the triangle sides into vectors
WB1 =  [best1(1)-worst(1) best1(2)-worst(2)];
WB2 =  [best2(1)-worst(1) best2(2)-worst(2)];
B1B2 = [best2(1)-best1(1) best2(2)-best1(2)];

%Then i find the length of each vector
lWB1 = sqrt(WB1(1)^2 + WB1(2)^2);
lWB2 = sqrt(WB2(1)^2 + WB2(2)^2);
lB1B2 = sqrt(B1B2(1)^2 + B1B2(2)^2);

c = [best1(1) best1(2)] + B1B2*0.5;
W1NP = c - [worst(1) worst(2)];
new_point = [worst(1) worst(2)] + W1NP*2;
best1 = best1;
best2 = best2;

end
```

Figure 11.3: Script for generating the simplex optimization

Bibliography

[1] Sóti Z, Magill J, Dreher R. Karlsruhe Nuclide Chart–New 10th edition 2018. EPJ Nuclear Sciences & Technologies. 2019;5:6. (document), 2.4, 2.1

[2] Meisenheimer J. Ueber reactionen aromatischer nitrokörper. Justus Liebigs Annalen der Chemie. 1902;323(2):205-46. (document), 3.3.3, 3.4

[3] Incremona JH, Martin JC. N-Bromosuccinimide. Mechanisms of allylic bromination and related reactions. Journal of the American Chemical Society. 1970;92(3):627-34. (document), 3.6

[4] Lu P, Sanchez C, Cornella J, Larrosa I. Silver-catalyzed protodecarboxylation of heteroaromatic carboxylic acids. Organic letters. 2009;11(24):5710-3. (document), 3.3.6, 3.7, 4.2.4, 4.2.5, 4.4.2

[5] Sandtorv AH, Bjørsvik HR. Fast Halogenation of Some N-Heterocycles by Means of N, N-Dihalo-5, 5-dimethylhydantoin. Advanced Synthesis & Catalysis. 2013;355(2-3):499-507. (document), 3.3.7, 3.8, 3.3.7, 4.2.6, 4.2.7, 4.4.2

[6] Yang Y, Zhang L, Deng GJ, Gong H. Simple, efficient and controllable synthesis of iodo/di-iodoarenes via ipsoiododecarboxylation/consecutive iodination strategy. Scientific Reports. 2017;7(1):40430. (document), 3.3.8, 3.9

[7] Fu Z, Li Z, Song Y, Yang R, Liu Y, Cai H. Decarboxylative halogenation and cyanation of electron-deficient aryl carboxylic acids via Cu mediator as well as electron-rich ones through Pd catalyst under aerobic conditions. The Journal of Organic Chemistry. 2016;81(7):2794-803. (document), 3.3.8, 3.9, 4.4.2

[8] Jones LH, Mohammed S, Newman S, Mowbray CE, Selby MD, Stupple PA, et al.. Sulphur-Linked Imidazone Compounds for the Treatment of Hiv/Aids. Google Patents; 2008. US Patent App. 10/599,707. (document), 3.3.8, 3.9, 4.2.1

[9] Pavia DL, Lampman GM, Kriz GS, Vyvyan JA. In: Introduction to spectroscopy. Cengage learning; 2014. p. 108. (document), 3.4.2, 3.10

[10] Pavia DL, Lampman GM, Kriz GS, Vyvyan JA. In: Introduction to spectroscopy. Cengage learning; 2014. p. 117. (document), 3.11, 3.4.2

[11] Gross JH. Mass spectrometry: a textbook. Springer Science & Business Media; 2006. (document), 3.11

[12] Pavia DL, Lampman GM, Kriz GS, Vyvyan JA. In: Introduction to spectroscopy. Cengage learning; 2014. p. 109. (document), 3.4.2, 3.12

[13] Lewis JS, Windhorst AD, Zeglis BM. In: Radiopharmaceutical Chemistry. Springer; 2019. p. 3. 2.1

[14] Lewis JS, Windhorst AD, Zeglis BM. In: Radiopharmaceutical Chemistry. Springer; 2019. p. 208. 2.1

[15] Lewis JS, Windhorst AD, Zeglis BM. In: Radiopharmaceutical Chemistry. Springer; 2019. p. 114. 2.1

[16] Heiss WD, Herholz K. Brain receptor imaging. Journal of Nuclear Medicine. 2006;47(2):302-12. 2.2, 2.3

[17] Taddei C, Pike VW. [11C] Carbon monoxide: advances in production and application to PET radiotracer development over the past 15 years. EJNMMI Radiopharmacy and Chemistry. 2019;4(1):1-31. 2.4, 2.4.1, 2.4.3, 2.4.3

[18] Lewis JS, Windhorst AD, Zeglis BM. In: Radiopharmaceutical Chemistry. Springer; 2019. p. 219. 2.4.1

[19] Lewis JS, Windhorst AD, Zeglis BM. In: Radiopharmaceutical Chemistry. Springer; 2019. p. 224. 2.4.2

[20] Lewis JS, Windhorst AD, Zeglis BM. In: Radiopharmaceutical Chemistry. Springer; 2019. p. 233. 2.4.3

[21] Eriksson J, Antoni G, Långström B, Itsenko O. The development of 11C-carbonylation chemistry: a systematic view. Nuclear Medicine and Biology. 2021;92:115-37. 2.4.3, 2.4.3

[22] Kihlberg T, Langstrom B. Method and apparatus for production and use of [11C] carbon monoxide in labeling synthesis. Google Patents; 2004. US Patent App. 10/480,093. 2.4.3

[23] Eriksson J, van den Hoek J, Windhorst AD. Transition metal mediated synthesis using [11C] CO at low pressure–a simplified method for 11C-carbonylation. Journal of Labelled Compounds and Radiopharmaceuticals. 2012;55(6):223-8. 2.4.3

[24] Rahman O, Takano A, Amini N, Dahl K, Kanegawa N, Långström B, et al. Synthesis of ([11C] carbonyl) raclopride and a comparison with ([11C] methyl) raclopride in a monkey PET study. Nuclear Medicine and Biology. 2015;42(11):893-8. 2.5

[25] Halldin C, Stone-Elander S, Thorell JO, Persson A, Sedvall G. 11C-labelling of Ro 15-1788 in two different positions, and also 11C-labelling of its main metabolite Ro 15-3890, for PET studies of benzodiazepine receptors. International Journal of Radiation Applications and Instrumentation Part A Applied Radiation and Isotopes. 1988;39(9):993-7. 2.6

[26] Beer HF, Bläuenstein PA, Hasler PH, Delaloye B, Riccabona G, Bangerl I, et al. In vitro and in vivo evaluation of iodine-123-Ro 16-0154: a new imaging agent for SPECT investigations of benzodiazepine receptors. Journal of Nuclear Medicine. 1990;31(6):1007-14. 2.6

[27] Ryzhikov NN, Seneca N, Krasikova RN, Gomzina NA, Shchukin E, Fedorova OS, et al. Preparation of highly specific radioactivity [18F] flumazenil and its evaluation in cynomolgus monkey by positron emission tomography. Nuclear medicine and biology. 2005;32(2):109-16. 2.6

[28] Grewal AS, Kumar K, Redhu S, Bhardwaj S. Microwave assisted synthesis: a green chemistry approach. International Research Journal of Pharmaceutical and Applied Sciences. 2013;3(5):278-85. 3.3.2

[29] McMurry J. In: Organic Chemistry. Cengage Learning; 2016. p. 704. 3.3.4

[30] Wohl A. Bromierung ungesättigter Verbindungen mit N-Brom-acetamid, ein Beitrag zur Lehre vom Verlauf chemischer Vorgänge. Berichte der deutschen chemischen Gesellschaft (A and B Series). 1919;52(1):51-63. 3.3.5

[31] Ziegler K, Schenck G, Krockow E, Siebert A, Wenz A, Weber H. Die synthese des cantharidins. Justus Liebigs Annalen der Chemie. 1942;551(1):1-79. 3.3.5

[32] Pavia DL, Lampman GM, Kriz GS, Vyvyan JA. In: Introduction to spectroscopy. Cengage learning; 2014. p. 215, 216, 217, 218, 219, 220, 221, 222, 223. 3.4.5

[33] Montgomery DC. In: Design and analysis of experiments. John wiley & sons; 2017. p. 11. 3.5.1

[34] Montgomery DC. In: Design and analysis of experiments. John wiley & sons; 2017. p. 183. 3.5.2

[35] Nortvedt R, Brakstad F, Kvalheim OM, Lundstedt T. In: Anvendelse av KJEMOMETRI innen forskning og industri. Tidsskriftforlaget Kjemi AS; 1996. p. 81, 82, 83, 84, 85, 86, 87. 3.5.2

[36] Nortvedt R, Brakstad F, Kvalheim OM, Lundstedt T. In: Anvendelse av KJEMOMETRI innen forskning og industri. Tidsskriftforlaget Kjemi AS; 1996. p. 101, 102. 3.5.2, 3.5.3

[37] Donohue SR, Dannals RF. A concise and efficient synthesis of flumazenil and its precursor for radiolabeling with fluorine-18. Tetrahedron Letters. 2009;50(52):7271-3. 4.1.1, 4.1.3, 4.4.1

[38] Cleij MC, Clark JC, Baron JC, Aigbirhio FI. Rapid preparation of [11C] flumazenil: captive solvent synthesis combined with purification by analytical sized columns. Journal of Labelled Compounds and Radiopharmaceuticals: The Official Journal of the International Isotope Society. 2007;50(1):19-24. 4.3.1, 4.3.3, 4.4.3

[39] Fahr A, Nayak AK, Kurylo MJ. The ultraviolet absorption cross sections of CH3I temperature dependent gas and liquid phase measurements. Chemical physics. 1995;197(2):195-203. 4.3.5

[40] Resende P, Almeida WP, Coelho F. An efficient synthesis of (R)-(-)-baclofen. Tetrahedron: Asymmetry. 1999;10(11):2113-8. 5.2.5

[41] Chow SY, Odell LR, Eriksson J. Low-Pressure Radical 11C-Aminocarbonylation of Alkyl Iodides through Thermal Initiation. European Journal of Organic Chemistry. 2016;2016(36):5980-9. 5.2.5

[42] E Ramsay MA, Luterman DL. Dexmedetomidine as a total intravenous anesthetic agent. The Journal of the American Society of Anesthesiologists. 2004;101(3):787-90. 5.2.5